

4-2018

ROLE OF THE SNF2 HOMOLOG, IRC20, IN YEAST GENOME MAINTENANCE

Deena Mohamed Galal Eldin Ahmed

Follow this and additional works at: https://scholarworks.uaeu.ac.ae/all_theses



Part of the [Biochemistry Commons](#), and the [Other Medicine and Health Sciences Commons](#)

United Arab Emirates University

College of Medicine and Health Sciences

ROLE OF THE SNF2 HOMOLOG, IRC20, IN YEAST GENOME
MAINTENANCE

Deena Mohamed Galal Eldin Ahmed

This dissertation is submitted in partial fulfilment of the requirements for the degree
of Doctor of Philosophy

Under the Supervision of Dr. Ahmed H. Hassan Al-Marzouqi

April 2018

Declaration of Original Work

I, Deena Mohamed Galal Eldin Ahmed, the undersigned, a graduate student at the United Arab Emirates University (UAEU), and the author of this dissertation entitled “*Role of the Snf2 Homolog, Irc20, in Yeast Genome Maintenance*”, hereby, solemnly declare that this dissertation is my own original research work that has been done and prepared by me under the supervision of Dr. Ahmed H. Hassan Al-Marzouqi, in the College of Medicine and Health Sciences at UAEU. This work has not previously been presented or published by others, or formed the basis for the award of any academic degree, diploma or a similar title at this or any other university. Any materials borrowed from other sources (whether published or unpublished) and relied upon or included in my dissertation have been properly cited and acknowledged in accordance with appropriate academic conventions. I further declare that there is no potential conflict of interest with respect to the research, data collection, authorship, presentation and/or publication of this dissertation.

Student's Signature: _____

Date: _____

Copyright © 2018 Deena Mohamed Galal Eldin Ahmed
All Rights Reserved

Advisory Committee

1) Advisor: Ahmed H Hassan Al- Marzouqi

Title: Associate Professor

Department of Biochemistry

College of Medicine and Health Sciences

2) Member: Farah Mustafa

Title: Associate Professor

Department of Biochemistry

College of Medicine and Health Sciences

3) Member: Samir Attoub

Title: Professor

Department of Pharmacology

College of Medicine and Health Sciences

4) Member: Starling Emerald Bright David

Title: Assistant Professor

Department of Anatomy

College of Medicine and Health Sciences

Approval of the Doctorate Dissertation

This Doctorate Dissertation is approved by the following Examining Committee Members:

- 1) Advisor (Committee Chair): Ahmed H Al- Marzouqi

Title: Associate Professor

Department of Biochemistry and Molecular Biology

College of Medicine and Health Sciences

Signature _____ Date _____

- 2) Member: Haider Raza

Title: Professor

Department of Biochemistry and Molecular Biology

College of Medicine and Health Sciences

Signature _____ Date _____

- 3) Member: Tahir Rizvi

Title: Professor

Department of Microbiology and Immunology

College of Medicine and Health Sciences

Signature _____ Date _____

- 4) Member (External Examiner): LeAnn Howe

Title: Associate Professor

Department of Biochemistry and Molecular Biology

Institution: University of British Columbia (UBC), Canada

Signature _____ Date _____

This Doctorate Dissertation is accepted by:

Dean of the College of Medicine and Health Sciences: Professor Ruth Langer

Signature _____ Date _____

Dean of the College of Graduate Studies: Professor Nagi T. Wakim

Signature _____ Date _____

Copy ____ of ____

Abstract

In eukaryotes, DNA is wrapped around histone proteins forming a highly compact structure, the chromatin. All DNA-based processes must occur within the complex organization of the chromatin, and this requires modulation of its structure when needed. This is accomplished by covalent histone modifications that alter histone-DNA contacts, as well as through the actions of ATP-dependent chromatin remodelers. These multi-subunit complexes play major roles in transcription regulation, replication and repairing DNA damage. This thesis aims to characterize a poorly studied member of the SWI/SNF family of ATPases/helicases, *Irc20*, from *Saccharomyces cerevisiae*. Previously, *Irc20* has been shown to be involved in recombinational repair and to possess ubiquitin ligase (E3) activity. The human homolog of *Irc20*, SHPRH, has also been implicated in repair via the poly-ubiquitylation of PCNA, the sliding clamp of the DNA polymerase. Loss of heterozygosity in the region containing the SHPRH gene is seen in a wide variety of cancers. In this study, using purified *Irc20*, we showed that it possesses DNA and nucleosome binding activities, as well as an ATP-hydrolyzing activity. However, despite homology to Snf2 catalytic domain, *Irc20* did not have the ability to alter chromatin structure. Using point mutations in different *Irc20* domains, we identified that the increased recombination centers observed in *irc20* null mutants is dependent on both its ATPase and ubiquitin ligase activities. Consistent with this, we observed higher recruitment or retention of the recombination repair factor Rad52 at a single induced double strand break in Δ *irc20* mutant, suggesting a regulatory role for *Irc20* in DNA repair. Furthermore, we observed a previously unidentified function for *Irc20* in regulating the levels of the endogenous yeast 2- μ m plasmid. In *irc20* null mutant, we observed a three to four-fold increase in 2- μ m levels, forming high molecular weight forms in a manner dependent on homologous recombination. We suggest this is, at least partially, through regulating the levels of Flp1 recombinase since we observed higher levels of Flp1 in Δ *irc20* mutant after shutting off expression from a repressible promoter. Collectively, our results show a regulatory

role for Irc20 in recombination underlying its role in stabilizing the genome and regulating the 2- μ m plasmid levels.

Keywords: *Saccharomyces cerevisiae*, Irc20, ATPase enzyme, ubiquitin ligase, DNA repair, 2- μ m plasmid, recombination, ubiquitin, SUMO.

Title and Abstract (in Arabic)

دور نظير Snf2، Irc20 ، في الحفاظ على الحمض النووي للخميرة

المخلص

في حقيقيات النواة ، يتم لف الحمض النووي حول بروتينات الهيستون التي تشكل بنية مدمجة للغاية، الكروماتين. يجب أن تحدث جميع العمليات القائمة على الحمض النووي ضمن التنظيم المعقد للكروماتين، وهذا يتطلب تعديل هيكله عند الحاجة. ويتم تحقيق ذلك من خلال تعديلات هيستون التساهمية التي تغير من اتصالات الهيستون بالحمض النووي، وكذلك من خلال تصرفات مقلدات الكروماتين المعتمدة على ATP. تلعب هذه المجمعات متعددة الوحدات الفرعية أدواراً رئيسية في تنظيم النسخ وتكرار وإصلاح أضرار الحمض النووي. تهدف هذه الأطروحة إلى وصف العضو الذي تمت دراسته بشكل ضعيف في عائلة SWI/SNF من *Saccharomyces cerevisiae*، Irc20، ATPases/helicases. في السابق، تم إثبات أن Irc20 يشارك في إصلاح التكاثر وأن يمتلك نشاط ubiquitin ligase E3. كما تم توريث نظير Irc20 في الإنسان، SHPRH، في إصلاح الحمض النووي عبر poly-ubiquitylation من PCNA، مشبك الانزلاق لبوليميراز الحمض النووي. وينظر إلى فقدان متغايرة الازيجوتية في المنطقة التي تحتوي على جين SHPRH في مجموعة واسعة من أنواع السرطان. في هذه الدراسة، باستخدام Irc20 منقى، أظهرنا أنه يمتلك أنشطة ربط الحمض النووي ونواة الجسيمات، بالإضافة إلى نشاط ATP-hydrolyzing. ومع ذلك ، على الرغم من انه مشابه ل Snf2، لم يكن لدى Irc20 القدرة على تغيير بنية الكروماتين. باستخدام طفرات في نقاط مختلفة في Irc20، حددنا أن زيادة مراكز إعادة التركيب الذي لوحظ في الخلايا التي تنقص جين irc20 يعتمد على كل من أنشطة ال ATPase و ubiquitin ligase. تماشياً مع ذلك، لاحظنا زيادة في توظيف أو الاحتفاظ بعامل إصلاح إعادة التركيب Rad52 عند حدوث كسر مزدوج للحبل مزدوج في متحولة irc20Δ، مما يشير إلى وجود دور تنظيمي لـ Irc20 في إصلاح الحمض النووي. علاوة على ذلك، لاحظنا وظيفة غير معروفة سابقاً لـ Irc20 في تنظيم مستويات من البلازميد 2 ميكرون الخاص بالخميرة. في الخلايا التي تنقص irc20، لاحظنا زيادة ثلاثة إلى أربعة أضعاف في مستويات البلازميد 2 ميكرون، وتشكيل أشكال ذات

وزن جزيئي عالي بطريقة تعتمد على إعادة التركيب المتماثل. نحن نقترح أن هذا، على الأقل جزئياً، من خلال تنظيم مستويات Flp1 recombinase لأننا لاحظنا مستويات أعلى من Flp1 في الخلايا التي تنقص جين irc20 بعد إغلاق التعبير الجيني من مشغل قابل للاغلاق. بشكل جماعي، تظهر نتائجنا دوراً تنظيمياً لـ Irc20 في إعادة التركيب التي تقوم على أساس دورها في تثبيت الجينوم وتنظيم مستويات البلازميد 2 ميكرون.

مفاهيم البحث الرئيسية: إصلاح الحمض النووي، البلازميد 2 ميكرون، إعادة التركيب المتماثل، *Saccharomyces cerevisiae*, Irc20, ATPase enzyme, ubiquitin, SUMO, ubiquitin ligase.

Acknowledgements

First of all, I would like to thank Allah for giving me strength to endure. I would like to thank the UAE University for the research opportunity and funding that allowed for this research to happen. I would also like to thank my advisor Dr. Ahmed H Hassan Al Marzouqi, for believing in me and giving me a chance in the lab, even though I had no prior research experience in this field. I would also like to thank him for the freedom he always gave during the research, for allowing me to learn from my own mistakes, and for always reminding me of the bigger picture when I had conflicts between my family and my PhD. He always gave me one reply to my every concern, 'Family comes first'. I will be forever grateful for that.

I would also like to thank the members of my thesis advisory committee, Dr. Farah Mustafa, Dr. Starling Emerald and Prof. Samir Attoub for their insightful comments, encouragement and for their questions and critiques during the course of my studies. I would also like to thank the members of my thesis examination committee, Prof. Haider Raza, Prof. Tahir A. Rizvi, and Dr. LeAnn Howe for providing valuable comments and suggestions that would undoubtedly help in making this research of better quality.

I would like to thank my fellow members in the lab, Dr. Jisha Chalissery, Dr. Zeina Al Natour, Ms. Mehwish Iqbal, Ms. Sanjana, and Ms. Zahra for the stimulating discussions, encouragement and support, and all the nice moments we had together as my second family during this period. I would like to particularly thank Jisha for being the best friend and mentor during the six years we spent together, for always

listening and for always managing to make everything available in the least possible time. I would definitely not have endured in the lab without her. I would like to thank Zeina, for introducing me to the molecular biology field. I would also like to thank Mehwish, for being my good luck charm.

I would like to thank my family especially my father for being my role model and my number one supporter. He taught me all the basics of research from his own experience, and always helped keep me grounded. I would like to thank my mother, for always making life easier so I can focus on my studies. I would like to thank my sisters, Heba and Lamis, for always listening and always encouraging me and supporting me when I was at my darkest moments. I would like to thank my brother, Waleed, for keeping me company for endless nights while writing and studying, and always managing to cheer me up. I would like to thank my husband, Ahmed, for bearing with me for 6 years and for always encouraging me to move forward when I wanted to quit, sacrificing his own happiness for mine. I would like to thank my son, Selim, who has definitely been the biggest push forward and the sunshine in my life.

I would also like to thank my friends, especially those who I got to know during my time in CMHS, Rawan, Salma, Heba, Amal, Nour Yahfoufi, and Nour Majbour. I would particularly like to thank Rawan and Salma for making my time in the CMHS fun, and giving me a shoulder to cry on everytime I needed it. I would also like to thank my friends in the hostel, Razan, Shaima, Hasna, Maysm and Haya, for being more than sisters. I would particularly like to thank Razan, for being the best friend any one could ask for.

Dedication

To my beloved son, Selim

Table of Contents

Title	i
Declaration of Original Work	ii
Copyright	iii
Advisory Committee	iv
Approval of the Doctorate Dissertation	v
Abstract	vii
Title and Abstract (in Arabic)	ix
Acknowledgements	xi
Dedication	xiii
Table of Contents	xiv
List of Tables	xvii
List of Figures	xviii
List of Abbreviations	xix
Chapter 1: Introduction	1
1.1 Overview	1
1.2 ATP-Dependent chromatin remodelers	2
1.3 The DNA Damage Response (DDR)	5
1.4 Ubiquitin and SUMO in DNA damage repair	12
1.4.1 The ubiquitylation process	12
1.4.2 Proteins of the ubiquitin regulatory network	15
1.4.3 The SUMOylation process	19
1.4.4 Ubiquitin and SUMO in DNA damage response	22
1.4.5 SUMO in Base Excision Repair (BER)	22
1.4.6 Ubiquitin and SUMO in Nucleotide Excision Repair (NER)	23
1.4.7 Ubiquitin and SUMO in Post-Replication Repair (PRR)	26
1.4.8 Ubiquitin and SUMO in Double Strand Break Repair (DSBR)	33
1.4.9 SUMO-targeted ubiquitin ligases (STUbLs) in DSB repair and perinuclear localization	37
1.4.10 The epigenetic role of Ubiquitin in DNA damage signalling and stress response	43
1.4.11 Ubiquitin and SUMO in the maintenance of rDNA regions and telomeres	45
1.5 The yeast 2- μ m plasmid	51
1.6 The Irc20 protein	57

1.6.1 The human homologs of Irc20 and their role as tumor suppressor genes	58
1.6.2 The role of Irc20 in DNA repair	60
1.6.3 The role of Irc20 in transcription regulation	61
1.7 Aims and objectives	63
Chapter 2: Materials and Methods	64
2.1 Yeast strain construction	64
2.1.1 One-step PCR-mediated gene deletion or tagging	64
2.1.2 <i>In vivo</i> site-specific mutagenesis (<i>delitto perfetto</i>)	67
2.2 Tandem Affinity Purification (TAP) of Irc20	77
2.2.1 Double affinity TAP purification	77
2.2.2 Single affinity TAP purification	80
2.3 Purification of CBP-tagged Snf6 for quantification of purified proteins	80
2.4 Size exclusion chromatography	81
2.5 Mass spectrometry analysis	81
2.6 Immobilized template binding assay	82
2.7 SalI accessibility assay	82
2.8 ATP-hydrolysis assay	83
2.9 Growth assay	84
2.10 Rad52 foci detection	84
2.11 Co-immunoprecipitation	84
2.12 ChIP at the HO cut site	85
2.13 Measuring the presence of the endogenous 2- μ m plasmid	86
2.14 Curing yeast cells from the endogenous 2- μ m plasmid	87
2.15 2- μ m plasmid loss assay	87
2.16 Analyzing 2- μ m plasmid levels	88
2.17 Southern blotting for analyzing 2- μ m species	89
2.18 Extraction of total cellular protein by TCA	90
2.19 Monitoring Flp1 levels	90
Chapter 3: Results – Biochemical Characterization of Irc20	92
3.1 Overview	92
3.2 Purification and characterization of Irc20 protein	92
3.2.1 Irc20 is normally expressed in low amounts and shows promiscuous protein interactions	92
3.2.2 Purification of overexpressed Irc20 produces sufficient yield and purity	97
3.3 Irc20 shows DNA and nucleosome binding activities	98
3.4 Irc20 shows ATP hydrolyzing activity	100
3.5 Irc20 does not show the ability to remodel the chromatin structure	101

3.6 Conclusion	102
Chapter 4: Results – Irc20 Recycles Rad52 from DSB Sites during Recombination	103
4.1 Overview	103
4.2 Both the ATPase and the ubiquitin ligase mutants of Irc20 show increased spontaneous Rad52 foci under non-damaging conditions.....	103
4.3 Irc20 deletion does not show sensitivities to DNA damaging agents and does not genetically interact with other repair factors.....	105
4.4 Irc20 interacts with Rad52	109
4.5 Irc20 facilitates the removal of Rad52 during DSB repair	110
4.6 Conclusion	113
Chapter 5: Results – Irc20 Regulates 2- μ m Plasmid Levels.....	115
5.1 Overview	115
5.2 Mutations in <i>IRC20</i> gene occasionally generate [cir ⁰] strains.....	115
5.3 The loss of 2- μ m plasmids does not occur if plasmids do not harbor the Flp1 gene	117
5.4 The 2- μ m plasmid copy numbers are elevated in Irc20 null mutant but not in point mutants	120
5.5 The elevation in 2- μ m plasmid copy number in Irc20 null mutant is dependent on HR	121
5.6 The Irc20 null mutant and the ATPase domain mutant both show production of a high molecular weight form of the 2- μ m plasmid	123
5.7 Irc20 controls copy number amplification of the 2- μ m plasmid by regulating the Flp1 protein levels in the cell	124
5.8 Conclusion	125
Chapter 6: Discussion and Future Prospectives	127
6.1 Irc20 is an ATPase that does not alter the chromatin structure	127
6.2 Irc20 interacts with multiple proteins in diverse pathways	128
6.3 The role of Irc20 in HR.....	130
6.4 Irc20 and Cdc48, opposing or similar roles?	133
6.5 The role of Irc20 in regulating the 2- μ m plasmid levels	136
References	140
Appendix	167

List of Tables

Table 1: Yeast strains used in this thesis.....	70
Table 2: Primers used in this thesis.....	72
Table 3: Top hits for mass spectrometry results for TAP-Irc20	167
Table 4: Top hits for mass spectrometry for TAP-Irc20 <i>C1239A</i>	175

List of Figures

Figure 1.1: Repair of Single Strand DNA Damage	8
Figure 1.2: Double Strand Break Repair Pathways	11
Figure 1.3: The Ubiquitylation Process	14
Figure 1.4: PCNA Modifications	27
Figure 1.5: The 2- μ m plasmid and its regulatory units.....	53
Figure 1.6: Irc20 and its human homologs	58
Figure 2.1: Overview of one-step PCR mediated gene tagging and deletion.....	67
Figure 2.2: Overview of <i>delitto perfetto</i>	69
Figure 2.3: Domains of Irc20 showing specific amino acids mutated in each domain	70
Figure 2.4: Tandem Affinity Purification (TAP) illustration.....	79
Figure 3.1: Purification of Irc20 under native expression conditions.....	93
Figure 3.2: Size exclusion chromatography.....	95
Figure 3.3: Overexpression and Purification of Irc20	98
Figure 3.4: Irc20 shows DNA and nucleosome binding activities	99
Figure 3.5: Irc20 hydrolyzes ATP	100
Figure 3.6: Irc20 does not show chromatin remodeling activity	101
Figure 4.1: Increased Rad52 foci in both ATPase and ubiquitin ligase mutants of Irc20	104
Figure 4.2: Irc20 does not show synthetic rescue with Mre11 or display genetic interactions with other DNA repair factors	108
Figure 4.3: Irc20 physically interacts with Rad52 weakly.....	110
Figure 4.4: Irc20 controls levels of Rad52 at an induced DSB.....	112
Figure 5.1: Absence of Irc20 ubiquitin ligase activity leads to the occasional loss of the endogenous 2- μ m plasmid.....	116
Figure 5.2: Δ <i>irc20</i> mutant only show loss in 2- μ m stability if the 2- μ m plasmid harbors a Flp1 gene	118
Figure 5.3: Elevated 2- μ m plasmid levels are observed in Δ <i>irc20</i> , but not in point mutants.....	120
Figure 5.4: The hyper-amplification of the 2- μ m plasmid in Δ <i>irc20</i> mutants is dependent on HR factors	122
Figure 5.5: Formation of high molecular weight forms of 2- μ m in Δ <i>irc20</i> and ATPase domain mutant <i>Irc20-DE534-535AA</i>	123
Figure 5.6: Irc20 regulates Flp1 levels	125
Figure 6.1: A model for the functional interaction between Irc20 and Cdc48	135

List of Abbreviations

BER	Base excision repair
Bp	Base pair
Bur-	Bypass of upstream activator sequence (UAS)
Cy5	Cyanine5
DDR	DNA damage response
DNA	Deoxyribo nucleic acid
DSB	Double strand break
DTT	1,4-Dithiothreitol
GCR	Gross chromosomal rearrangements
GGR	Global genome repair
HR	Homologous Recombination
HO	Homothallic switching endonuclease
HU	Hydroxyurea
ICL	Intrastrand crosslink
IgG	Immunoglobulin G
MMR	Mismatch repair
MMS	Methyl methane sulphonate
NER	Nucleotide excision repair
Nt	nucleotide
PCR	Polymerase chain reaction
PIP/PIM	PCNA interacting protein/motif

PRR	Post replication repair
SCJs	Sister chromatid junctions
SDSA	Synthesis dependent strand annealing
SIM	SUMO interacting motif
STUbLs	SUMO targeted ubiquitin ligases
SUMO	Small ubiquitin like modifier
TAP	Tandem affinity purification
TCA	Trichloroacetic acid
TCR	Transcription coupled repair
TLS	Translesion synthesis
TS	Template switching
UV	Ultra-violet light

Chapter 1: Introduction

1.1 Overview

DNA encodes the genetic information required for the development, functioning and survival of all living organisms. In eukaryotes, the DNA double helix is wrapped around histones, forming nucleosomes. Linker histones and other scaffold proteins further compact this structure into higher order chromatin structures. This wrapping, while serves in compacting around two meters of DNA into the nucleus, also severely impedes many important DNA-based processes. Access to chromatin is regulated by covalent posttranslational modification of histone proteins, and by the action of ATP-dependent remodeling enzymes. DNA is under continuous attack from both endogenous and exogenous damaging agents. To protect itself from the severe consequences of DNA damage, the cell has evolved an intricate multi-faceted response, called the DNA Damage Response (DDR). This involves two parallel concerted events; the first is the activation of a signaling network that works to sense the damaged lesion, and activate cell cycle checkpoints. The second event in DDR is the recruitment of various proteins of the DNA repair system, which work to process and repair the damaged region. Several tumors are thought to evolve from improper repair of damaged lesions and mutations in DDR machinery. Timely activation and regulation of repair protein functions are vital for cell survival. Post-translational modification of repair factors by ubiquitylation and SUMOylation provides a quick reversible way of signaling and targeting, making responses to cellular changes rapid and dynamic. In the coming sections, I will discuss some of the classes of ATP-dependent chromatin remodelers, the DDR and

its regulation by ubiquitin and SUMO. This will be followed by an account on the yeast episomal DNA, the 2- μ m plasmid. Finally, the specific interest in Irc20 protein in yeast and its human homologs will be discussed.

1.2 ATP-Dependent chromatin remodelers

ATP-dependent remodelers are large multi-subunit complexes that couple ATP hydrolysis to remodel the structure of chromatin. The first identified ATP-dependent chromatin remodeler was the yeast SWI/SNF complex. It was discovered through genetic screens, for genes important in yeast mating type *switching* (SWI), and for *SUC2* gene expression, which encodes the enzyme invertase required for utilizing sucrose - *sucrose non fermenting* (Laurent, Treich, & Carlson, 1993). The SWI/SNF proteins form a large multi-subunit complex of 12 different proteins, with a core catalytic subunit, SWI2/SNF2. This subunit harbors a helicase-like ATPase domain consisting of two tandem RecA-like folds and contains seven conserved helicase-related sequence motifs that classify it as part of the Superfamily 2 (SF2) grouping of helicase-like proteins (Flaus, Martin, Barton, & Owen-Hughes, 2006). Several other proteins were found to resemble the Snf2 domain that lead to a separate grouping into the Snf2 family. The Snf2 family can be further divided into 24 subfamilies based on similarities within these Snf2-specific motifs, four of which are well characterized chromatin remodelers (Flaus et al., 2006). These are the SWI/SNF, ISWI, CHD and INO80 subfamilies. While all four utilize ATP hydrolysis to alter histone-DNA contacts and share a similar ATPase domain, they are all specialized for particular purposes, because of unique domains residing in their

catalytic ATPase subunits and by their unique associated (helper) subunits (Clapier & Cairns, 2009).

The SWI/SNF subfamily remodelers are composed of 8 to 14 subunits. Most eukaryotes have two related SWI/SNF family remodelers, the SWI/SNF and the RSC complexes, with two related catalytic subunits, the SNF2/SWI2 and the STH1 subunits, respectively. The catalytic ATPase subunit includes an HSA (helicase-SANT) domain, which binds unmodified histone tails, and a bromodomain, which recognizes acetylated lysine residues on histone N-terminal tails. This family has many activities, and it slides and ejects nucleosomes at many loci and for diverse processes such as DNA replication initiation (Flanagan & Peterson, 1999), transcriptional regulation (Cairns et al., 1996; Laurent et al., 1993; C. J. Wilson et al., 1996) and DNA repair (Chai, Huang, Cairns, & Laurent, 2005; J. Huang, Liang, Qiu, & Laurent, 2005; Klochendler-Yeivin, Picarsky, & Yaniv, 2006).

The ISWI (imitation switch) subfamily remodelers contain 2 to 4 subunits. Most eukaryotes contain multiple ISWI family complexes using one or two different catalytic subunits, namely the Isw1 and Isw2 in yeast, with specialized associated proteins. A characteristic set of domains reside at the C terminus of ISWI family of ATPases. A SANT domain adjacent to a SLIDE domain (SANT-like ISWI), which together form a nucleosome-recognition module that binds to an unmodified histone tail and DNA, is present in many of these remodelers (Boyer, Latek, & Peterson, 2004). The other subunits of the ISWI subfamily of remodelers contain DNA-binding histone fold motifs, bromodomains and plant homeodomains (PHD), which is a methyl-lysine interaction motif. Many ISWI family complexes, such as ACF and

CHRAC, optimize nucleosome spacing to promote chromatin assembly and repress transcription (Langst, Bonte, Corona, & Becker, 1999; Yang, Madrid, Sevastopoulos, & Narlikar, 2006).

The CHD (chromodomain, helicase, DNA binding) subfamily of remodelers, usually contain 1 to 10 subunits and were first purified from *Xenopus laevis*. These include Mi-2 and Chd1 in *S. cerevisiae*. Characteristic features of members of this subfamily include two tandemly arranged chromodomains on the N terminus of the catalytic subunit, which allow it to preferentially bind to methylated lysines on the histone terminal tails. The catalytic subunit of this subfamily remodelers is monomeric in lower eukaryotes but can be in large complexes in vertebrates. Associated proteins of these subfamily remodelers often bear DNA-binding domains as well as PHD and SANT domains. CHD1 promotes transcription elongation and the formation of regularly spaced nucleosomal arrays *in vitro*. The Mi-2/CHD complex can also deacetylate chromatin, repress transcription, and regulate development and promote nucleosome sliding *in vitro* (Bowen, Fujita, Kajita, & Wade, 2004; Lusser, Urwin, & Kadonaga, 2005).

The INO80 (inositol requiring 80) subfamily of remodelers contain more than 10 subunits and include the SWR1-related complexes that were initially purified from *Saccharomyces cerevisiae*. Orthologs of INO80 in higher eukaryotes also contain histone acetyl transferase (HAT) activity. The defining feature of the INO80 subfamily members is a 'split' ATPase domain, with a long insertion present in the middle of the ATPase domain. INO80 has diverse functions, including promoting transcriptional activation and DNA repair (Morrison et al., 2004). Although highly

related to INO80, SWR1 is unique in its ability to restructure the nucleosome by removing canonical H2A-H2B dimers and replacing them with H2A.Z-H2B dimers. Individual families are conserved from yeast to human, although there is some variation in their protein composition.

1.3 The DNA Damage Response (DDR)

The ability to deal effectively with spontaneous or environmentally-induced DNA damage is crucial for cellular survival and the maintenance of genomic stability, as inaccuracies in these processes can lead to chromosomal aberrations and cancer. Consequently, as part of the DDR, cells have evolved sophisticated surveillance mechanisms termed DNA damage checkpoints that monitor the successful completion of cell cycle events and initiate a coordinated cellular response when DNA damage is detected (Bartek & Lukas, 2007; Weinert & Hartwell, 1988). Activation of the DNA damage checkpoint results in cell cycle arrest, activation of transcriptional programs from genes like the ribonucleotide reductase (RNR) gene and thus initiation of DNA repair or, if the damage is too severe, cellular senescence or programmed cell death. These mechanisms act in concert to preserve genomic integrity and thus the fidelity of cell propagation. Once repair is completed, the DNA damage checkpoint response is down-regulated and cells re-enter the cell cycle in a process known as recovery. Alternatively, if the lesion is irreparable, cells may undergo adaptation and eventually re-enter the cell cycle in the continued presence of DNA damage (Clemenson & Marsolier-Kergoat, 2009).

The other essential aspect of the DDR is the repair of the damaged lesions. According to the type of damage, a specific repair pathway is employed. DNA lesions are mostly repaired by base excision repair (BER), in which the damaged base is first excised from the DNA by DNA glycosylases (such as Ung1, Mag1, Ogg1, Ntg1 and Ntg2) creating an abasic or apurinic/aprimidinic (AP) site (Figure 1.1.1). This AP site is recognized by AP endonucleases (Apn1 and Apn2), which nick the DNA backbone 5' to the damaged lesion, creating a 3'-substrate for DNA polymerase (Pol δ) to fill, and followed by DNA ligase (Cdc9) to seal the nick. Bulkier lesions that cause distortion of the DNA helix are repaired by nucleotide excision repair (NER), in which the lesion is recognized by Rad4-Rad23 and Rad14 repair factors, followed by excision of 24-27 nucleotide (nt) long oligo around the DNA lesion by the action of endonucleases, Rad2 and Rad1-Rad10 (Figure 1.1.1). The oligonucleotide is then removed by the action of TFIIH and Rad3 helicases, together with Mms19, and RPA. The lesion recognition step of NER is divided into two pathways: transcription coupled repair (TCR) and global genome repair (GGR). TCR refers to lesions encountered by RNA Pol II that cause it to stall, and thus repairs lesions on the template strand. TCR requires the additional function of either Rad26 or the Rpb9 subunit of RNA Polymerase II for damage detection. GGR can repair damage on template and non-template strands and involves the Rad16-Rad7 heterodimer. Global Mismatch repair (MMR) is used when replication errors or damaged lesions cause mispairing between bases. MUTS α and MUTS β complexes identify the mismatch, and together with MUTL α translocate along the DNA to the nearest nick site to differentiate the mismatched daughter strand from the parent

strand. They then recruit repair factors such as the exonuclease Exo1, DNA polymerase δ and ϵ , and DNA ligase Cdc9 to repair the lesion.

In case a damaged lesion is encountered by the DNA replication machinery, it can be bypassed by the post-replication repair (PRR) pathway. This pathway involves two sub-pathways, the error-prone translesion synthesis (TLS) and the error-free template switching (TS) (Figure 1.1.1). PRR primarily involves proteins of the Rad6 epistasis group, which mostly consists of ubiquitin conjugating enzymes (E2s) and ubiquitin ligases (E3s) (Prakash, Sung, & Prakash, 1993; Ulrich, 2002). The Rad6/Rad18 (E2/E3) proteins mono-ubiquitylate the proliferating nuclear cell antigen (PCNA), which is the sliding clamp that provides processivity to the replicative DNA polymerase (Hoegge, Pfander, Moldovan, Pyrowolakis, & Jentsch, 2002). This activates the TLS sub-pathway, and signals the recruitment of TLS polymerases from the Y family of DNA polymerases, such as Rev1 and pol η , and the B-family polymerase pol ζ , which can incorporate nucleotides, correctly or incorrectly, opposite the damaged one (Torres-Ramos, Prakash, & Prakash, 2002; Waters et al., 2009; Xiao, Chow, Broomfield, & Hanna, 2000; Xiao et al., 1999). Further ubiquitylation of PCNA by Ubc13-Mms2/Rad5 (E2/E3) proteins (Hoegge et al., 2002; Torres-Ramos et al., 2002), activates the error-free subpathway, TS, which involves the use of the newly replicated sister chromatid as a template to accurately copy past the lesion (Branzei, 2011). Both modes of PRR are considered DNA damage tolerance (DDT) pathways, which allows the replication machinery to bypass the damage, and the lesion to be repaired at a later time. This provides the

most prominent example of how ubiquitylation is involved in DNA repair, and will be discussed in greater detail in the following section.

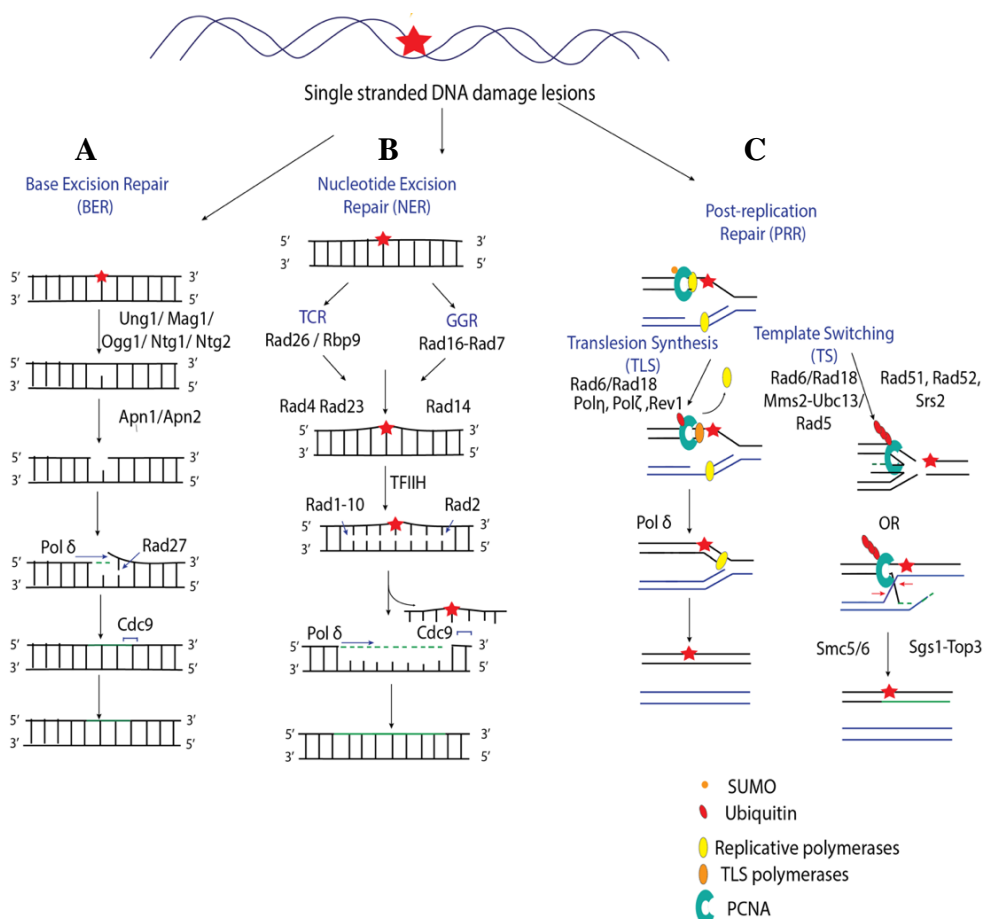


Figure 1.1: Repair of Single Strand DNA Damage

A. Base excision repair (BER), DNA N-glycosylases excise the damaged base creating an AP site. This is recognised by AP endonucleases, which nick the DNA backbone creating a 3'-substrate for DNA polymerase to fill, followed by DNA ligase to seal the nick. B. Nucleotide Excision Repair (NER), bulkier lesions that cause distortion of the DNA helix are recognised by Rad4-Rad23 and Rad14 repair factors, followed by excision of 24-27 long oligonucleotide around the DNA lesion by the action of endonucleases and helicases. NER is divided into two pathways: transcription coupled repair (TCR), which depends on Rad26 and Rbp9 and global genome repair (GGR), which depends on Rad7-Rad16. C. Post-replication repair (PRR), in case a damaged lesion is encountered by the DNA replication machinery, it can be bypassed by one of two sub-pathways, translesion synthesis (TLS) and template switching (TS). The Rad6/Rad18 proteins mono-ubiquitylate PCNA, activating the TLS sub-pathway, and signals the recruitment of TLS polymerases such as Rev1, Pol η , and Pol ζ . Further ubiquitylation of PCNA by Ubc13-Mms2/Rad5 activates TS, which involves the use of the newly replicated sister chromatid as a template to accurately copy past the lesion. TS involves proteins of the HR pathway.

DSBs, in which both strands of the DNA are broken, can be repaired by two main pathways (Figure 1.2). The first is simple re-ligation of the broken ends, through non-homologous end joining (NHEJ), which occurs throughout the cell cycle. NHEJ can be error-prone, as loss of nucleotides around the break can lead to mutagenesis. NHEJ depends on lesion recognition by MRX (Mre11-Rad50-Xrs2) complex and Yku70- Yku80 heterodimer. The Yku70-Yku80 complex binds the broken ends and mediate their ligation by the DNA Ligase IV complex (Dnl4-Lif1-Nej1) (T. E. Wilson, Grawunder, & Lieber, 1997). The second pathway to repair DSBs is homologous recombination (HR), which involves the use of the sister chromatid as a template to copy past the DSB. HR can only occur after DNA has replicated during the S phase, and thus after the sister chromatid becomes available. HR involves the concerted action of various DNA repair factors. The MRX complex first binds the free broken ends, and together with Sae2 removes aberrant DNA end structures, and resects 50-100 nts at the 5' end, forming a 3'-overhang (Krejci, Altmannova, Spirek, & Zhao, 2012). Further resection is achieved by the action of two nucleases, Exo1 exonuclease and Dna2 5'-flap endonuclease, which partners with Sgs1-Top3-Rmi3 helicase-topoisomerase complex. This creates long 3' ssDNA tails that become bound by the ssDNA binding protein RPA. RPA is then displaced by Rad51, forming a nucleoprotein filament that together with Rad52 protein, invade the sister chromatid forming a D-loop in search for homologous regions. Once found, Rad51 dissociates from the synaptic region, and DNA polymerases Pol δ or Pol ϵ extend at the 3' end of the invading strand. The second end of the DSB can be captured to form double Holliday junctions (dHJs), where their resolution could

result in crossovers or non-crossovers. Helicases such as Sgs1, Mph1, and Srs2 promote strand displacement through a subpathway called synthesis dependent strand annealing (SDSA), which is preferred during mitosis and results in non-crossovers. When the second end of the DSB is lost, break-induced replication (BIR) can occur where the D-loop turns into a replication fork copying the entire chromosome arm, as seen in alternative lengthening of critically short telomeres in telomerase-deficient cells. DSBs between repeats can be repaired by single strand annealing (SSA), where end resection reveals homologous regions on the same DNA strand, and through the action of Rad52 and Rad59, anneal to each other, resulting in the loss of the middle region. SSA and some types of BIR are Rad51-independent.

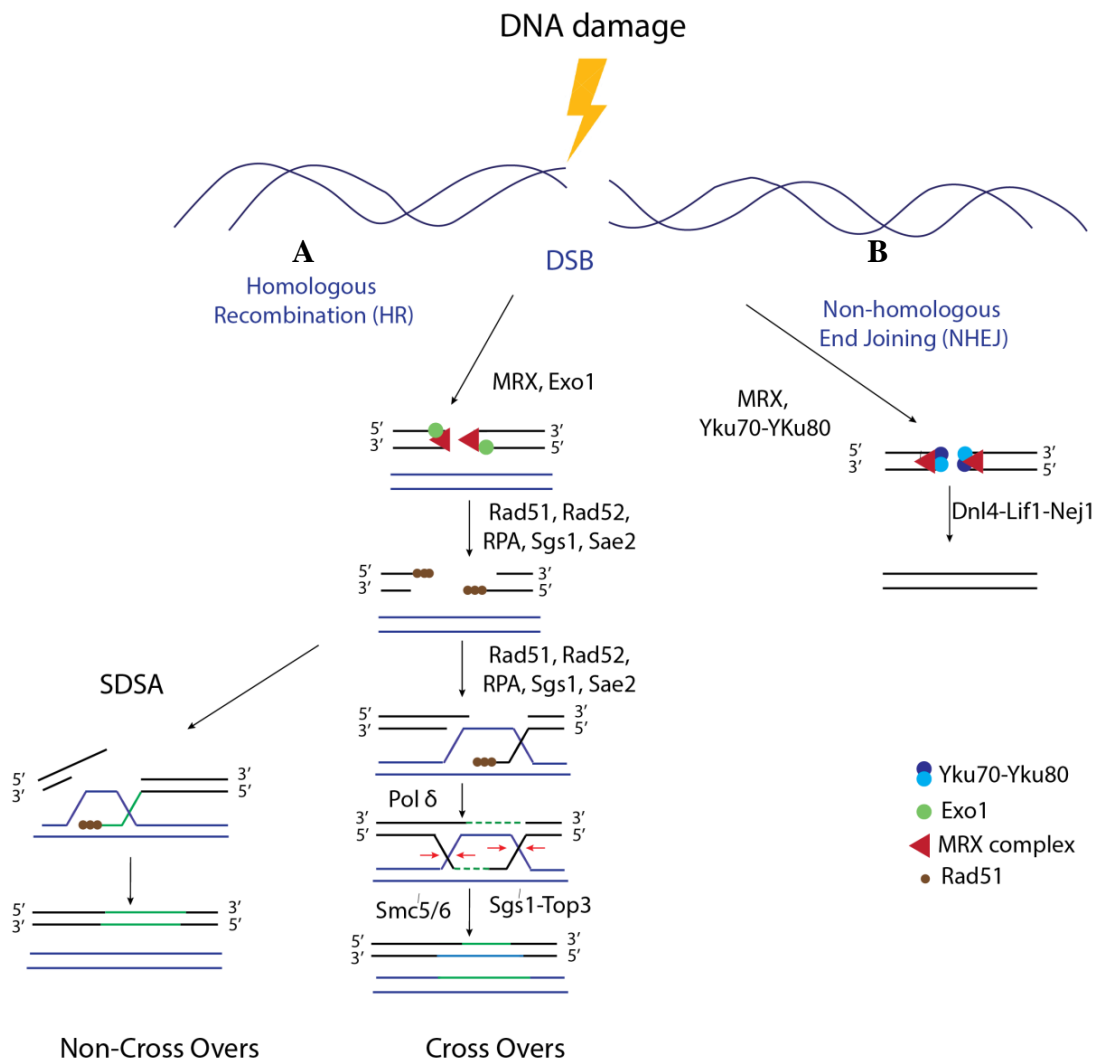


Figure 1.2: Double Strand Break Repair Pathways

A. DSB repair (DSBR), in case of DSBs simple re-ligation of the broken ends can occur through non-homologous end joining (NHEJ). This depends on lesion recognition by MRX (Mre11-Rad50-Xrs2) and Yku70-Yku80 complexes. Ligation is mediated by the DNA Ligase IV complex. B. The second pathway to repair DSBs is homologous recombination (HR), which involves the use of the sister chromatid as a template to copy past the DSB. MRX complex first binds the free broken ends, and together with Sae2, removes aberrant DNA end structures, and resects 50-100 nts forming a 3'-overhang. Further resection is achieved by the action of Exo1 and Dna2 along with Sgs1-Top3-Rmi3. This creates long 3'-ssDNA tails that become bound by RPA. RPA is then displaced by Rad51 forming a nucleoprotein filament, which together with Rad52 invade the sister chromatid forming a D-loop in search for homologous regions. Once found, Rad51 dissociates and DNA polymerases extend at the 3'-end of the invading strand. The second end of the DSB can be captured to form double Holliday junctions (dHJs), where their resolution could result in crossovers.

1.4 Ubiquitin and SUMO in DNA damage repair

Most of the basic mechanisms and factors involved in the DNA damage response are well understood; however, what remains a mystery is how these pathways are regulated, and the crosstalk that exists between them. One of these regulatory mechanisms is post-translational modifications on proteins involved in DNA damage response, namely ubiquitylation and SUMOylation. Hence, ubiquitin, SUMO and the enzymes involved in their conjugation and processing, are now regarded as critical players in maintaining genome stability [reviewed in (Jalal, Chalissery, & Hassan, 2017)]. This section focuses on the role that ubiquitin and SUMO play in the DDR.

1.4.1 The ubiquitylation process

The process of conjugating ubiquitin molecules onto a protein is ATP-dependent and involves several steps; first is ubiquitin activation by an activating enzyme (E1), followed by conjugating enzymes (E2) and ligases (E3) [(Kerscher, Felberbaum, & Hochstrasser, 2006) and Figure 1.3]. Successive conjugation of ubiquitin results in poly-ubiquitin chains, which can conjugate on any of the seven lysine residues (K6, K11, K27, K29, K33, K48, and K63) of the attached ubiquitin forming topologically distinct branched poly-ubiquitin chains (Peng et al., 2003; Xu et al., 2009). More than one ubiquitin can also be added to different sites on the substrate protein through the process of multi-ubiquitylation. These attached ubiquitin molecules act as an interaction surface for proteins having ubiquitin binding domains, such as ubiquitin-associated (UBA), ubiquitin-interacting motifs (UIM), and ubiquitin-binding zinc finger (UBZ) domains (Kirkin & Dikic, 2007).

The canonical K48 linked chains usually signal for protein degradation, while the non-canonical K63 linked chains usually provide regulatory and signalling roles. Other linkages are less common, and provide different roles depending on the substrate and interacting protein [reviewed in (Komander & Rape, 2012; Pickart, 2000)]. Hence, the type of poly-ubiquitin chain and its length makes binding to particular proteins harbouring specific binding domains highly specific. Ubiquitin modification not only mediates protein-protein interactions through ubiquitin binding domains, but may also act to prevent or loosen protein-protein interactions due to their bulkiness. Ubiquitylation is a highly reversible process, where deubiquitylating enzymes (DUBs) can cleave off the ubiquitin moiety when it is no longer needed.

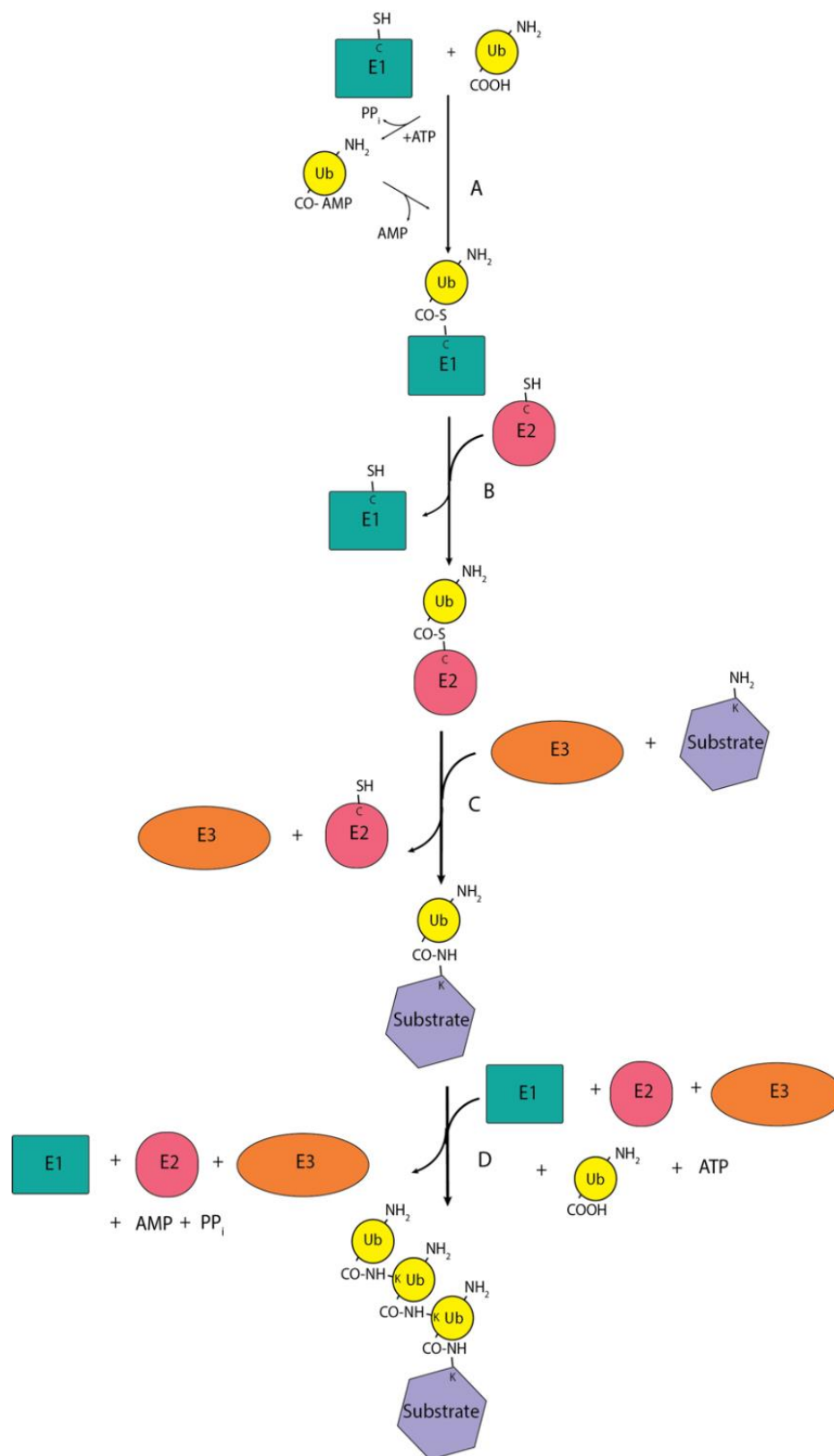


Figure 1.3: The Ubiquitylation Process

The ubiquitylation process involves three steps; A. E1 activating enzymes use the energy of ATP to form a ubiquitin-adenylyl intermediate followed by the conjugation of ubiquitin to a cysteine in E1 through thioester bond and the release of AMP. B. E2 ubiquitin conjugating enzymes that catalyze the transfer of ubiquitin from E1 to the active site cysteine of E2. C. Ligation of ubiquitin to the substrates through the activity of E3 ubiquitin ligases which catalyze the creation of an isopeptide bond between substrate protein and C-terminal glycine of ubiquitin. D. Multiple rounds of ubiquitin ligation creates poly-ubiquitylated substrates, which commonly target proteins for proteasomal degradation.

1.4.2 Proteins of the ubiquitin regulatory network

E1 Ubiquitin Activating Enzyme. There is only one E1 in *S. cerevisiae*, Uba1. This is an essential enzyme, responsible for forming a high energy thioester bond with the main-chain carboxyl group of the terminal glycine residue of ubiquitin. [(McGrath, Jentsch, & Varshavsky, 1991) and Figure 1.3A].

E2 Ubiquitin Conjugating Enzymes. There are 11 identified E2s in *S. cerevisiae* and are named Ubc1, Ubc2 (Rad6), Ubc3 (Cdc34), Ubc4, Ubc5, Ubc6, Ubc7, Ubc8, Ubc10, Ubc11 and Ubc13. These enzymes catalyze a transesterification reaction where ubiquitin is transferred from the E1 to the active site cysteine on the E2. E1s and E3s bind to the same site on E2, which ensures the dissociation of E1 before the binding to E3 and thus the unidirectional transfer of ubiquitin from the E1 to the substrate (Figure 1.3B). E2s together with E3s provide substrate specificity of ubiquitylation. Ubiquitin conjugating enzymes can also operate sequentially, causing the formation of poly-ubiquitin chains as seen with Ubc1 and Ubc4 together with the E3 anaphase promoting complex/cyclosome (APC/C). This process involves 2 steps; the first is mono-ubiquitylation catalyzed by Ubc4, followed by cycles of ubiquitin chain elongation catalyzed by Ubc1. The ubiquitin associated domain (UBA) of Ubc1 allows its interaction with mono-ubiquitylated substrates and is required for optimal processivity of this step.

E3 Ubiquitin Ligases. This class of enzymes catalyzes the transfer of the ubiquitin moiety to the substrate protein (Figure 1.3C). There are 60-100 putative E3s in *S. cerevisiae* based on sequence homology to the E3 domains, and they confer specificity to the ubiquitylation process. They are classified into two classes, RING (Really Interesting New Gene) domain E3s, and HECT (Homologous to the E6-AP Carboxyl Terminus) domain E3s (Scheffner, Nuber, & Huibregtse, 1995). The two classes differ in their mechanisms to catalyze ubiquitin ligation. HECT domain E3s contain a cysteine within the active site, which forms a thioester bond with ubiquitin received from an E2 before its transfer to the substrate. RING E3s, on the other hand, do not form thioester intermediates, and instead enable ubiquitin transfer by bringing the ubiquitin charged E2 in close proximity to the acceptor lysine of the substrate. Some ubiquitin ligases function only on mono-ubiquitylated substrates to extend the ubiquitin chain (Koegele et al., 1999), and are, thus, considered E4s and usually paired with an E3 forming an E3/E4 complex, as seen with Ubr1/Ufd4 (Hwang, Shemorry, Auerbach, & Varshavsky, 2010). Substrate recruitment – the key function of ubiquitin ligases – may be achieved through specific substrate binding domains in the E3, or through interaction with other subunits harbouring substrate receptors forming a multi-subunit complex. The most prominent multi-subunit E3 complex is the APC/C complex, which is composed of 13 subunits and is responsible for mitotic and meiotic cell cycle progression. Another important example of multi-subunit E3 complex is the cullin-RING ligases (CRLs), which is composed of 4 main subunits; cullin (1), on its N-terminal a substrate receptor protein (2) joined with a linker (3), and on its C-terminal, a small RING subunit Roc1 (also called Hrt1 or Rbx1) (4),

which interacts with E2 and catalyzes the transfer of ubiquitin from E2 to substrate (Petroski & Deshaies, 2005; Zimmerman, Schulman, & Zheng, 2010). Because of the enormous amount of ubiquitin ligases in yeast, they will not be specified in this thesis except in the context of DNA repair later.

Deubiquitylating Enzymes (DUBs). These enzymes catalyze the hydrolysis of the isopeptide bond that links ubiquitin to its substrate proteins (Reyes-Turcu, Ventii, & Wilkinson, 2009). There are 20 deubiquitylating enzymes in yeast, belonging to four families; Usp, Otu, JAMM, and Uch families (Finley, Ulrich, Sommer, & Kaiser, 2012). DUBs not only function to remove the ubiquitin signal from proteins when it is no longer needed, they also work to recycle ubiquitin before the target protein is degraded by the proteasome (Amerik, Li, & Hochstrasser, 2000; Amerik, Nowak, Swaminathan, & Hochstrasser, 2000). Defects in this leads to reduced levels of ubiquitin in the cell, a condition that causes several stress sensitivities (Chernova et al., 2003; Hanna, Leggett, & Finley, 2003). DUBs also play a very important role in the biosynthesis of ubiquitin. Ubiquitin is synthesized from four genes, Ubi1-4, as a fusion product. Ubi1-3 have ubiquitin moieties bound to ribosomal proteins (Finley, Bartel, & Varshavsky, 1989), while Ubi4 expression is induced upon DNA damage and consists of six tandem repeats of ubiquitin (Finley, Ozkaynak, & Varshavsky, 1987; Ozkaynak, Finley, & Varshavsky, 1984). All four ubiquitin gene products require deubiquitylating enzyme activity to release ubiquitin from the C-terminus.

Cdc48 ATPase Protein. Cdc48 is a chaperone protein of the AAA family of ATPases. Its exact mechanism of action remains to be revealed, however, it was

shown to play important roles in the ubiquitin regulatory system. Together with its cofactors, Ufd1 and Npl4, it was shown to work as a segregase, which disassembles protein complexes (Rape et al., 2001; Shcherbik & Haines, 2007; Verma, Oania, Fang, Smith, & Deshaies, 2011). Other studies have also shown Cdc48 to export poly-ubiquitylated proteins from the endoplasmic reticulum as part of the endoplasmic reticulum-associated degradation (ERAD) pathway (Jarosch et al., 2002; Rabinovich, Kerem, Frohlich, Diamant, & Bar-Nun, 2002; Ye, 2006).

The Ubiquitin-Proteasome. The 26S ubiquitin proteasome is found in all eukaryotes and is highly conserved between species. It is composed of two sub-assemblies; the 19S regulatory particle (RP) and the 20S core particle (CP) [reviewed in (Finley et al., 2012)]. This complex is responsible for degrading ubiquitin marked proteins, typically those that are poly-ubiquitylated using K48 linkage. The 19S RP contains ubiquitin receptor proteins that harbour ubiquitin binding domains, and recognize the poly-ubiquitin linked to the substrate (X. Wang & Terpstra, 2013). The 20S CP contains the proteolytic active sites sequestered within the interior space, ensuring that access to these sites is strictly controlled and nonspecific degradation is minimized (Finley et al., 2012). Substrates are directed from the RP to the CP through a narrow substrate translocation channel. Globular proteins must be unfolded by distinct hexameric ATPases in the RP, to traverse this channel. The high specificity of substrate recognition for targeting to the ubiquitin-proteasomal system provides a highly regulated pathway for protein degradation and recycling (Belle, Tanay, Bitincka, Shamir, & O'Shea, 2006).

1.4.3 The SUMOylation process

Although ubiquitin and SUMO only share 20% sequence identity, the conjugation of SUMO (Smt3 in *S. cerevisiae*) to proteins shows high resemblance to the ubiquitylation process [reviewed in (Hay, 2005; Muller, Hoege, Pyrowolakis, & Jentsch, 2001; Ulrich, 2009b)]. It also includes the action of E1-E2-E3 cascade of enzymes, and is conjugated to a large number of substrates. SUMOylation, however, is a simpler process. It involves an initial step of processing of Smt3 to expose a diglycine residue at the C-terminus, followed by activation by the E1 activating enzyme complex, Aos1-Uba2 (Johnson, Schwienhorst, Dohmen, & Blobel, 1997). This is followed by conjugation to the E2 conjugating enzyme, Ubc9, and finally ligation to a substrate protein by a few E3s ligases including Siz1, Siz2 (Johnson & Gupta, 2001), Mms21 (also called Nse2 part of Smc5/6 complex) and Cst9 (meiosis specific E3) (Lindroos et al., 2006). Ubc9 usually binds to substrates directly; however, E3s confer higher selectivity to the process. The final ligation step of SUMOylation involves the formation of an isopeptide bond between the C-terminal glycine of Smt3 and an internal lysine in the protein. Typically, SUMOylated sites are lysines within a consensus motif Ψ KXE, where Ψ represents a large hydrophobic amino acid and X represents any amino acid (Hay, 2013). Other SUMOylated lysine sites, however, have also been reported (Hoege et al., 2002; Zhou, Ryan, & Zhou, 2004). Similar to ubiquitin, SUMO can also be attached as a single moiety (mono-SUMOylation), as several moieties at multiple sites (multi-SUMOylation), or as a chain (poly-SUMOylation (Mullen & Brill, 2008)). Poly-SUMO chains are attached through one of the three lysines in the N-terminus of SUMO (K11, K15 and K19 in

Smt3). While SUMO is essential for yeast viability, polySUMOylation is not (Bylebyl, Belichenko, & Johnson, 2003). The SUMO signal is removed by SUMO proteases, Ulp1, Ulp2 and Wss1. Ulp1 is the major desumoylating enzyme and is localized to the nuclear pores (Elmore et al., 2011; Palancade et al., 2007; Panse, Kuster, Gerstberger, & Hurt, 2003). It is responsible for the maturation of Smt3 as well as deconjugating SUMO from SUMOylated substrates (Hickey, Wilson, & Hochstrasser, 2012). Its major role in the cell is shown by the inviability of *ulp1* null mutants. Ulp2 is present throughout the nucleus and specifically involved in desumoylating poly-SUMOylated substrates (Bylebyl et al., 2003; Li & Hochstrasser, 2000). The absence of Ulp2 in cells renders them viable but with growth defects. The conjugated SUMO moieties are recognized by two types of motifs; SUMO Interacting Motif (SIM), and Zn finger (ZZ) motif (Danielsen et al., 2012; Song, Durrin, Wilkinson, Krontiris, & Chen, 2004). The presence of tandem SIMs in a protein allows it to specifically bind poly-SUMOylated proteins (Tatham et al., 2008).

Unlike ubiquitylation, SUMOylation of target proteins does not serve as a signal for degradation. In fact, it has been shown to be involved in signalling in a large number of cellular processes such as nuclear transport, gene transcription, and DNA repair (Bermudez-Lopez et al., 2015; Bologna et al., 2015; Branzei, Vanoli, & Foiani, 2008; Danielsen et al., 2012; Hoege et al., 2002; Kolesar, Altmannova, Silva, Lisby, & Krejci, 2016). Large scale SUMOylation of DNA repair proteins of all repair pathways has been shown to occur upon DNA damage, in a manner analogous to, but independent of, the phosphorylation network by checkpoint kinases in the

DDR. This was termed DNA damage-induced SUMOylation (DDIS) (Bermudez-Lopez et al., 2015; Bologna et al., 2015; Branzei et al., 2008; Cremona et al., 2012; Danielsen et al., 2012; Hoege et al., 2002; Kolesar et al., 2016; Psakhye & Jentsch, 2012). The SUMOylation process is very intriguing in that it includes a very small number of conjugating enzymes, and that the modified substrates represent a small fraction of the total substrates, yet the signal is transduced effectively. This was best explained by highlighting the protein group modification nature of the SUMO-conjugating system, where the SUMOylation reaction does not target a specific substrate, but a group of proteins resulting in an additive or redundant effect (Psakhye & Jentsch, 2012). This protein group modification is mediated by a highly specific trigger (Psakhye & Jentsch, 2012). Interestingly, SUMO and ubiquitin modifications have been shown to occur on the same lysine residues leading to different signals, signifying the cross-talk between both pathways. This was also further shown by the identification of SUMO-targeted Ubiquitin Ligases (STUbLs), which are E3 ubiquitin ligases having SIMs, and thus target SUMOylated proteins for ubiquitylation (Sriramachandran & Dohmen, 2014). These enzymes also have the ability to conjugate ubiquitin at the growing end of SUMO chain, forming SUMO-ubiquitin hybrid chains, which may function to terminate the growing SUMO chain, or to target the protein for proteasomal degradation as seen with Slx5-Slx8 STUbLs (Mullen & Brill, 2008). The interplay between ubiquitylation and SUMOylation will be discussed further in the context of DNA repair in the following sections.

1.4.4 Ubiquitin and SUMO in DNA damage response

As discussed earlier, the cell genome is under continuous attack by DNA damaging agents which warrants for a complex DNA damage response. Proteins of the DNA damage response include DNA repair factors such as nucleases, helicases, scaffold proteins, as well as signalling factors. Interactions between repair factors need to be switched on and off in a rapid, reversible, and dynamic manner in response to DNA damage. The conjugation of ubiquitin or SUMO moieties to those proteins offers a dynamic way for their regulation. The coming sections, I will provide a detailed account of the role of ubiquitin and SUMO in the DNA damage response as currently known.

1.4.5 SUMO in Base Excision Repair (BER)

Many proteins of the BER pathway were found to be SUMOylated upon DNA damage, such as the N-glycosylases Ogg1, Ntg1, Ntg2 and Mag1, and the AP endonuclease Apn1 (Cremona et al., 2012; Griffiths et al., 2009). Ntg1 and Ntg2 have similar functions but show different cellular localization (Alseth et al., 1999; H. J. You et al., 1999). Under normal growth conditions as well as oxidative stress, Ntg1 localizes to both nucleus and mitochondria, while Ntg2 shows exclusive nuclear localization (Alseth et al., 1999; Griffiths et al., 2009; H. J. You et al., 1999). The SUMOylation of the nuclear fraction of Ntg1 was found to be increased five-folds upon both nuclear and mitochondrial oxidative stress (Griffiths et al., 2009). This SUMOylation was found to be important for the nuclear re-localization of Ntg1 upon oxidative DNA damage, and for full oxidative damage resistance. Whether re-localization of SUMO-Ntg1 is due to increased nuclear transport, increased nuclear

retention, or a combination of factors is still unclear. Nevertheless, SUMOylation of Ntg1 provides an example of how SUMOylation affects re-localization of a DNA repair protein, and is thus crucial for conferring cellular survival following oxidative stress.

1.4.6 Ubiquitin and SUMO in Nucleotide Excision Repair (NER)

NER is the primary repair pathway responsible for repair of bulky DNA lesions such as cyclobutane dimers resulting from UV-damage. Proteins involved in the NER pathway have been shown to be ubiquitylated and SUMOylated, which affects their repair activities. The repair proteins involved in NER are grouped into NEF1 complex, consisting of Rad1, Rad10 and Rad14, NEF2 complex, consisting of Rad4 and Rad23, and NEF4 complex, consisting of Rad7, Rad16, Elc1, and the cullin protein, Cul3. Rad23 possesses an Ubl domain which mediates its interaction with some components of the 19S RP of the proteasome (Schauber et al., 1998), an Uba domain that mediates its interaction with poly-ubiquitylated proteins, and a R4B domain for interaction with Rad4 (Ortolan, Chen, Tongaonkar, & Madura, 2004; Watkins, Sung, Prakash, & Prakash, 1993). Both the Ubl and R4B domains of Rad23 were shown to be important for NER repair (Bertolaet et al., 2001; Watkins et al., 1993). Contrary to initial belief, the binding of Rad23 to proteins, including Rad4, does not target it to the proteasome; instead, it actually stabilizes and prevents their proteolytic degradation (Raasi & Pickart, 2003). Stabilizing Rad4, however, is not the only contribution of Rad23 to NER (Ortolan et al., 2004). The 19S RP of the proteasome was shown to play a non-canonical role in regulation of NER mediated through interaction with Ubl domain of Rad23 (Russell, Reed, Huang, Friedberg, &

Johnston, 1999). This is possibly through coordinating the binding and disassembly of NER machinery at damaged sites.

The NEF4 complex was also shown to control Rad4 stability (Gillette et al., 2006; Ramsey et al., 2004). Rad16 is a Swi2/Snf2-related ATPase and an E3 ubiquitin ligase. Together with Rad7, Rad16 was shown to be important in repairing heterochromatic and non-template strand lesions through GGR (Bang, Verhage, Goosen, Brouwer, & van de Putte, 1992; Mueller & Smerdon, 1995; Terleth, Schenk, Poot, Brouwer, & van de Putte, 1990; Verhage et al., 1994). The ATPase activity of Rad16-Rad7 was suggested to provide translocase activity to scan for damage on the DNA (Guzder, Habraken, Sung, Prakash, & Prakash, 1995; Guzder, Sung, Prakash, & Prakash, 1998). The ubiquitin ligase activity of the NEF4 complex is believed to function in a redundant pathway with Rad23 to maintain Rad4 levels. The NEF4 complex was shown to ubiquitylate Rad4 upon UV damage and target it for proteasomal degradation (Gillette et al., 2006). The ubiquitylation of Rad4, but not the subsequent proteasomal degradation, activates *de novo* synthesis of Rad4 (Gillette et al., 2006). This ubiquitin mediated transcriptional activation of Rad4 expression, and possibly of other repair factors, provide the basis of a transcriptional pathway. Altogether, the ubiquitin-proteasome was shown to affect NER via two pathways. The first involves interaction between Rad23 and subunits of the 19S RP, which results in a non-canonical function of the proteasome, possibly coordinating the binding and disassembly of NER machinery at damaged sites. The second pathway involves the ubiquitylation of Rad4 by Rad7-Rad16 ECS complex and activates the *de novo* transcription of Rad4 (Reed & Gillette, 2007).

Ubiquitylation also plays a crucial role in the removal of stalled RNA Pol II at an encountered lesion to be repaired by TCR. The ubiquitylation of RNA Pol II requires the sequential addition of ubiquitin on the Rpb1 subunit, through the action of Rsp5 and Elc1 E3 ligases (Harreman et al., 2009). The Cdc48/Ufd1/Npl4 segregase complex, as well as the adaptor proteins Ubx4 and Ubx5, were shown to be important in proteasomal degradation of RNA Pol II during NER by assisting the proteasomal AAA-ATPases in the segregation and disassembly of the RNA Pol II subunits (Verma et al., 2011). Removal of RNA Pol II from the DNA allows repair by TCR or the subsequent recognition of the damaged lesion by GGR machinery Rad7-Rad16.

SUMO was also shown to play a role in NER, where $\Delta siz1\Delta siz2$ double mutants were shown to be sensitive to UV damage (Silver, Nissley, Reed, Hou, & Johnson, 2011). Genetic data suggest that Siz1 and Siz2 act in the Rad16- and Rpb9-sub-pathways of NER. Several NER proteins were found to be SUMOylated upon UV irradiation, such as Rad16, Rad7 and Rad4, as well as NER proteins which are also involved in other repair pathways, such as Rad1, Rad10, Rpb4, Rad3 and several others (Sarangi et al., 2014; Silver et al., 2011). SUMOylation of Rad1 was suggested to facilitate its dissociation from DNA post-cleavage, allowing it to handle the high amount of damaged lesions that occur at high doses of camptothecin and UV irradiation (Sarangi et al., 2014).

Complex DNA lesions such as DNA-protein crosslinks (DPCs) and protein-protein adducts can be produced enzymatically as an intermediate step in some DNA processes such as topoisomerase-DNA intermediate complexes, and non-

enzymatically by some kinds of DNA damaging agents such as formaldehyde (Stingele, Schwarz, Bloemeke, Wolf, & Jentsch, 2014). Small DPCs can be resolved and repaired by NER such as camptothecin-stalled Top1 DNA cleavage complexes which are resolved by tyrosyl-DNA phosphodiesterase I (Tdp1) (Pommier et al., 2006). In the absence of Tdp1 or in the case of larger DPCs, the SUMO system is involved. A dual acting SUMO-ligase protease, Wss1, has been recently implicated in resolution of DPCs (Iyer, Koonin, & Aravind, 2004). Under normal conditions and when first recruited to DNA damage, Wss1 catalyzes the formation of poly-SUMO chains and is thus considered a SUMO-ligase (Balakirev et al., 2015). Polymeric SUMO possibly leads to further recruitment of Wss1 at damaged sites and its oligomerization and activation of its SUMO-processing activities (Balakirev et al., 2015). At sites of damage, Wss1 was found to partner with Cdc48/Doa1 forming a ternary complex acting to disassemble proteins from the damaged sites and target them to the vacuole for processing (Balakirev et al., 2015; Stingele et al., 2014). This provides an additional involvement of SUMO-mediated processing of complex DNA structures and targeting them for vacuolar autophagy.

1.4.7 Ubiquitin and SUMO in Post-Replication Repair (PRR)

Perhaps the most studied role for the ubiquitylation and SUMOylation pathway is in regulating and resolving events involved in the PRR pathway and much of that role depends on the modification of PCNA. PCNA (Pol30) not only interacts with DNA polymerase as part of the replisome, but also interacts with proteins involved in downstream processing of the newly synthesized DNA such as nucleosome assembly and sister chromatid cohesion, and with DNA repair proteins

at stalled replication forks. These interactions are mediated through direct interaction with hydrophobic PCNA regions through PIP (PCNA-interacting protein) box or through interaction with PCNA after its modification with ubiquitin and SUMO. PCNA has 18 lysines that can be modified, however the most frequently ubiquitylated and SUMOylated site is K164 [(Tsutakawa et al., 2015) and Figure 1.4].

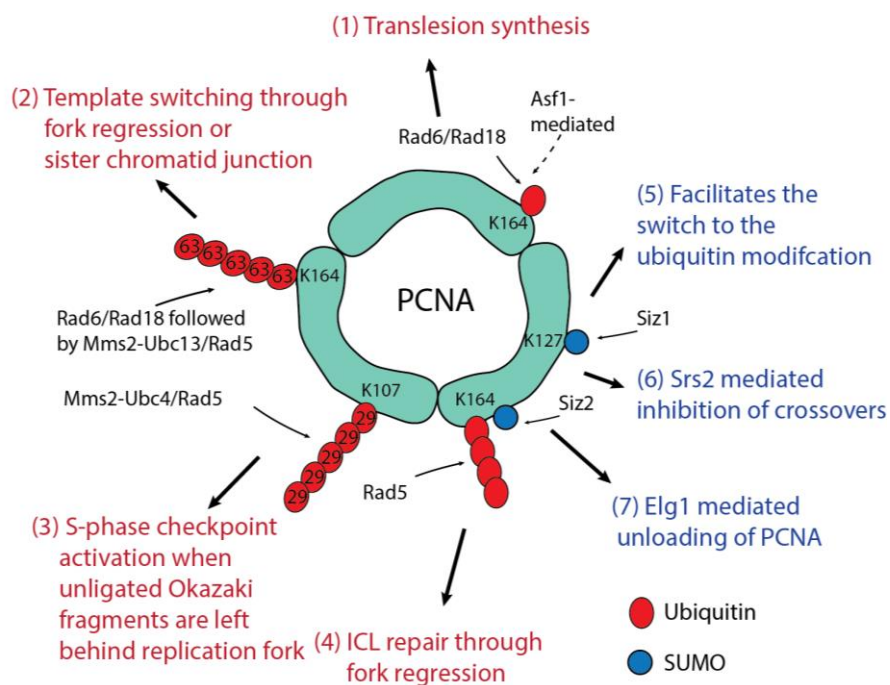


Figure 1.4: PCNA Modifications

(1) Ubiquitylation of K164 of PCNA is mediated by Rad6/Rad18 and to a minor extent Asf1 and unknown E2/E3 and leads to translesion synthesis, by recruiting TLS polymerases to damage site. (2) K63 linked Poly-ubiquitylation on K164 is mediated by Mms2-Ubc13/Rad5 and requires the prior mono-ubiquitylation by Rad6/Rad18. It results in template switching through either fork regression or SCJs. (3) K29 linked poly-ubiquitylation on K107 by Mms2-Ubc4/Rad5 results in response to accumulation of unligated Okazaki fragments left behind replication forks, results in activation of S-phase checkpoint. (4) Poly-ubiquitylation on K164 by Rad5 signals intrastrand crosslink repair through fork regression. (5) SUMOylation on K164 by Siz2 or K127 by Siz1 mediates interaction with Rad18 through Rad18 SIM, thus switching to the ubiquitin modification upon DNA damage. (6) SUMOylation of PCNA also serves to recruit Srs2, leading to inhibition of Pol δ/ϵ limiting D-loop extension and crossovers. (7) SUMOylation of PCNA also facilitates its interaction with Elg1 alternative clamp loader, to unload PCNA from DNA upon completion of DNA synthesis.

The proteins of the *RAD6* epistasis group coordinate PRR, and most of its members are ubiquitin conjugating and ligating enzymes. This group includes Rad6, Rad18, Rad5, Ubc13, Mms2, Pol30, Rev1, Rev3, Rev7 and Srs2. Although it was termed post-replication repair, the belief has been that it happens coupled to the replication fork. Several studies, however, have recently shown that PRR mostly occurs after bulk replication has occurred, in the late S/G2 phase (Karras & Jentsch, 2010). When a lesion is encountered by the replicative DNA polymerase, lesion bypass coupled to the replication fork can be attempted or the replication can restart downstream of the lesion leaving behind a ssDNA gap opposite the lesion, which can be bypassed behind the replication fork or after bulk replication occurs in the late S/G2 phase (gap-filling repair). Bypass of the lesion, whether during replication or post-replication, can occur by translesion synthesis (TLS), or by error-free template switching (TS) and HR. The choice and regulation of the pathways involved are currently being extensively studied, and is largely regulated by ubiquitylation and SUMOylation of several proteins.

TLS polymerases are each specialized in the type of lesion that they can accurately bypass. Pol η (Rad30) accurately bypasses UV-induced cyclobutane dimers (Cleaver, 1972), whereas Rev1 is a highly specialized polymerase that predominantly incorporates a C opposite any template nucleotide, making it accurately bypass lesions opposite of G in the template strand. Rev1 also has the ability to interact with Pol η , Pol ζ and some subunits of Pol δ (Acharya, Johnson, Prakash, & Prakash, 2006). Pol ζ consists of four subunits, Rev7, Pol31, Pol32, and the catalytic subunit Rev3 (Gomez-Llorente et al., 2013). Pol ζ is highly proficient in

extending mismatched terminal nucleotide pairs as well as nucleotides incorporated opposite damaged lesions by other polymerases, and generally has a higher fidelity in incorporating nucleotides opposite undamaged DNA (Acharya et al., 2006; Kochenova, Soshkina, Stepchenkova, Inge-Vechtomov, & Shcherbakova, 2011). While Pol η promotes error-free TLS across cyclobutane dimers, Pol ζ and Rev1 contribute to UV-induced mutagenesis (Prakash, Johnson, & Prakash, 2005). Whereas proficient replication past some lesions like UV-induced cyclobutane dimers and 8-oxo-guanines requires only one polymerase, other lesions require the action of two TLS polymerases, one to insert the nucleotide opposite the lesion, and another for subsequent extension (Prakash et al., 2005). How the recruitment of each is regulated is currently being studied, and largely depends on modifications on PCNA.

Rad18 is recruited to stalled replication forks through interaction with RPA coated ssDNA regions, and results in mono-ubiquitylation of PCNA on K164 [(Davies, Huttner, Daigaku, Chen, & Ulrich, 2008), Figure 1.4]. Ubiquitylation of PCNA on K164 can also occur at a minor level through an Asf1-mediated manner independent of Rad6-Rad18, involving yet-to-be identified E2 and E3 enzymes (Kats, Enserink, Martinez, & Kolodner, 2009). Mono-ubiquitylated PCNA leads to the recruitment of Pol η through its UBZ domain that binds to Ub-PCNA and Rad18, and bypasses UV-lesions accurately (Waters et al., 2009). Pol η was shown to be ubiquitylated during G1 phase leading to its proteasomal degradation, with a decrease in ubiquitylation during S phase and upon UV damage, thus becoming more available for TLS repair (McIntyre & Woodgate, 2015; Pabla, Rozario, & Siede,

2008; Parker, Bielen, Dikic, & Ulrich, 2007). Ub-PCNA can also result in error-prone TLS where it acts as an interaction domain for Rev1. Hence, ubiquitylation of PCNA acts as the switch that regulates the recruitment of different TLS polymerases to the DNA damage site.

Error-free lesion bypass, on the other hand, is triggered by the subsequent poly-ubiquitylation of mono-ubiquitylated PCNA on K164 by Ubc13-Mms2/Rad5 E2/E3 complex through the non-canonical K63 linkage [(Gazy & Kupiec, 2012; Torres-Ramos et al., 2002; Ulrich, 2009a), Figure 1.4]. How the undamaged nascent sister chromatid is used as a template for lesion bypass is still unknown. Several *in vitro* studies have proposed a fork-regression model in which a Rad5-dependent ‘chicken-foot structure’ is formed (Blastyak et al., 2007; Choi et al., 2015). Another model is recombinational template switching, in which the invasion of the nascent undamaged sister chromatid results in pseudo-Holliday junctions or sister chromatid junctions (SCJs). This model has been supported by the accumulation of X-shaped structures when their resolution is impaired (Branzei et al., 2008; Hoege et al., 2002). Smc5/6 is one of the structural maintenance of chromosomes (SMC) complexes which include cohesin (Smc1/3) and condensin (Smc2/4), that are responsible for sister chromatid cohesion and chromosome condensation, respectively (Bermudez-Lopez et al., 2010). Smc5/6 complex was shown to play a role in resolving DNA-mediated linkages and was proposed to be named ‘resolvin’ (Bermudez-Lopez et al., 2010). The Smc5/6 complex is composed of two SMC subunits, Smc5 and Smc6, as well as 6 non-SMC elements, Nse1 (an E3 ubiquitin ligase), Nse2 (Mms21), and Nse3-6 (Stephan, Kliszczak, & Morrison, 2011). Recombinational TS through SCJ

formation involves proteins of the homologous recombination pathway, such as Rad51 and Rad52. HR also operates as a salvage pathway for gap-filling, and is tightly regulated by SUMOylation of PCNA and the Srs2 helicase (Antony et al., 2009; Armstrong, Mohideen, & Lima, 2012; Friedl, Liefshitz, Steinlauf, & Kupiec, 2001; Hishida, Hirade, Haruta, Kubota, & Iwasaki, 2010).

The Rad5 activities responsible for either mode of error-free lesion bypass has been under intense study. Rad5 has two functional domains, an ATPase domain with SWI2/SNF2 family homology, and a RING finger E3 ubiquitin ligase domain (Choi et al., 2015). Although it was originally thought that the action of Rad5 in the PRR pathway is dependent on its interaction with Ubc13-Mms2, the sensitivity of *rad5* mutants to IR was much higher than *ubc13* and *mms2* mutants indicating a role for Rad5 unrelated to poly-ubiquitylation of PCNA (Friedl et al., 2001). The Rad5 helicase domain was found to be responsible for non-recombinational damage avoidance through fork regression and dispensable for recombinational TS that requires the E3 ligase activity of Rad5 (Choi et al., 2015). Rad5 also contributes to UV-induced mutagenesis through recruitment of TLS polymerases to damaged site (Kuang et al., 2013; Pages et al., 2008). The Rad5 ubiquitin ligase activity also functions in a pathway independent of Rad6, Rad18 or Ubc13, where it mono- and poly-ubiquitylates PCNA on K107 through the non-canonical K29 linkage, together with the E2 complex Ubc4-Mms2, in response to DNA ligase I *cdc9* mutations, which leave un-ligated Okazaki fragments in the lagging strand behind the replication fork [(Das-Bradoo et al., 2010), Figure 1.4]. This modification was shown to trigger S-phase checkpoint, and the subsequent fork progression was found to be

Rad59-dependent (Nguyen et al., 2013). Rad5 was also shown to play a role in the recently identified intra-strand crosslink (ICL) repair pathway reminiscent of the mammalian Fanconi-Anemia ICL repair pathway (Dae et al., 2012). Here, Rad5 was shown to poly-ubiquitylate PCNA on K164 when an ICL is encountered by the replication machinery independent on Rad6/Rad18 (Figure 1.4). This mediates the Mph1 helicase-mediated fork regression and repair of the lesion (Dae et al., 2012; Dae & Myung, 2012; Ward et al., 2012).

SUMOylation of PCNA provides the switch that regulates damage avoidance pathways. It occurs constitutively in the S-phase typically at K164 by the E3 SUMO ligase Siz1 (Pfander, Moldovan, Sacher, Hoegge, & Jentsch, 2005), and less efficiently at K127 by Siz2 (Parker et al., 2008), and thus competes with ubiquitylation on K164 (Figure 1.4). However, since PCNA is a homotrimer, it is possible that SUMO and ubiquitin can co-exist on the same PCNA molecule (Hoegge et al., 2002). SUMO-PCNA recruits the anti-recombinase helicase Srs2, which works to dismantle Rad51-nucleofilaments and thus keeps HR in check during DNA replication (Antony et al., 2009; Armstrong et al., 2012; Friedl et al., 2001; Hishida et al., 2010; Pfander et al., 2005). SUMO-PCNA is also a prerequisite for the Rad6/Rad18 pathway for PCNA ubiquitylation (Branzei et al., 2006; Branzei et al., 2008). Mms21 SUMO ligase, which is part of the Smc5/6 complex, was shown to be important in resolving Rad18-dependent SCJs, together with the helicase/nuclease complex Sgs1-Top3 (Branzei et al., 2008). Studies suggest that in a strain having functional SUMOylation activity, Rad18 is the predominant error-free damage avoidance pathway, and that Mms21-dependent SUMOylation contributes to

resolution of SCJs formed during template switching. Mms21 was shown to SUMOylate the Smc5 subunit, as well as play a minor contribution to the SUMOylation of Sgs1, amongst other yet-to-be revealed substrates (Branzei et al., 2008; Choi, Szakal, Chen, Branzei, & Zhao, 2010; Stephan et al., 2011). SUMOylation of PCNA was found to be increased in *cdc9-1* mutants which harbour un-ligated Okazaki fragments; however, it is unclear if this is due to increased retention of PCNA on DNA or due to increased SUMOylation *per se* (Das-Bradoo et al., 2010). SUMOylation on K164 also mediates the interaction of PCNA with the alternative clamp loader Elg1, leading to its unloading from DNA (Kubota, Nishimura, Kanemaki, & Donaldson, 2013; Parnas et al., 2010). SUMOylation on K127 of PCNA deters PCNA interactions with PIP box containing proteins, like Eco1 and Rfc1, as this modification occurs at the inter-domain-connecting loop of PCNA (Moldovan, Pfander, & Jentsch, 2006).

1.4.8 Ubiquitin and SUMO in Double Strand Break Repair (DSBR)

As discussed earlier, large-scale SUMOylation of DNA repair proteins occurs in response to DNA damage as part of the DDR (Cremona et al., 2012; Psakhye & Jentsch, 2012). This is evident where the repair proteins involved in DSB processing and subsequent repair are highly SUMOylated in response to damaging agents and SUMO-deficient strains exhibit high sensitivity to DSB inducing agents (Cremona et al., 2012; Psakhye & Jentsch, 2012). This involves proteins in both NHEJ and HR pathways of DSBR. The SUMOylation wave is catalyzed by Siz2 and is triggered in response to ssDNA exposure by Exo1 and Sgs1 nucleases at DSBs (Psakhye & Jentsch, 2012), similar to the phosphorylation wave (Chung & Zhao, 2015; Marechal

& Zou, 2015). The SUMOylation wave was shown to enhance interactions between the repair proteins through multiple SIMs that decorate them, acting primarily as a molecular glue at damage sites (Psakhye & Jentsch, 2012). Almost all HR proteins have been shown to be SUMOylated in response to DSB damage, including RPA subunits, Rfa1 and Rfa2, MRX complex subunits, Rad50 and Xrs2, Rad52, Rad59, Srs2, and Sae2.

One of the best studied SUMOylated HR protein is Rad52. Methyl methane sulphonate (MMS)-induced SUMOylation of Rad52 was found to primarily occur when cells are entering S-phase, but not when blocked in the G1 or G2 phase (Ohuchi et al., 2008). SUMOylation of Rad52 depends on the MRX complex (Psakhye & Jentsch, 2012; Sacher, Pfander, Hoegge, & Jentsch, 2006), and is stimulated by Rad52 binding to ssDNA (Altmannova et al., 2010). Rad52 SUMOylation facilitates its interaction with Rad51 C-terminal SIM (Bergink et al., 2013) and facilitates the loading of Rad51 onto ssDNA. SUMO-Rad52 results in both pro- and anti-recombinational effects. The pro-recombinational effects of SUMO-Rad52 are shown by the reduction of MMS-induced inter-chromosomal recombination to approximately half in nonSUMOylatable Rad52 mutants. On the other hand, SUMO-Rad52 helps prevent superfluous recombination where it facilitates the recruitment of Cdc48-Ufd1 segregase to dislodge improperly loaded Rad51-Rad52 from DNA, surpassing the need for the anti-recombinational activities of Srs2. SUMOylation of Rad52 re-localizes it out of the nucleolus, inhibiting recombination at the rDNA repeat-rich sequences (Torres-Rosell et al., 2007). SUMO-Rad52 was proven to be an *in vitro* substrate for the STubL complex Slx5-

Slx8, which poly-ubiquitylates SUMOylated substrates and target them for degradation (Xie et al., 2007). However, neither $\Delta slx5$ nor $\Delta slx8$ mutants displayed slower degradation or accumulation of SUMO-Rad52. In fact, *in vivo* results indicated less SUMOylated Rad52 and several other HR proteins in $\Delta slx8$ and $\Delta slx5$ cells upon MMS-induced DNA damage (Burgess, Rahman, Lisby, Rothstein, & Zhao, 2007). On the other hand, SUMOylated Rad52 was shown to be subject to Slx5-Slx8 mediated degradation at replication forks tethered to nuclear pores after fork collapse during replication of trinucleotide CAG repeats (Su, Dion, Gasser, & Freudenreich, 2015). To this end, SUMO-Rad52 promotes CAG stability (Su et al., 2015).

The Srs2 helicase is another protein that is SUMOylated. Srs2 has helicase and translocase activities and was shown to possess both anti- and pro-recombinational roles *in vivo*. The multiple roles of Srs2 in DNA repair entail proper regulation of its function. Srs2 possesses a SIM and PCNA interacting motif (PIM), which allows it to interact with SUMO-PCNA, and recruits it to stalled replication forks to dismantle Rad51-nucleofilament formation through its translocase activity, and thus inhibit unwarranted HR (Antony et al., 2009; Friedl et al., 2001). The pro-recombinational role of Srs2 depends on its helicase activity, where it promotes SDSA and involves branch migration and non-crossover products (Miura, Shibata, & Kusano, 2013), Rad51-dependent and -independent recombination (Hishida et al., 2010; Ira, Malkova, Liberi, Foiani, & Haber, 2003; Kolesar, Sarangi, Altmannova, Zhao, & Krejci, 2012). The SIM domain of Srs2 is also important for mediating the pro-recombinational role of Srs2, and thus depends on the PCNA-unbound pool of

Srs2 (Kolesar et al., 2012). Srs2 is SUMOylated in response to DNA damage and, most of it, is dependent on Ubc9 without the need for Siz1 or Siz2. The interaction between Srs2 and SUMO-charged Ubc9 is mediated by Srs2-SIM, thus SUMO-PCNA Srs2 interaction inhibits SUMOylation of Srs2 by outcompeting Ubc9 (Kolesar et al., 2012). The SUMOylation and SIM of Srs2 also mediates its interaction with other HR proteins, such as Rad51, Rad52, Mre11 and to a lesser extent Rad59 (Kolesar et al., 2016). These interactions are enhanced in *srs2 Δ PIM* strains, indicating that competition exists between PCNA and HR proteins in binding to Srs2 and regulating its recombinational role (Kolesar et al., 2016). SUMOylated Srs2 was also shown to increase recombination at rDNA regions (Kolesar et al., 2016). In summary, PIM and SIM of Srs2 seem to promote its anti-recombination activity by recruiting it to stalled replication forks by SUMO-PCNA to dismantle Rad51 filaments. Whereas, in the absence of SUMO-PCNA interaction, SUMO and SIM of Srs2 mediate its interaction with HR proteins to promote recombination. These results show how SUMOylation coordinates the pro- and anti-recombination activities of Srs2, and how it can modulate sometimes opposing functions of a protein. Collectively, the effects of SUMOylation of HR proteins indicate a role for SUMO in enhancing HR repair upon induction of DSB.

NHEJ proteins such as the Yku70, Yku80, and Lif1 (part of the DNA IV ligase complex Dnl4-Lif1-Nej1) were also shown to get SUMOylated upon DSB induced damage. Yku70 gets SUMOylated upon DNA damage induction through treatment with zeocin or other replication blocking agents and requires prior binding to DNA and interaction with Yku80 (Hang et al., 2014). SUMOylation of Yku70

stimulates NHEJ through increased DNA binding (Hang et al., 2014). SUMOylation of Yku70 also affects its role in telomere maintenance, and will be discussed further in the coming sections of the introduction. Another NHEJ protein whose SUMOylation was recently studied is the Lif1 protein. Lif1 was shown to be SUMOylated at a basal level, as well as induced upon DNA damage in a non cell-cycle dependent manner (Vigasova et al., 2013). Unlike Rad52, binding of Lif1 to ssDNA inhibits its SUMOylation (Vigasova et al., 2013). Lif1 SUMOylation decreases its ssDNA binding activity, as well as its self-association, however, it does not affect its interaction with downstream repair factors (Vigasova et al., 2013). This results in inhibition of NHEJ, particularly at persistent DSBs (Vigasova et al., 2013).

1.4.9 SUMO-targeted ubiquitin ligases (STUbLs) in DSB repair and perinuclear localization

The ubiquitin and SUMO pathways converge to regulate DSB repair as seen in the involvement of Slx5-Slx8 STUbLs in recombinational repair. Slx5-Slx8 is a heterodimeric complex, which consists of the Slx8 RING finger E3 ligase that interacts with Ubc4 E2 enzyme and catalyzes the conjugation of ubiquitin to substrates. Slx5 harbours multiple SIMs causing it to be specifically targeted to poly-SUMOylated substrates to mediate their ubiquitylation and subsequent degradation (Ii, Mullen, Slagle, & Brill, 2007; Uzunova et al., 2007; Xie et al., 2007). They were initially identified in screens for genes required for viability in *sgs1* null mutants, and displayed synthetic lethality (gene χ), highlighting their role in recombinational repair (Mullen, Kaliraman, Ibrahim, & Brill, 2001). This was further shown by an increase in gross chromosomal rearrangements (GCRs) in Δ *slx5* and

Δslx8 mutants, which includes loss of the chromosome arm followed by *de novo* telomere addition or nonreciprocal translocations with or without microhomology (Zhang, Roberts, Yang, Desai, & Brown, 2006). An increase in mutation rates was also observed in these mutants, as well as higher levels of Rad51-dependent and -independent recombination, suggesting spontaneous damage (Burgess et al., 2007; Zhang et al., 2006). This was further proven by increased repair foci as well as higher levels of Rad53 phosphorylation, indicative of checkpoint activation in *Δslx5* and *Δslx8* mutants (Burgess et al., 2007; Zhang et al., 2006). Slx5 and Slx8 also localize to replication forks as indicated with co-localization with PCNA, suggesting that the increased damage foci is due to replication defects resulting in increased incidence of damage as well as delayed DNA repair (Burgess et al., 2007). Slx8 also localizes to rDNA regions, with higher incidence of Rad52 nucleolar foci in *Δslx8* mutants, suggesting a role in inhibiting recombination in these repeat-rich regions which could lead to amplifications and contractions (Burgess et al., 2007). The involvement of the Slx5-Slx8 complex in SUMO pathway was highlighted by the clonal lethality exhibited by *Δslx5* and *Δslx8* cells in the presence of the endogenous 2- μ m plasmid, similar to that seen in SUMO pathway defective mutants (Chen, Reindle, & Johnson, 2005). This clonal lethality depended on proteins of the Rad51-independent recombinational repair and the levels of SUMOylation of these proteins was found to be decreased in *Δslx5* and *Δslx8* cells, indicating a role in regulating their SUMOylation. This is in contrast to the general hyperSUMOylation observed in *Δslx5*, *Δslx8*, and *Δsgs1* mutants (Mullen & Brill, 2008). Recently, the Slx5-Slx8 complex was shown to play a role in repressing spontaneous Sgs1 foci. This is in

addition to repressing the localization of Sgs1 foci upon hydroxyurea (HU)-induced replication stalling, while not affecting the general Sgs1 levels, thus possibly preventing Sgs1 localization at stalled replication forks inhibiting superfluous recombination (Bohm, Mihalevic, Casal, & Bernstein, 2015). These results suggest that Slx5-Slx8 functions to regulate homologous recombination during DNA replication, presumably through ubiquitylation and subsequent degradation of a SUMOylated factor that normally promotes HR, thus keeping unneeded HR in check.

A recently identified intriguing SUMO-related phenomenon is the re-localization of recalcitrant DSBs to the nuclear periphery, in a manner similar to telomere and rDNA nuclear membrane anchoring and the re-localization of actively transcribed genes to the nuclear pores (Oza, Jaspersen, Miele, Dekker, & Peterson, 2009; Schober, Ferreira, Kalck, Gehlen, & Gasser, 2009). Links between the SUMO pathway and nuclear organization have long been suggested by the localization of the Ulp1 protease and the STUbL complex Slx5-Slx8 at the nuclear pores. Ulp1 localization at nuclear pores is mediated through interaction with the inner pore basket proteins Mlp1 and Mlp2, and was shown to be crucial for nuclear transport and genome stability (Zhao, Wu, & Blobel, 2004). Slowly repaired DSBs are tethered to the inner nuclear envelope to inhibit ectopic recombination, thus preventing GCRs resulting from collapsed forks or unrepaired DSBs (Oza et al., 2009; Oza & Peterson, 2010). This involves the recruitment of components of the telomerase machinery like Cdc13, Est1, Est2, and Yku70/80 to DSBs to mediate the interaction with Mps3 envelope protein (Oza et al., 2009; Oza & Peterson, 2010).

Recruitment to nuclear periphery and interaction with telomerase machinery can, but not necessarily result in *de novo* telomere addition during cell adaptation with unrepaired DSBs. The relocalization to the nuclear periphery was suggested to involve the histone variant H2A.Z (Htz1), where it gets deposited around DSB sites early after DSB induction and subsequently SUMOylated. SUMO-H2A.Z, Rad51, and checkpoint activation are all important factors for the localization of DSBs to nuclear periphery (Kalocsay, Hiller, & Jentsch, 2009). However, since H2A.Z is important for the Mps3 envelope protein localization at the nuclear envelope, further studies need to be done on whether the defects in DSB relocation in *htz1* mutants is merely due to impaired nuclear envelope proteins assembly (Gardner et al., 2011). Some studies suggested a sequential shuttling of unrepaired DSBs from nuclear envelope to nuclear pores, similar to the re-localization of critically short telomeres in telomerase deficient cells to be repaired by an alternative recombinational pathway involving Slx5-Slx8 (Khadaroo et al., 2009; Su et al., 2015). This is reminiscent to the alternative lengthening of telomeres (ALT) pathway that occurs in PML bodies in human cells lacking telomerase, which involves proteins of the Rad51-independent recombination repair pathway (Khadaroo et al., 2009).

A recent study, however, clarified that the cell cycle stage and length of SUMO chain determine the subnuclear location for a persistent DSB. They showed that in the S/G2 phase, mono-SUMOylation, mediated by the Rtt107-stabilized Smc5/6-Mms21 SUMO E3 ligase complex, results in persistent DSB association with the Mps3 nuclear envelope protein and inhibition of recombinational repair (Horigome et al., 2016). In the G1 phase, however, DSBs are directed to the nuclear

pores by the Slx5-Slx8 complex following a polySUMOylation signal mediated by the sequential activities of Mms21 and Siz2 SUMO ligases (Horigome et al., 2016). Slx5-Slx8 ubiquitylates targets at the DSB site to mediate nuclear pore association which favours ectopic break-induced replication (BIR) and imprecise end joining (Horigome et al., 2016). Slx5-Slx8 mediated relocation to nuclear pores was, however, shown to not entirely depend on the ubiquitin ligase activity of Slx8, but rather on the interaction of Slx5 with poly-SUMO chains and the Nse5 subunit of the Smc5/6 complex as well as with the nuclear pore Nup84 complex (Horigome et al., 2016). Interestingly, the nucleoplasmic domain of Mps3 is required for the genome instability observed in $\Delta slx5$ strains (Oza et al., 2009), suggesting a lost balance in the regulation of recombination between nuclear pores and envelope. These data show the importance of SUMO and its chain length in perinuclear localization of DSBs.

Collapsed replication forks at trinucleotide repeats, on the other hand, were shown to interact only with nuclear pore proteins such as Nup84, but not Mps3 (Su et al., 2015). At these difficult to replicate regions, Slx5-Slx8 association with Nup84 serves to inhibit Rad52-dependent recombination, and thus prevent contractions and expansions resulting from recombinational repair at these regions (Su et al., 2015). This role was suggested to involve degradation of Rad52 in a SUMO-dependent manner (Su et al., 2015). Together these results indicate a role for SUMOylation for DNA damage adaptation and repair pathway choice. It also indicates a role for Slx5-Slx8 at nuclear pores to inhibit *de novo* telomere addition, and depending on the type and region of damage, either mediate Rad51-independent recombination, or inhibit

Rad52 recombinational events and thus maintain genome stability (Oza & Peterson, 2010; Su et al., 2015).

Another STUbL that was recently linked to DSB repair is Uls1. This protein belongs to the Swi2/Snf2 family of ATPases, and harbours a Snf2 helicase domain and a ubiquitin ligase RING finger domain. Uls1 also interacts with Ubc4 and possesses multiple SIMs similar to Slx5-Slx8, suggesting a possible role in ubiquitylation of SUMOylated substrates, although this biochemical activity has not yet been demonstrated. Originally identified to play a role in antagonizing silencing during mating type switching, evidence is accumulating for its role in the preservation of genomic integrity. Owing to its translocase activity, Uls1 was shown to remove Rad51 nucleofilaments and inhibit unneeded recombination, particularly in strains lacking Rdh54, which predominantly removes Rad51 depositions on dsDNA (Shah et al., 2010). Uls1 was also shown to be important for the S phase progression in the presence of DNA damage (Cal-Bakowska, Litwin, Bocer, Wysocki, & Dziadkowiec, 2011). Moreover, it displays genetic interaction with several proteins DNA repair factors, such as Rad52, Mus81, and Sgs1 (Cal-Bakowska et al., 2011). These genetic interactions suggest that Uls1 works upstream of Sgs1 in an ATPase-dependent manner (Cal-Bakowska et al., 2011; Kramarz et al., 2014). Physical and genetic evidence also suggest that Uls1 antagonizes Slx5 activity (Tan, Wang, & Prelich, 2013). Altogether, despite clear evidence that the STUbLs Slx5-Slx8 and Uls1 are involved in replication stress response, their molecular targets remain unknown.

1.4.10 The epigenetic role of Ubiquitin in DNA damage signalling and stress response

The Rad6 E2 enzyme was implicated in checkpoint signalling and Rad51-dependent recombination in a manner independent on Rad18 or PRR (Game & Chernikova, 2009; Game, Williamson, Spicakova, & Brown, 2006). This was evident by the higher X-ray sensitivities exhibited in *Δrad6* mutants compared to *Δrad18* mutants, which results in DSBs that are primarily repaired by HR. Rad6 is known to interact with other E3 ligases, such as Bre1 (which forms a complex with Lge1) and Ubr1. The Rad6/Bre1 complex, together with the Paf1 transcription-related complex, RNA Pol II and Bur1/Bur2 kinase complex, are responsible for ubiquitylating histone H2B at K123, a histone mark that is found at promoters and throughout genes during transcription (Game & Chernikova, 2009). A major function of ubiquitylation of H2B is to facilitate di- and tri- methylation of histone H3 at K4 and K79 by the methyltransferases Set1 and Dot1, respectively (Briggs et al., 2002; Ng, Xu, Zhang, & Struhl, 2002). Unlike the ubiquitin modification which was found to be transient, the H3-K4 and H3-K79 methylation is constitutively found in the cells and affects several cellular processes such as transcription regulation and gene silencing as well as a recently identified role in DNA damage checkpoint signalling and repair (Game & Chernikova, 2009; Giannattasio, Lazzaro, Plevani, & Muzi-Falconi, 2005). Unlike H3-K79 methylation mutants (*Δdot1*), mutants in H3-K4 methylation (*Δset1*) do not exhibit major irradiation sensitivities. The irradiation sensitivities of strains defective in H2B ubiquitylation at K123 (*Δrad6*, *Δbre1* and *Δlge1*), are epistatic to *Δdot1*, demonstrating this as the main function of the H2B modification in irradiation resistance (Game et al., 2006). Checkpoint activation was

found to be impaired in cells deficient in H2B-K123 ubiquitylation as well as H3-K79 methylation, particularly in the G1 and intra-S checkpoints (Giannattasio et al., 2005). The methylated H3-K79 is usually embedded within the nucleosome and becomes accessible when chromatin remodelling occurs around the DSB (Huertas, Sendra, & Munoz, 2009). This contributes to the concentration of Rad9 at damaged regions through interaction with the Rad9-Tudor domain, facilitating Rad9 phosphorylation by Mec1 kinase and downstream checkpoint activation (Giannattasio et al., 2005; Grenon et al., 2007). The ubiquitylation of histone H2B provides additional understanding into how ubiquitylation produces local changes in the chromatin structure impacting DNA damage signalling.

The importance of ubiquitylation and SUMOylation in replication fork progression during replicative stress is further highlighted by the sensitivities observed in *RTT107* mutant (Hang et al., 2015). Rtt107 is a scaffold protein that interacts with the cullin-ubiquitin ligase Rtt101-Mms22, the SUMO-ligase complex Smc5/6, and the endonuclease Slx4, forming mutually exclusive complexes. The Rtt101 complex is implicated in ubiquitylating acetylated histone H3 to facilitate nucleosome assembly during replication (Han, Zhang, Wang, Zhou, & Zhang, 2013). Rtt101 also acts directly at replication forks by counteracting the activity of Mrc1, the replicative and checkpoint protein which is part of the replisome progression complex (RPC), thus promoting HR at stalled replication forks (Buser et al., 2016). The Smc5/6 complex was found to be responsible for SUMOylating the Pole subunit Pol2, and Mcm2 (Hang et al., 2015). Both of these functions were found to be

important for replication fork progression in the presence of DNA-damaging agents (Hang et al., 2015).

1.4.11 Ubiquitin and SUMO in the maintenance of rDNA regions and telomeres

Repetitive DNA sequences are commonly found in the genome, particularly at rDNA regions in the nucleolus and at telomeres. Replication past rDNA regions is particularly challenging as repetitive sequences commonly form secondary structures which stall the replication fork and could lead to replication fork collapse (Su et al., 2015). Repair of damage at the rDNA regions requires special care to avoid expansions and contractions of the rDNA repeats, which commonly occurs during recombinational repair between repeats. Telomeres on the other hand require protection from being recognized as DSBs by the repair machinery, which could result in telomere fusions. Ubiquitylation and SUMOylation have been shown to play an important role in maintaining the integrity of these special DNA structures and are described below.

rDNA resides in a special nuclear sub-compartment called the nucleolus and is composed of 100-200 tandem repeats encoding the 35S and 5S ribosomal RNA in *S. cerevisiae*. The importance of SUMOylation in rDNA maintenance is highlighted by accumulation of fluorescently tagged Smt3 in the nucleolus when deconjugation is impaired (Takahashi & Strunnikov, 2008). In conditional triple mutant lacking the three E3 SUMO ligases, Siz1, Siz2, and Mms21, rDNA stability is severely impaired (Takahashi et al., 2008). Several SUMOylation targets responsible for the observed rDNA instability have been studied. Top1 and Top2 are examples of proteins that are

SUMOylated by Siz1 and Siz2, and contribute to rDNA stability by facilitating rDNA replication and transcription (Takahashi et al., 2008). Top2 SUMOylation deficient mutants exhibit a decrease in rDNA number as well as altered localization at the rDNA locus (Takahashi et al., 2008). Cohesin and condensin subunits (Smc1, 2, and 3) were identified as Mms21 SUMOylation substrates essential for rDNA maintenance and their binding to 5S rDNA region (Takahashi et al., 2008). Mms21 is also shown to SUMOylate the Smc5 subunit of the Smc5/6 complex in which Mms21 is part of. Smc5/6 complex was shown to be important for chromosome segregation at repetitive sequences. Cells having mutant *smc5* and *smc6* display accumulation of X-shaped structures at the rDNA region as well as hyper-recombination, in a Rad52-dependent manner (Torres-Rosell et al., 2005; Torres-Rosell et al., 2007). The Smc5/6 complex contributes to the exclusion of Rad52 foci from the nucleolus, thereby inhibiting recombination at these repetitive sequences which could result in repeat expansion or contraction (Torres-Rosell et al., 2007). Although SUMOylation of Rad52 also excludes Rad52 from the nucleolus, it does not depend on the Smc5/6 complex but instead depends on the Siz2 E3 ligase. Another contributor to the exclusion of Rad52 foci from nucleolus is the Slx5-Slx8 STUbL complex (Burgess et al., 2007). Interestingly, it was shown that a DSB induced in rDNA requires its transient exit to be repaired by the nuclear Rad52 pool (Torres-Rosell et al., 2007).

Other SUMOylated substrates that were recently identified are the nucleolus associated proteins Net1, Fob1, and Tof2 (Gillies et al., 2016). Net1 is part of the RENT complex that plays a role in silencing the rDNA region, inhibiting

recombination, and repressing RNA Polymerase II transcription. Fob1 acts to block the progression of replication fork and recruits subunits of the RENT complex and Tof2. Tof2 was shown to be SUMOylated in response to MMS damage. These proteins were found to be hyperSUMOylated in *Δulp2*, *Δslx5*, and *Δslx5Δulp2* cells with reduced binding to rDNA in *Δulp2* cells that is rescued in absence of Slx5 (Gillies et al., 2016). This suggests that the hyperSUMOylation that occurs when deconjugation is impaired, targets them for Slx5-Slx8-mediated ubiquitylation and possibly proteasomal degradation (Gillies et al., 2016). The accumulation of hyperSUMOylated species of Net1, Fob1, and Tof1 could be the more deleterious species that cannot bind rDNA resulting in hyper-recombination at these regions (Gillies et al., 2016). This partly explains the rDNA defects observed in *Δulp2* cells and the contribution SUMO plays in rDNA maintenance.

Telomeres represent another specialized DNA structure that requires dedicated machinery to protect and replicate. Telomeres are the ends of the linear DNA molecule that forms the chromosome. They very much resemble DSBs, thus have to be carefully distinguished from them to avoid recombinational or end-joining repair. They pose a particular challenge for replication by the replication machinery, and are thus subject to shortening and erosion with each cell cycle. This necessitates a special DNA polymerase that belongs to the family of reverse transcriptases to replicate it, called telomerase. The telomerase complex consists of several subunits, Est1, Est2 (catalytic subunit), Est3, and TLC1 (telomerase RNA) (Wellinger & Zakian, 2012). The telomeres consist of 75-150 repeats of C₁₋₃A/TG₁₋₃ with a terminal 3'-tail called the G-tail, followed by sub-telomeric regions called the X and

Y' regions, which also consist of repetitive sequences (Grandin & Charbonneau, 2008; Wellinger & Zakian, 2012). Special proteins bind to the telomeric DNA to make up the telomere. Cdc13 binds the ssDNA at the G-tails, and together with Stn1 and Ten1 form a complex resembling RPA. Rap1 protein binds the double-stranded TG repeat region and together with its interacting partners Rif1 and Rif2 inhibit the telomerase activator Tel1 (Grandin & Charbonneau, 2008; Wellinger & Zakian, 2012). Additionally, the Yku70-Yku80 complex binds DNA ends similar to its function at DSBs and protects the DNA ends from resection by nucleases, whereas the Sir2-Sir3-Sir4 complex functions to silence telomeric regions. The Yku70-Yku80 complex and the Sir2-Sir3-Sir4 complex also bind the telomeric ends and tether them to the inner nuclear membrane through interaction with the inner nuclear membrane protein Esc2. This anchoring, however, is dynamic and subject to regulation by post-translational modification like all other DNA based processes. HR provides an alternative way of lengthening short telomeres in telomerase-deficient cells.

Several lines of evidence show that SUMO plays a major role in maintaining telomere integrity and telomere anchoring. This is evident by the high SUMOylation status of several of the telomeric proteins, such as Yku70-Yku80, Sir4, and Esc2. While single mutants of each of the three E3 ligases Siz1, Siz2, and Mms21 exhibit longer telomeres (Hang, Liu, Cheung, Yang, & Zhao, 2011), only *Δsiz2* cells exhibit loss of telomere anchoring (Ferreira et al., 2011). The longer telomeres seen in *Δsiz2* mutants were shown to be due to telomerase mediated lengthening, not Rad52-dependent recombinational lengthening (Ferreira et al., 2011). Siz2 was also found to be the major E3 ligase SUMOylating Sir4 and Yku80, as well as contribute to

SUMOylation of Yku70. Together, this suggests Siz2-dependent SUMOylation of the Yku70-Yku80 complex, Sir-complex, and possibly other targets, promotes anchoring of telomeres to the nuclear envelope and inhibits telomerase mediated lengthening (Ferreira et al., 2011).

The Smc5/6 complex is also enriched at telomeres. As in HR, Smc5/6 was shown to resolve intermediates of HR mediated ALT, thus slowing senescence in telomerase-deficient cells (Chavez, George, Agrawal, & Johnson, 2010). This function depends on the SUMO ligase activity of Mms21. It was also shown to localize to sub-telomeric regions upon MMS damage, in a manner dependant on the Mms21 subunit (Pebernard, Schaffer, Campbell, Head, & Boddy, 2008). Highlighting the role of Smc5/6 complex in telomere maintenance is the defect in telomere clustering observed in *mms21-11* cells (Noel & Wellinger, 2011). Smc5/6 complex is also important for efficient replication at the repetitive telomeric region as observed in rDNA region and this contributes to the growth defects observed in the *smc5/6* mutants. It was suggested that the increased senescence observed in *smc5/6* mutants is due to telomere breaks resulting from inefficient replication and resolution of recombination intermediates at the telomeres as well as throughout the genome (Chavez et al., 2010; Noel & Wellinger, 2011). It is unclear, however, whether it is strictly the SUMO ligase activity of Smc5/6 complex or the structural maintenance activity of the complex that is required for its function at rDNA and telomeres. Either way, these results indicate that SUMO and Smc5/6 complex contribute to tethering telomeres to the nuclear envelope as well as resolving intermediates that arise during replication and recombination at the telomeres. In

addition to the role of SUMO in maintaining telomere anchoring, it also affects the stability and activity of the telomere-associated proteins. MMS treatment induces the SUMOylation of several of the telomere binding proteins, such as Rap1, Cdc13, Pif1, and Yku70-Yku80 (Hang et al., 2011).

Uls1 has also been implicated in maintaining telomere end-joining inhibition through its ubiquitin ligase activity. Moreover, Uls1 was shown to regulate the levels of poly-SUMOylated Rap1, a telomere binding protein that functions to inhibit NHEJ and protect the telomeric ends from nuclease activity as well as checkpoint signalling (Lescasse, Pobiega, Callebaut, & Marcand, 2013). SUMOylation of Rap1 results in a decreased NHEJ inhibition activity except through the pathway depending on Sir4 which remains functional (Lescasse et al., 2013). The translocase and E3 ligase activities of Uls1 mediate the proteasomal degradation of poly-SUMOylated Rap1 clearing the non-functional forms and allowing for the unmodified functional Rap1 molecules to bind and thus ensure permanent NHEJ inhibition (Lescasse et al., 2013). These findings suggest a role for Uls1 as a general molecular sweeper to dislodge poly-SUMOylated proteins through its translocase and ubiquitin ligase activities (Lescasse et al., 2013).

In contrast to SUMO activities in inhibiting recombination at telomeres, SUMOylation of Sgs1 has been shown to promote telomere-telomere recombination, and thus provides a means for ALT in telomerase-deficient cells. Sgs1 is SUMOylated by Siz1 and Siz2 SUMO ligases on K621, which lies between Top3 binding site and the helicase domain (Lu, Tsai, Brill, & Teng, 2010). Non-SUMOylatable *sgs1-K621R* mutants exhibited less telomere-telomere recombination

in telomerase-deficient cells particularly in formation of Type II recombinants, which show amplified telomeric repeats as opposed to Type I recombinants, which show amplified sub-telomeric Y'-repeats (Lu et al., 2010). On the other hand, the SUMOylation of Sgs1 was shown not to be important in recombinational repair, replication intermediates resolution, or rDNA recombination. The rescue of short telomeres in telomerase-deficient cells by recombination indicates their recognition as DSBs. This sensing requires the conventional DSB repair proteins, MRX complex and Tel1, for checkpoint activation. Resection and exposure of ssDNA recruits RPA and the rest of the repair and checkpoint machinery. This also requires the re-localization of telomeres to the nuclear pores, which are known to contain several of the SUMO pathway proteins, indicating a possible regulatory mechanism for SUMO in recombinational repair at telomeres (Khadaroo et al., 2009).

1.5 The yeast 2- μ m plasmid

The 2- μ m plasmid present in budding yeast is a selfish circular DNA element ubiquitously found in almost all *S. cerevisiae* strains (Strope et al., 2015). Unlike other extrachromosomal circular DNA (eccDNA) found in eukaryotic cells which readily accumulate in mother cells, the 2- μ m plasmid shows stability close to chromosome status. This high stability, with a loss rate of only about 10^{-4} - 10^{-5} per generation, is remarkable since the 2- μ m plasmid adds to the replicative burden without conferring any competitive advantage to the host cell (A B Futcher & Cox, 1983).

The 2- μ m plasmid is small in size (6.3 kb) and is generally present at high copy number (40-60 copies) per haploid cell. Its small sequence, highly optimized for self-serving ends, contains four protein coding sequences (*FLP1*, *REP1*, *REP2*, and *RAF1*) and four *cis*-acting DNA elements (two Flp Recombination Target *FRT* inverted repeats, an origin of replication, and the stability *STB* partitioning locus) [(Yen Ting et al., 2014) and Figure 1.5]. Together with some of the host's cellular machinery, these sequences are divided into three functional units to ensure: (i) the duplication of the 2- μ m plasmid sequence using its origin of replication, (ii) the faithful partitioning of the 2- μ m plasmid molecules into the mother and daughter cells without bias through the action of Rep1, Rep2, and the *STB* locus, and (iii) the maintenance of high copy number in the individual cells, in case of a drop in the 2- μ m plasmid copy number, through site specific recombination at the *FRT* repeats by the Flp1 recombinase. The amplification of the 2- μ m plasmid is tightly regulated and inter-connected to ensure stable maintenance without runaway increase in copy number, through the regulated expression of Flp1 (Figure 1.5). Rep1-Rep2 form a transcription repression complex regulating the expression of Flp1 within a 100-fold range as well as the expression of Rep1 and Raf1 (Murray, Scarpa, Rossi, & Cesareni, 1987; Som, Armstrong, Volkert, & Broach, 1988). Raf1 antagonizes the repression of Rep1-Rep2, thereby acting to positively regulate the amplification system and thus fine-tuning the amplification signal for rapid response to a decreased copy number (Murray et al., 1987). 2- μ m derived plasmids have been utilized in molecular biology as high copy expression vectors owing to their high copy number and stability in host cells. The FLP-FRT system has also been utilized as a

recombination-based *in vivo* DNA editing tool, similar to the Cre-Lox system (Luo & Kausch, 2002; Schweizer, 2003; Stricklett, Nelson, & Kohan, 1999; Theodosiou & Xu, 1998; Weasner, Zhu, & Kumar, 2017).

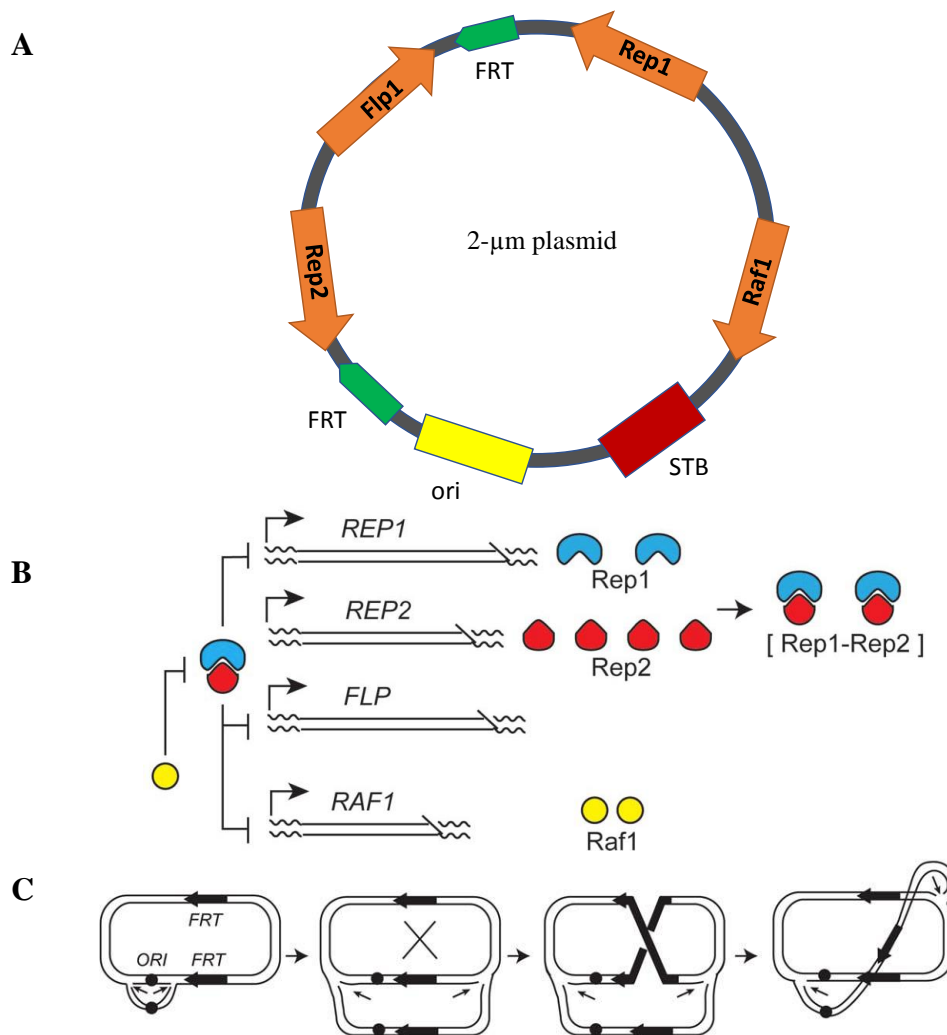


Figure 1.5: The 2- μ m plasmid and its regulatory units

A. Diagram of 2- μ m plasmid and its functional sequences. Ori is the origin of replication. Rep1, Rep2 and the *STB* locus constitute the partitioning system. Flp1 with its recognition sites (FRTs) constitute the copy number amplification system. **B.** Rep2 is constitutively expressed, and together with Rep1 forms a transcriptional repressor complex which represses the transcription of Rep1, Flp1, and Raf1. [Adapted from Sau 2015 (Sau, Liu, Ma, & Jayaram, 2015)]. **C.** Flp1-induced cut early during replication causes the shift from theta mode to double rolling circle. This results in spooling out a long concatemer of several plasmids connected end to end. These are then resolved into plasmid monomers by Flp1 or homologous recombination [Adapted from Yen Ting 2015 (Yen Ting et al., 2014)].

The partitioning system of the 2- μ m plasmid is comprised of two coding sequences (*REP1* and *REP2*) and a *cis*-acting DNA element *STB* (*REP3*) locus. The Rep1 and Rep2 proteins form a complex at the *STB* locus and together with other host-encoded factors, help in segregating the replicated plasmid into the mother and daughter cells. Like yeast centromeres (*CENs*), the *STB* locus recruits sophisticated factors to aid in the partitioning. The chromatin remodeling complex RSC2 (Wong, Scott-Drew, Hayes, Howard, & Murray, 2002), the nuclear motor Kip1 (Cui, Ghosh, & Jayaram, 2009), the histone H3 variant Cse4 (C. C. Huang, Chang, Cui, & Jayaram, 2011; C. C. Huang, Hajra, Ghosh, & Jayaram, 2011), the cohesin complex (Ghosh, Hajra, & Jayaram, 2007; Mehta et al., 2002), and the microtubules (Prajapati, Rizvi, Rathore, & Ghosh, 2017) are among the factors common between *STB* and *CEN* loci, even though the levels are largely sub-stoichiometric. Studies on the kinetics of partitioning have shown the temporal recruitment of these factors to ensure the proper segregation of 2- μ m plasmids to daughter cells (Ma et al., 2013). The RSC2 complex is amongst the first recruited, and was shown to play a role in retaining Rep1 and Rep2 at the *STB* locus. Following this, one to two Cse4 containing nucleosomes are deposited at the *STB* locus allowing the chromatin to be favorable for proper Rep1-Rep2 complex retention at *STB*. The Kip1 nuclear motor followed by cohesin then culminate the partitioning complex. The acquisition of the host factors required for partitioning was shown to depend on the nuclear location of the 2- μ m plasmid. Rep1 and Rep2 were shown to form specific nuclear foci co-localizing with Ulp1 (Dobson et al., 2005). This sub-nuclear localization requires the microtubule associated proteins Bim1 and Bik1 (Prajapati et al., 2017). This system

requires coupling with replication to ensure perfect partitioning between mother and daughter cells.

Despite the similarities in factor recruitment between *STB* and *CEN*, there is no evidence for direct spindle assembly, or kinetochore complex formation at the *STB*. Additionally, the insertion of two or more *STB* loci on the 2- μ m plasmid does not lead to instabilities as observed with *CEN* sequences. The current accepted model is of hitchhiking as a mode of coupling plasmid segregation to chromosome segregation (Liu, Chang, Ma, & Jayaram, 2016; Liu, Ma, & Jayaram, 2013). The exact molecular details of this mechanism are still unknown, but it is thought to involve coupling plasmid sisters with chromosome sisters by the cohesin complex to ensure equal segregation between mother and daughter cells. Papilloma and gamma herpes virus episomes use a similar chromosome tethering mechanism to persist in latently infected cells (Botchan, 2004; J. You, Croyle, Nishimura, Ozato, & Howley, 2004).

In rare mis-segregation events of plasmid molecules, the drop in copy number is corrected by the Flp1 recombinase. The lower than normal copy number makes the levels of Rep1-Rep2 repressor drop below the threshold required to repress Flp1 expression, thus prompting the recombination-induced copy number amplification. The accepted model for copy number amplification, the Futcher model, depends on the Flp-FRT system and the asymmetric placement of the *ori* in respect to FRT inverted repeats. At one point of time early during replication, one of the FRT repeats would have replicated while the other would have not, causing three FRTs to

exist within the same molecule (Figure 1.5). Flp-induced recombination between one of the replicated FRTs and the unreplicated one reverses the orientation of the replication forks. This converts the bi-directional replication forks into a mono-directional rolling circle replication (A. B. Futcher, 1986; Volkert & Broach, 1986), thus generating multiple copies of the plasmid connected end to end as concatemers. The tandem array of 2- μ m produced are resolved by a Flp- or a HR-induced recombination reaction.

The SUMO and ubiquitin pathways have been shown to participate in the regulation of the 2- μ m plasmid to maintain it at the normal innocuous levels. Perturbations in any of these pathways cause 2- μ m related cell toxicities. The first implication of the SUMO pathway in 2- μ m plasmid regulation was the identification of a mutation that led to nibbled colony morphology in cells that harbor the 2- μ m plasmid (Holm, 1982). This morphology, referred to as clonal lethality, is due to the formation of a subpopulation of abnormally large cells with higher than normal copy number of the 2- μ m plasmid (Holm, 1982). This mutation was identified to be in *ulp1* deSUMOylating enzyme (Dobson et al., 2005). The loss of Mlp1-dependent nuclear pore anchoring of Ulp1 causes the same effect, showing that the Ulp1 nuclear localization and not just its activity is needed to prevent the abnormal increase in copy number (Zhao et al., 2004). Mutations in the SUMO-conjugating enzyme Ubc9 (Burgess et al., 2007) and the SUMO-ligases Siz1 and Siz2 also cause 2- μ m -dependent cell toxicities associated with high copy numbers (Chen et al., 2005). Rep1, Rep2, and Flp1 have all been shown to be SUMOylated (Chen et al., 2005; Pinder, McQuaid, & Dobson, 2013), suggesting that SUMO may participate in

2- μ m plasmid copy number regulation by directly targeting plasmid-encoded proteins.

Rep1 is SUMOylated at 3 sites, whereas Rep2 is SUMOylated at around 13 lysine residues (Pinder et al., 2013). Loss of SUMOylation of either Rep1 or Rep2 results in the loss of their association at *STB* partitioning locus, without affecting their interaction together or their stability (Pinder et al., 2013). The SUMOylation of Flp1 seems to regulate Flp-mediated recombination similar to the regulatory role of SUMO on HR repair. Loss of Flp1 SUMOylation leads to an abnormal increase in its activity, leading to the formation of toxic recombination species, in a manner dependent on HR factors (Xiong, Chen, Silver, Ahmed, & Johnson, 2009).

The involvement of the ubiquitin pathway is shown by the increased copy number in mutants of the ubiquitin conjugating enzyme Ubc4 (Sleep, Finnis, Turner, & Evans, 2001) as well as the clonal lethality observed in null mutants of the STUbL complex Slx5-Slx8 (Burgess et al., 2007). The abnormal increase in 2- μ m copy number in Slx5-Slx8 mutants is dependent on HR factors, and is associated with a general reduction in their SUMOylation (Burgess et al., 2007). Together these suggest the general inhibitory role that the SUMO modification plays in recombination underlies its role in modulating 2- μ m plasmid copy number.

1.6 The Irc20 protein

Irc20 has sequence homology to the SWI2/SNF2 ATPase domain and is a product of the gene locus YLR247C. It is classified in the SHPRH subfamily of the Snf2 family of helicases, and shares sequence homology to the mammalian proteins

SHPRH (Snf2 Histone-linker PHD RING Helicase) and HLTF (Helicase like transcription factor). SHPRH contains in addition to its Snf2 ATPase domain and RING-type E3 ubiquitin ligase domain, a plant homeodomain (PHD), which normally recognizes methylated histones, and a linker histone H1/H5 globular domain (H15 domain). HLTF contains HIP116 Rad5p N-terminal (HIRAN) domain that is predicted to function as a DNA-binding domain that recognizes features associated with damaged DNA or stalled replication forks (Figure 1.6).

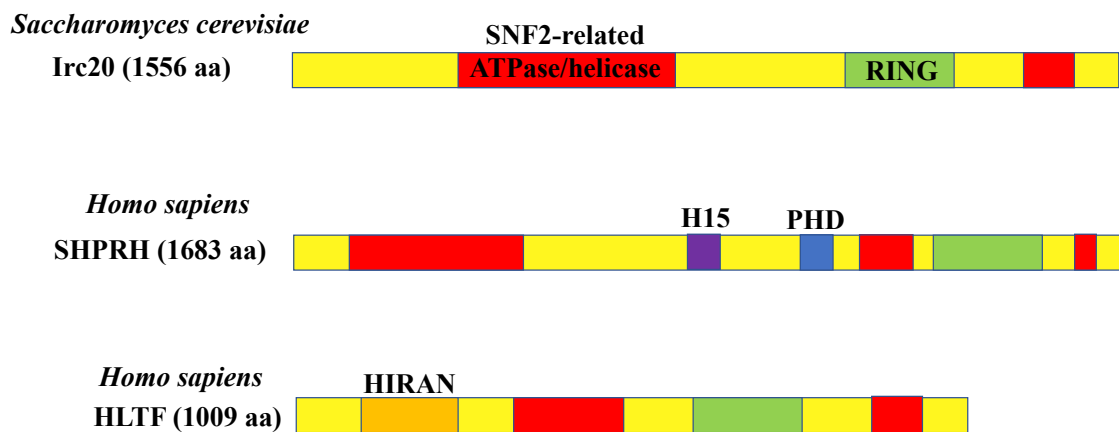


Figure 1.6: Irc20 and its human homologs

Irc20 and its closest human homologs, SHPRH and HLTF, are shown. They share a SNF2-related ATPase/helicase domain (shown in red as a split domain), and a RING finger domain (green) characteristic for ubiquitin ligase enzymes. SHPRH also possesses other domains such as H15 (purple), and PHD domains (blue). HLTF possesses a HIRAN domain (orange) in addition to the Snf2-ATPase domain, and the RING finger domain.

1.6.1 The human homologs of Irc20 and their role as tumor suppressor genes

In humans, the proteins most similar to Irc20 are SHPRH and HLTF, two RING finger-containing ATPases which play important roles in transcription regulation (Dhont, Mascaux, & Belayew, 2016; Ding et al., 1996), Wnt signaling

(Qu et al., 2016; Qu, Kalland, & Ke, 2017), and rRNA transcription (Lee et al., 2017). Silencing of the HLTF gene expression (Dhont et al., 2016; Hibi, Kodera, Ito, Akiyama, & Nakao, 2005; Hibi et al., 2003; Moinova et al., 2002) and point mutations of the SHPRH gene (Sood et al., 2003) have been observed in human ovarian and colorectal cancer cells. As homologs of the yeast Rad5, they participate in maintaining genomic stability at stalled replication forks, via the poly-ubiquitylation of PCNA thus allowing for template switching (Motegi et al., 2008). In mammalian cells, the error-prone TLS pathway regulated by PCNA ubiquitylation allows for somatic hypermutations and immunoglobulin diversification, which are important for proper immune response (Tomi et al., 2014).

Besides the function of HLTF and SHPRH in template switching, they also employ distinct mechanisms to control the recruitment of an appropriate polymerase for TLS. Using an elegant experimental design, Lin *et al.* (2011) found that HLTF and SHPRH contribute in differential ways to specify DNA damage induced mutagenesis (Lin, Zeman, Chen, Yee, & Cimprich, 2011). HLTF was shown to be required for correct bypass of UV lesions, while SHPRH was required for MMS-induced lesions. They recognized that this pattern corresponded to the differential participation of TLS polymerases η and κ in DNA damage tolerance. Specifically, polymerase η can accurately insert the correct base pairs across UV lesions, while polymerase κ can bypass alkylated bases (i.e., the kinds of lesions typically induced by MMS) ten-folds more accurately than other polymerases. Their findings indicate that, following UV, HLTF enhances PCNA mono-ubiquitylation and recruitment of translesion synthesis polymerase η , while also inhibiting SHPRH function. In

contrast, MMS promotes the degradation of HLTF and the interactions of SHPRH with Rad18 and polymerase κ , together with poly-ubiquitylation of PCNA. The ubiquitylation of Rad18 plays an additional role for the regulation of this pathway. Ubiquitylated Rad18 interacts with an unmodified Rad18, inhibiting its interaction with SHPRH or HLTF. Upon MMS or UV damage, deubiquitylation of Rad18 occurs, allowing for its interaction with SHPRH and HLTF, the ubiquitylation of PCNA, and subsequent DNA repair events (Zeman, Lin, Freire, & Cimprich, 2014).

1.6.2 The role of Irc20 in DNA repair

Global analysis of gene expression of novel helicase genes, showed YLR247C gene upregulation upon heat shock and UV irradiation, suggesting a role in DNA repair (Shiratori et al., 1999). Moreover, the loss of Irc20 results in increased spontaneous Rad52 foci in diploid cells and hence the name Increased Recombination Centers 20 (Alvaro, Lisby, & Rothstein, 2007). Rad52 foci are formed on a 3'-single-strand tails generated by resection, to mediate D-loop formation by Rad51 and copying from the undamaged sister chromatid. This suggests a defect in DNA repair that makes DSB more persistent and visible or a preference to longer-range resection in absence of Irc20. The closest Irc20 budding yeast homolog is Rad5, which is the ubiquitin ligase responsible for poly-ubiquitylation of PCNA as part of template switch signaling of post replicative repair.

Recently, using novel yeast genetic assays, Miura *et al.* (2012) showed that Irc20 helps in guiding DSB repair into a more error-free mode (Miura et al., 2012).

They showed that Irc20 plays a role in both NHEJ and HR and helps in both maintaining precise end joining during NHEJ, and in directing HR into SDSA, thus maintaining proper repair of the DSB. This was, however, not visible as a growth phenotype, as knockouts of Irc20 ($\Delta irc20$) did not show increased sensitivity to DNA damaging agents such as bleomycin, MMS, HU, or camptothecin. Interestingly though, Irc20 was shown to possess a negative genetic interaction with Mre11, the exonuclease which works as part of the MRX complex to process DSB ends shortly after they occur. The authors suggested that since $\Delta irc20$ suppresses the $\Delta mre11$ growth defect phenotype, Irc20 may work to direct DSB end processing by Mre11 and its absence allows other exonucleases to process the DSB ends to repair the break (Miura et al., 2012). They assigned this role to its ATPase domain, and a possible helicase activity required prior to the Mre11 exonuclease.

1.6.3 The role of Irc20 in transcription regulation

Richardson *et al.*, (Richardson, Gardner, & Prelich, 2013) recently showed that Irc20 possesses ubiquitin ligase activity *in vitro*, as well as a role in transcription regulation. They used a genetic approach to identify transcriptional regulators in *S. cerevisiae*, screening for mutations that increase transcription from the Upstream Activator Sequence (UAS)-less $suc2\Delta uas(-1900/-390)$ reporter. This Bur- (Bypass UAS Requirement) selection has been very successful, revealing mutations in genes that regulate transcription such as TATA Binding Protein, RNA polymerase II, and histones. A yeast strain containing the $suc2\Delta uas(-1900/-390)$ reporter was screened for genes whose overexpression caused the Bur- phenotype, and resulted in the isolation of a single gene, Irc20. The overexpression phenotype is only visible when

a functional Irc20 is expressed, not when mutations are introduced in the ATPase and RING domains, or when Irc20 is C-terminally tagged. They also demonstrated that Irc20 possesses ubiquitin E3 activity *in vitro*, and that it interacts with an important ATPase in the proteasomal degradation system, Cdc48. The interaction with Cdc48 seems to be functionally relevant as it also requires a functional Irc20. They demonstrated that Cdc48 and Irc20 function in opposing manners, as an increase in Irc20 activity produced a Bur- phenotype, while a recessive and presumably loss-of-function mutation in Cdc48 did the same. Based on these findings, they suggested one of two models. The first model predicts that Cdc48 inhibits *suc2Δuas(-1900/-390)* transcription with Irc20 having an overall activating role by inhibiting Cdc48 and is consistent with the antagonistic relationship between the two genes. An equally plausible model proposes that Irc20 functions as an activator of *suc2Δuas(-1900/-390)* transcription and that Cdc48 functions upstream as an Irc20 inhibitor. Based on this model, Irc20 is normally kept inactive by Cdc48-mediated inhibition, but its overexpression overwhelms the ability of Cdc48 to inhibit its function. Likewise, the *cdc48-R369K* mutation might impair the ability of Cdc48 to inhibit Irc20. In either case, increasing Irc20 activity by overexpression is sufficient for promoting transcription from the *suc2Δuas(-1900/-390)* reporter. Finally, Richardson *et al.* (2013) suggested that Irc20 serves as a SUMO-targeted ubiquitin ligase (STUbL), as they observed an increase in SUMO-conjugated Irc20 in a RING finger domain mutant of Irc20 (Richardson *et al.*, 2013). Because STUbLs typically target substrates for proteolytic degradation, their inactivation often leads to an increase in

the levels of SUMO conjugates of their target substrates, consistent with what was observed for Irc20 itself (SUMO-dependent auto-ubiquitylation).

1.7 Aims and objectives

The yeast Irc20 protein can be identified as a Snf2 family member based upon sequence homology. To gain insight into the mechanism of action of this protein, it will be of value to determine what activities it possesses, how it interacts with other repair factors and how it contributes to the maintenance of genome stability. Our overall objective is to better understand the mechanisms by which the Irc20 protein is involved in DNA repair and genome stability. The specific aims of this thesis are:

- I) Characterization of the *in vitro* biochemical activities of Irc20
- II) Investigating the role of Irc20 in regulating recombination foci formation
- III) Identifying how Irc20 contributes to 2- μ m plasmid stability and copy number control.

To achieve this, we will use a combination of genetic, biochemical, and molecular approaches to study the mechanism of action of the putative helicase and ubiquitin ligase, Irc20. Results obtained from these studies should be valuable to the scientific community regarding the mechanisms of genome maintenance, as well as to the medical community since mutations in the human homolog of Irc20, SHPRH, are associated with cancer and other diseases.

Chapter 2: Materials and Methods

2.1 Yeast strain construction

2.1.1 One-step PCR-mediated gene deletion or tagging

Yeast strains were made using the one-step PCR-mediated gene deletion or tagging method (Longtine et al., 1998). With this method, a null mutant of a gene can be generated or proteins can be tagged at their C-terminus. In general, for gene deletion, the whole gene is replaced with a DNA cassette containing a selection marker using the cell's homologous recombination. Depending on the type of selection marker, a strain will either acquire resistance to an antibiotic or it will be able to grow on synthetic media lacking a specific amino acid. For gene deletions, DNA inserts having either KanMX, His3 or Trp1 gene cassettes were amplified by PCR from pFA6a-KanMX6, pFA6a-His3MX6 or pFA6a-TRP1 plasmids, respectively (generous gifts from Professor Danesh Moazed, HMS, USA). The primers used for amplifications were designed in a way that would allow the proper integration of the inserted DNA. For gene deletions, the forward primers had 40-45 nts complementary to the sequence upstream of the start codon of the gene of interest, followed by a sequence that acted as a forward primer for amplifying the cassette from the plasmid. The reverse primers had 40-45 nts complementary to the sequence downstream of the stop codon of the gene of interest, followed by a sequence that acted as a reverse primer for amplifying the cassette from the plasmid. The primers for tagging the protein of interest at the C-terminal were designed similarly; however, the forward primers for these constructs had 40-45 nts

complementary to the sequence upstream of the stop codon of the gene of interest. DNA inserts containing the 13Myc tag were amplified from either pFA6a-13Myc-kanMX6 or pFA6a-13Myc-His3MX6 plasmids (Addgene). DNA inserts containing the N-terminal TAP tag were amplified from pBS1761. DNA inserts containing the GFPEnvy tag were amplified from pFA6a-link-GFPEnvy-SpHis5 (Addgene). DNA inserts containing the *GALI*-promoter were amplified from pFA6a-kanMX6-PGAL1 (Addgene). A diagram illustrating gene deletion and tagging by one-step PCR-mediated replacement is shown in below in Figure 2.1.

For all yeast strain constructions, the following was done. Briefly, following PCR amplification (using Taq DNA Polymerase/with thermoPol buffer for amplifying cassettes for the deletions and Phusion HF polymerase (New England Biolabs) for amplifying cassettes for tagging) of the appropriate cassette that would be inserted in the genome, and following confirmation of the size of the PCR product on an agarose gel, the inserts were ethanol precipitated, and dissolved in 15 μ L of distilled water, and transformed into yeast cells. For yeast transformation, a single colony of wild type yeast BY4741 strain was grown in 50 ml YPD media (1% yeast extract, 2% Bacto-Peptone, 2% Glucose) until an OD_{600} of 0.5. Cells were then pelleted by centrifugation at 2,000 RPM for 3 minutes, washed with 10 ml of sterile distilled water, and resuspended and incubated in 1 ml of buffer containing 100 mM lithium acetate and 0.5X TE (5 mM Tris-HCl pH 7.5, 0.5 mM EDTA) for 10 to 60 minutes at room temperature. One hundred μ L of the cell suspension were then initially mixed with 10 μ L of 10 mg/ml salmon sperm DNA (Life technologies) and 15 μ L of PCR product, followed by the addition of 700 μ L of a mix of 100 mM

Lithium acetate, 1X TE (10mM Tris-HCl pH 7.5, 1mM EDTA), and 40% polyethylene glycol. Cells were mixed and incubated at 30°C for 30 minutes with continuous shaking. Eighty five μ L of DMSO was added and cells were heat shocked by incubation at 42°C for 15 minutes. Cells were then kept on ice for 2 minutes, then pelleted by spinning at 2,500 RPM for 5 minutes. Cells were then resuspended in either 1 ml YPD broth and grown overnight (for KANMX6 transformations) and plated next day on YPD-Geneticin (YPD containing 0.03% Geneticin) plates, or resuspended in 1X TE buffer and plated directly (for nutritional markers). After plates were grown for 3 days, single colonies were re-streaked on selective plates. Single colonies are then grown, genomic DNA isolated, and checked for proper cassette integration by PCR with primers specific to the region of interest. An illustration of one-step PCR mediated gene tagging and deletion is given in Figure 2.1.

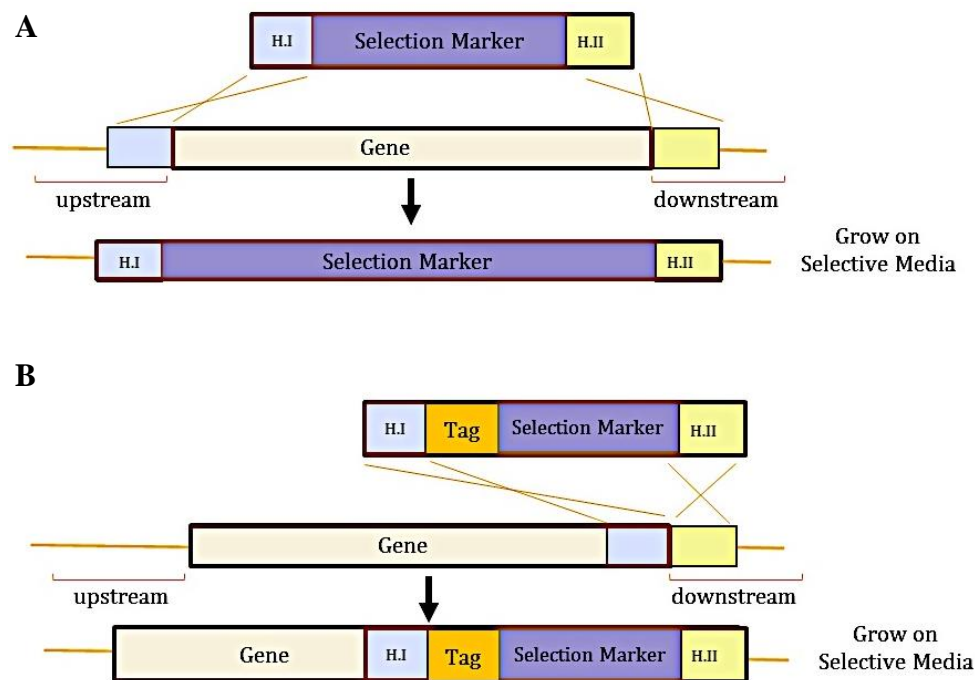


Figure 2.1: Overview of one-step PCR mediated gene tagging and deletion

A. Diagram illustrating gene deletion using one-step PCR amplified cassette. The cassette is designed to contain 2 regions homologous to upstream and downstream of the gene to be deleted (H.I and H.II) using the cell's own homologous recombination machinery, the cassette replaces the gene of interest leaving behind a selection marker that can be used to select for positive transformants. **B.** Diagram illustrating gene C-terminal tagging using one-step PCR amplified cassette. As previously described except that the H.I is homologous to end of gene, just upstream of stop codon. This results in tag placement at the end of the desired gene, in addition to a selection marker to select for positive transformants.

2.1.2 *In vivo* site-specific mutagenesis (*delitto perfetto*)

In vivo site-specific mutagenesis was used in gene manipulations that require absence of a selection marker following the gene manipulation (Stuckey, Mukherjee, & Storici, 2011). This method involves two transformation steps. The first step of *delitto perfetto* involves the insertion of a COunterselectable REporter (CORE) cassette containing two markers. The two CORE markers are used for selection purposes and consist of the following: an antibiotic resistance marker (REporter) –

which confers resistance to the antibiotic Geneticin (G418) – and a COUNTERselectable marker, the KIURA3 gene (a URA3 homolog from *Kluyveromyces lactis*), which can be selected against using 5-FOA. In addition, the CORE cassette includes the gene for the restriction endonuclease I-SceI under an inducible *GALI*-promoter. This is used to induce a DSB at the 18-nt I-SceI break site inserted at the desired region to enhance the second transformation efficiency. Amplification of the CORE cassette from pGSKU (Gift from Francesca Storici, GT, USA) plasmid by PCR is accomplished using primers which contain 40-nts tails of homology to either side of the target site to drive the integration of the CORE to its desired location in the first step of *delitto perfetto*. The second step involves replacement of the entire cassette with oligonucleotides or larger pieces of DNA to yield the expected modification to the original segment of chromosomal DNA. Transformations were done as described previously in Section 2.1.1, with the exception that in the second transformation step, cells were grown overnight in YEPLactate media (1% yeast extract, 2% Bacto-peptone, 3% glycerol, 2% lactic acid, pH adjusted to 6.6 by NaOH), 2% galactose was then added for 3-5 hours to induce the I-SceI cut at the desired location. Cells were then pelleted and transformed with oligonucleotides or PCR-amplified tag as described previously in Section 2.1.1. The N-terminal tagged Irc20 and point mutants were prepared using the *delitto perfetto* method. An overview of *delitto perfetto* is given in Figure 2.2. The domains in which point mutations of Irc20 are introduced are shown in Figure 2.3. The strains used in this thesis and primers used to construct the strains and plasmids used are listed in Table 1 and 2, respectively.

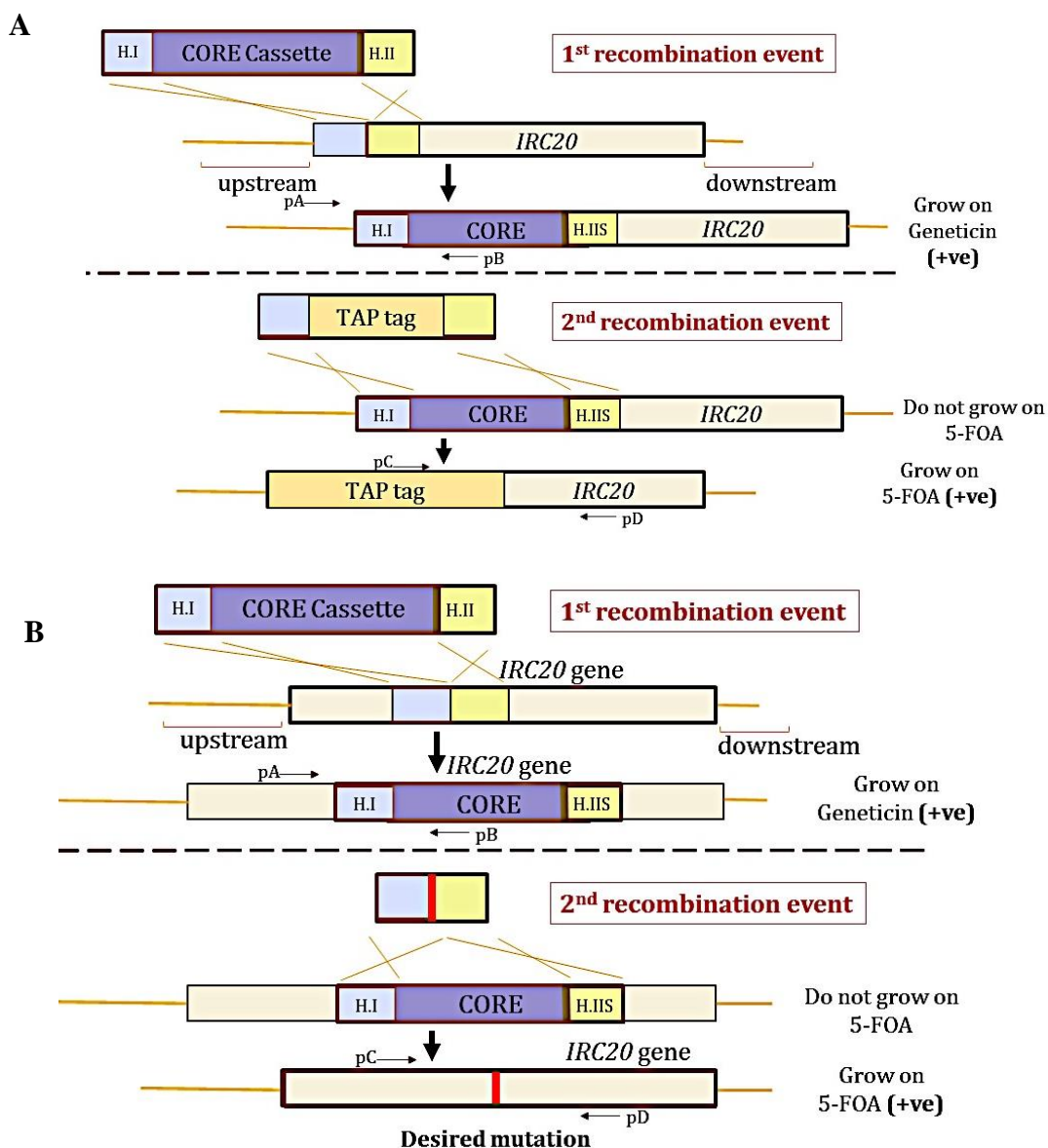


Figure 2.2: Overview of *delitto perfetto*

A. Diagram illustrating *delitto perfetto* to tag genes at the N terminus. The first transformation step involves insertion of the CORE cassette, consisting of a REporter selectable marker and a COunterselectable marker. The CORE cassette is designed to contain regions of homology H.I and H.IIS, with H.IIS also containing an I-SceI cut site to improve efficiency of the second transformation. The second step of *delitto perfetto* involves removal of CORE cassette using a cassette amplified containing the tag of interest without selection marker, thus allowing for tagging at N-terminus without interfering with the native promoter. B. Diagram illustrating *delitto perfetto* to make point mutants in genes. As described above, with the exception that the second transformation is using oligonucleotides containing the desired mutation. pA and pB are primers used to check the integration of the CORE cassette at the correct locus. pC and pD are primers used to check the proper insertion of the tag, or to amplify the region to be sequenced to confirm the insertion of mutation.

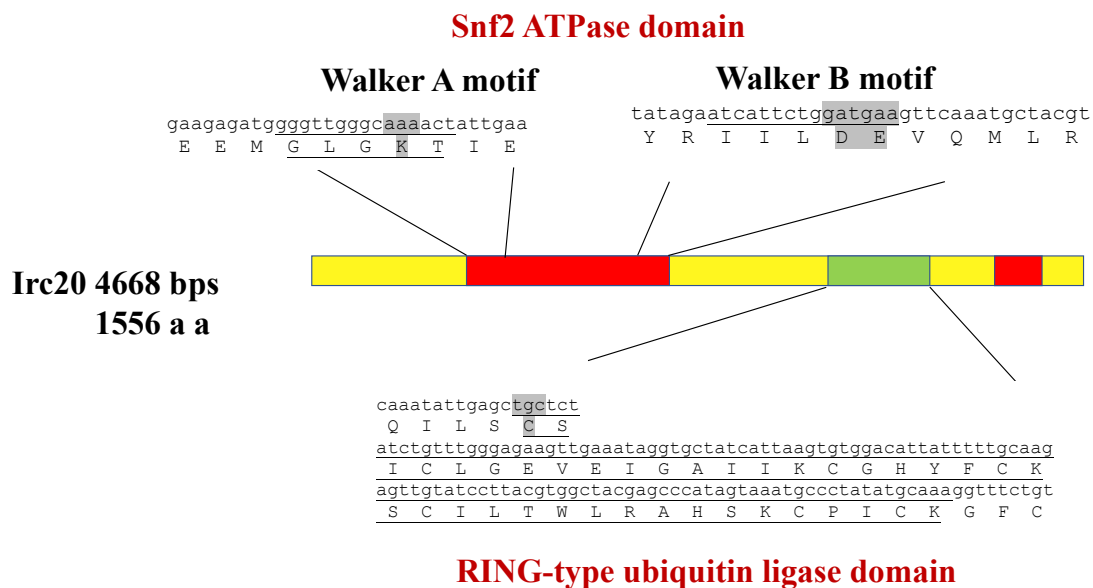


Figure 2.3: Domains of Irc20 showing specific amino acids mutated in each domain

The Irc20 ATP hydrolyzing domain consists of Walker A motif (consensus sequence: G-x(4)-GK-[TS], G= glycine, K=lysine, T=threonine, S=Serine, x=any amino acid) and Walker B motif (consensus sequence: hhhhDE, h=hydrophobic aminoacid, D=aspartic acid, E=glutamic acid). To abolish the ATP hydrolyzing activity of Irc20, mutations in the Walker A motif (K397A), and in the Walker B motif at (DE534-535A) were introduced. The RING finger ubiquitin ligase domain of Irc20 (containing C₃HC₄ amino acid motif; C=cysteine, H=histidine). To abolish the ubiquitin ligase activity of Irc20 the first cysteine in the RING finger was mutated to C1239A.

Table 1: Yeast strains used in this thesis

Strain	Description	Source
BY4741 (WT)	MATa; his3Δ1; leu2Δ0; met15Δ0; ura3Δ0	Euroscarf
JKM139	MATa Δho Δhml::ADE1 Δhmr::ADE1 ade1-100 leu2-3,112 lys5 trp1::hisG ura3-52 ade3::GAL::HO	Haber lab
ADJ5	BY4741; TAP-tagged at N terminus of IRC20 using <i>delitto perfetto</i>	This study
ADJ9	BY4741; Δirc20 using <i>delitto perfetto</i>	This study
ADJ17	BY4741; 13Myc Nt IRC20 using <i>delitto perfetto</i>	This study
ADJ22	ADJ5; ATPase mutant K397A of TAP-IRC20 using <i>delitto perfetto</i>	This study
AJC22	BY4741; Δmre11::KANMX6	This study
ADJ38	ADJ9; Δrad6::KANMX6	This study

Table 1: Yeast strains used in this thesis (continued)

Strain	Description	Source
ADJ40	BY4741; <i>irc20DE534-535AA</i> using <i>delitto perfetto</i>	This study
ADJ41	BY4741; <i>irc20C1239A</i> using <i>delitto perfetto</i>	This study
ADJ43	BY4741; $\Delta rad6::KANMX$	This study
ADJ44	BY4741; $\Delta rad18::KANMX$	This study
ADJ45	ADJ9; $\Delta rad18::KANMX$	This study
ADJ47	BY4741; Nt-TAP IRC20 C1239A	This study
ADJ55	BY4741; Rad52-GFPEnvy::His	This study
ADJ56	BY4741; $\Delta irc20$ Rad52-GFPEnvy::His	This study
ADJ57	BY4741; <i>irc20DE534-535AA</i> Rad52-GFPEnvy::His	This study
ADJ58	BY4741; <i>irc20C1239A</i> Rad52-GFPEnvy::His	This study
ADJ63	BY4741; <i>GAL1pr::KANMX</i> Nt-TAP $\Delta irc20$	This study
ADJ72	BY4741; <i>GAL1pr::KANMX</i> Nt-TAP <i>irc20K397A</i>	This study
ADJ73	<i>GAL1pr::KANMX</i> Nt-TAP <i>irc20DE534-535AA</i>	This study
ADJ77	BY4741; $\Delta rsc2::His3MX6$	This study
ADJ78	BY4741 [cir^0] (made using pBIS-GalkFLP1-URA)	This study
ADJ79	ADJ9 [cir^0] (made using pBIS-GalkFLP1-URA)	This study
ADJ80	BY4741; $\Delta irc20::His3MX6$	This study
AJC51	JKM139; Rad52-13Myc:kanMX6	This study
ADJ101	JKM139; Rad52-13Myc:kanMX6 $\Delta irc20::Trp1$	This study
ADJ102	JKM139; Rad52-13Myc:kanMX6	This study
ADJ103	BY4741; $\Delta mre11::KANMX6$ $\Delta irc20::His3MX6$	This study
ADJ104	BY4741; $\Delta rad52::KANMX6$ $\Delta irc20::His3MX6$	This study
ADJ108	13Myc Nt IRC20 Rad52-GFPEnvy::His	This study

Table 2: Primers used in this thesis

Name	Sequence	Description
0.18R HO FP	CCTGGTTTTGGTTTTGTAGAGTG G	Specific to 0.18 kb to the right of HO cut site at MAT locus.
0.18R HO RP	GAGCAAGACGATGGGGAGTTT C	
2.1R HO FP	GCCTCTATGTCCCCATCTTGTC TC	Specific to 2.1 kb to the right of HO cut site at MAT locus.
2.1R HO RP	GTGTTCCCGATTCAGTTTGACG	
ACT1 FP	TGTCACCAACTGGGACGATA	Primers used as control for HO ChIP experiments.
ACT1 RP	GGCTTGGATGGAAACGTAGA	
IRC20 Nt-CoRE FP	GCCAACTTATTCGACGGTAAT TCGTACGCTGCAGGTCGAC	Primers used to amplify the CORE cassette from pGSKU to introduce into the N-terminus of Irc20. In bold are sequences complementary to the plasmid, the rest are complementary to the beginning and upstream of the Irc20 gene. Underlined is the IScel cut site.
IRC20 Nt-CoRE RP	<u>AGCGCACCTACTGCAGACATT</u> <u>AGGGATAACAGGGTAATCCG</u> <u>CGCGTTGGCCGATTCAT</u>	
GUB-5' Cy5	GATCCTCTAGACGGAGGACA	Primers used to amplify the GUB Cy5 labelled template from pGUB.
GUB RP	GATCCCTCGATTCCATGG	
DJ8 Deletion FP	AGGAATGAACTCCAGGAAAGG CCAACCTTATTCGACGGTAATAT ATTAAAATATTTAATCTTTTGA ATTTTTATATAAACG	Oligos used to delete <i>IRC20</i> using <i>delitto perfetto</i> .
DJ9 Deletion RP	CGTTTATATAAAAATTCAAAA GATTAAATATTTTAATATATTA CCGTCGAATAAGTTGGCCTTTC CTGGAGTTCATTCT	
DJ10 TAP FP	AGGAATGAACTCCAGGAAAGG CCAACCTTATTCGACGGTAAT GGCAGGCCTTGCGCAA	Primers used to amplify the TAP tag from pBS1761 to introduce at the N terminus of Irc20. In bold are sequences complementary to the plasmid, the rest are complementary beginning and upstream of <i>IRC20</i> .
DJ11 TAP RP	CGTTGTACTCCCTTGCTAATAG CGCACCTACTGCAGACATAAG CTTATCGTCATCATC	

Table 2: Primers used in this thesis (continued)

Name	Sequence	Description
DJ25 Myc FP	AGGAATGAACTCCAGGAAAGG CCAACCTTATTCGACGGTAAATC CCCGGGTTAATGAACGGTGA ACAA	Primers used to amplify 13Myc tag from pFA6a-13Myc plasmids to introduce at N terminus of Irc20. In bold complementary to plasmid, rest complementary to gene of interest.
DJ27 Myc RP	CGTTGTA CTCCCTTGCTAATAG CGCACCTACTGCAGACATGGC GCGAATTGACGAGTGATTGAT	
DJ18 ATPase mut CORE FP	AGTTTGTGCAAAGGGGGTGTTA GCAGAAGAGATGGGGTTGTTC GTACGCTGCAGGTCGAC	Primers used to amplify the CORE cassette from pGSKU to introduce into <i>IRC20</i> at position K397. In bold are sequences complementary to the plasmid, the rest are complementary to an internal region in <i>IRC20</i> . Underlined is the ISceI cut site.
DJ19 ATPase mut CORE RP	ATTCCTTCTATTTAAGAGTATT AGTGATAAAATTTCAAT TAGG GATAACAGGGTAATCCGCGC GTTGGCCGATTCAT	
IRC20 mutant F	TGTGCAAAGGGGGTGTTAGCA GAAGAGATGGGGTTGGGCGCT ACTATTGAAATTTTACTACTAA TACTCTTAAATAGAAG	Oligos used to introduce K397A mutation in <i>IRC20</i> using <i>delitto perfetto</i> . Underlined is the introduced mutation.
IRC20 mutant R	CTTCTATTTAAGAGTATTAGTG ATAAAATTTCAATAGTAGCGCC CAACCCCATCTCTTCTGCTAAC ACCCCTTTGCACA	
DJ34 CoRE DE534-535AA FP	ATGACTATTCTTCACCGTTAGC TTTGATGCAGTTTTATAGAATC ATTCTGTT CGTACGCTGCAGG TCGAC	Primers used to amplify the CORE cassette from pGSKU to introduce into <i>IRC20</i> at position DE534-535. In bold are sequences complementary to the plasmid, the rest are complementary to an internal region in <i>IRC20</i> . Underlined is the ISceI cut site.
DJ35 CoRE DE534-535AA RP	AAACTCGTGCATTTTGCAGAAT ATGTTGATGAACTACGTAGCAT TTGAACT AGGGATAACAGGGT AATCCGCGCGTTGGCCGATT CAT	
DJ36 DE534-535AA FP	ACCGTTAGCTTTGATGCAGTTT TATAGAATCATTCTGGCTGCTG TTCAAATGCTACGTAGTTCATC AACATATTCTGCAA	Oligos used to introduce DE534-535AA mutation using <i>delitto perfetto</i> . Underlined is the introduced mutation.
DJ37 DE534-535AA RP	TTGCAGAATATGTTGATGAACT ACGTAGCATTTGAACAGCAGCC AGAATGATTCTATAAAACTGCA TCAAAGCTAACGGT	

Table 2: Primers used in this thesis (continued)

Name	Sequence	Description
DJ42 CoRE C1239A FP	TGTCCACACTTAATGATAGCAC CTATTTCAACTTCTCCCAAACA GATAGATTCGTACGCTGCAG GTCGAC	Primers used to amplify the CORE cassette from pGSKU to introduce into <i>IRC20</i> at position C1239. In bold are sequences complementary to the plasmid, the rest are complementary to an internal region in <i>IRC20</i> . Underlined is the ISceI cut site.
DJ43 CoRE C1239A RP	AATTTGTCCAGATTGAAAGAC ACATTAAACGATAATCAAATA TTGAGCTAGGGATAACAGGG <u>TAATCCGCGCGTTGGCCGAT</u> TCAT	
DJ46 C1239A Foligo	GATTGAAAGACACATTAAACG ATAATCAAATATTGAGCGCTTC TATCTGTTTGGGAGAAGTTGA <u>AATAGGTGCTATCATT</u>	Oligos used to introduce C1239A mutation using <i>delitto perfetto</i> . Underlined is the introduced mutation.
DJ47 C1239A Roligo	AATGATAGCACCTATTTCAACT TCTCCCAAACAGATAGAAGCG CTCAATATTTGATTATCGTTA ATGTGTCTTTCAATC	
JC30 Del Rad52 FP	CAAGAACTGCTGAAGGTTCTG GTGGCTTTGGTGTGTTGTTG CGGATCCCCGGGTTAATTAA	Primers used to amplify the deletion cassette from pFA6a plasmids to delete <i>RAD52</i> . In bold are sequences complementary to the plasmid, the rest are complementary to upstream and downstream of <i>RAD52</i> .
JC31 Del Rad52 RP	TAA TGA TGC AAA TTT TTT ATT TGT TTC GGC CAG GAA GCGTTGAATTCGAGCTCGTTT AAAC	
JC54 Del Mre11 FP	GACGCAAGTTGTACCTGCTCA GATCCGATAAAACTCGACTCG GATCCCCGGGTTAATTAA	Primers used to amplify the deletion cassette from pFA6a plasmids to delete <i>MRE11</i> . In bold are sequences complementary to the plasmid, the rest are complementary to upstream and downstream of <i>MRE11</i> .
JC55 Del Mre11 RP	GTT ATA AAT AGG ATA TAA TAT AAT ATA GGG ATC AAG TACAAGAATTCGAGCTCGTTT AAAC	
DJ51 delRad6 FP	GAATTCCAAAGATTATTTTATAG GCAGACAGAGACTAAAAGATA AAGCGTCCGGATCCCCGGGT TAATTAA	Primers used to amplify the deletion cassette from pFA6a plasmids to delete <i>RAD6</i> . In bold are sequences complementary to the plasmid, the rest are complementary to upstream and downstream of <i>RAD6</i> .
DJ52 delRad6 RP	AATTCATAATATCGGCTCGGC ATTCATCATTAAGATTCTTTTG ATTTTTCGAATTCGAGCTCGT TAAAC	

Table 2: Primers used in this thesis (continued)

Name	Sequence	Description
DJ54 delRad18 FP	ATCCGCAAGTGAGCATCACAG CTACTAAGAAAAGGCCATTTT TACTACTCCGGATCCCCGGGT TAATTAA	Primers used to amplify the deletion cassette from pFA6a plasmids to delete <i>RAD18</i> . In bold are sequences complementary to the plasmid, the rest are complementary to upstream and downstream of <i>RAD18</i> .
DJ55 delRad18 RP	TTAACAAATGTGCACAAGCTA ACAAACAGGCCTGATTACATA TACACACCGAATTCGAGCTC GTTTAAAC	
DJ57 Rad52 GFP FP	GAGAAGTTGGAAGACCAAAGA TCAATCCCCTGCATGCACGCA AGCCTACTGGTGACGGTGCT GGTTTA	Primers used to amplify the GFPEnvy tag from pFA6a-link-GFPEnvy-SpHis5 plasmid to introduce at the C-terminus of Rad52. In bold are sequences complementary to the plasmid, the rest are complementary to beginning and upstream of <i>RAD52</i> .
DJ58 Rad52 GFP RP	AGTAATAAATAATGATGCAAA TTTTTTATTTGTTTCGGCCAGG AAGCGTTTCGATGAATTCGA GCTCG	
DJ69 Rad52 myc FP	GAGAAGTTGGAAGACCAAAGA TCAATCCCCTGCATGCACGCA AGCCTACTCGGATCCCCGGG TTAATTAA	Primers used to amplify the 13Myc cassette from pFA6a plasmids to tag Rad52 at the C-terminus. In bold are sequences complementary to the plasmid, the rest are complementary to beginning and upstream of <i>RAD52</i> .
DJ70 Rad52 myc RP	AGTAATAAATAATGATGCAAA TTTTTTATTTGTTTCGGCCAGG AAGCGTTGAATTCGAGCTCG TTTAAAC	
DJ74 Gal1 insertion FP	AGGAATGAACTCCAGGAAAGG CCAACCTTATTCGACGGTAAGA ATTCGAGCTCGTTTAAAC	Primers used to amplify <i>GAL1</i> -promoter from pFA6a-PGAL1 plasmids to introduce upstream of <i>Irc20</i> gene.
DJ75 Gal1 insertion RP	ATTTGTTGTCCACGGCTTCATC GTGTTGCGCAAGGCCTGCCAT TTTGAGATCCGGGTTTT	In bold complementary to plasmid, rest complementary to gene of interest.

Table 2: Primers used in this thesis (continued)

Name	Sequence	Description
DJ78 Y sub-telomeric element FP	ACAATGGCCTTCGACTCTGGT TC	Primers used as control for measuring 2- μ m levels by qPCR.
DJ79 Y sub-telomeric element RP	ATCACAGCCCGAAGAAGCAC T	
DJ80 2- μ m qPCR FP	CACAAGATAGTACCGCAAAA CGA	Primers used to measure 2- μ m levels by qPCR.
DJ81 2- μ m qPCR RP	CACCTTTGCTGCTTTTCCTTA ATT	
DJ82 2- μ m presence PCR FP	ACAGCGCTGATATAACAATG	Primers used to detect presence of 2- μ m plasmid by normal PCR.
DJ83 2- μ m presence PCR RP	CTGTCGGCTATTATCTCCG	
DJ91 rsc2 deletion FP	AGAACCAGACGAAGCGGAGA ATATTCTACATTGACAGTGCC GGATCCCCGGGTTAATTAA	Primers used to amplify the deletion cassette from pFA6a plasmids to delete <i>RSC2</i> . In bold are sequences complementary to the plasmid, the rest are complementary to upstream and downstream of <i>RSC2</i> .
DJ92 rsc2 deletion RP	GGAAGATATTATGCTGCCATT GCTTTTACAATAAAGGTGAG AATTCGAGCTCGTTTAAAC	
DJ117 FLP1 Xba1 FP	ACGATCTCTAG <u>AAAAAAAAAT</u> GTCTATGCCACAATTTGGTAT ATT	Primers used to amplify <i>FLP1</i> having Xba1 restriction site (underlined) to clone into pRS416-Gal1 plasmid.
DJ118 Flp1 BamH1 RP	ACGATCGGATCC TATGCGTCTATTTATGTAGG	Reverse primer used to amplify <i>FLP1</i> having BamH1 restriction site (underlined) to clone into pRS416-Gal1 plasmid.
DJ126 Southern 2um probe 1	Biotin- GCCGTGGCCAGGACAACGTA TACTCATCAGATAACAGCAA TACCTGATCACTACTTCGCAC TAGTTTCTCGGTACTATGC	Biotinylated probe used to detect 2- μ m size.

Table 2: Primers used in this thesis (continued)

Name	Sequence	Description
DJ127 Southern 2um probe 2	Biotin- ATATGATCCAATATCAAAGG AAATGATAGCATTGAAGGAT GAGACTAATCCAATTGAGGA GTGGCAGCATATAGAACAGC	Biotinylated probe used to detect 2- μ m size.
DJ124 His3MX6 STB	AGGCATCCCCGATTATATTCT ATACCGATGTGGATTGCGCC GGATCCCCGGGTTAATTAA	Primers used to amplify the HIS3MX6 cassette from pFA6a plasmids to insert into 2- μ m plasmid. In bold are sequences complementary to the plasmid, the rest are complementary to regions within the 2- μ m plasmid.
DJ125 His3MX6 STB	GAAGAATCATCAACGCTATC ACTTTCTGTTCACAAAGTATG AATTTCGAGCTCGTTTAAAC	

2.2 Tandem Affinity Purification (TAP) of Irc20

2.2.1 Double affinity TAP purification

For the *in vitro* assays, purified Irc20 TAP-tagged at its N-terminus was used. The strain was constructed as described earlier in Section 2.2.1. The TAP method allows the purification of a protein over two affinity beads. The Irc20 TAP-tagged yeast strain was first streaked on a fresh YPD plate, allowed to grow for three days at 30°C, followed by inoculation of a single yeast colony in YPD media for native expression or YP 2% Galactose media for overexpression from *GALI*-promoter, until an OD₆₀₀ of 2-3. Cells from 6 liters of culture were then pelleted at 4,000 RPM for 20 minutes, resuspended in an equal volume of TAP extraction buffer (20 mM HEPES pH 7.4, 10% glycerol, 250 mM NaCl, 0.1% Tween-20, 0.5 mM DTT) supplemented with protease inhibitors (1 μ g/ml pepstatin, 2 μ g/ml leupeptin, 2 μ g/ml aprotinin, and 1 mM PMSF), and lysed by bead-beating (Hamilton Bead-beater). Bead beating was done for 30 seconds followed by 1 minute on ice, and repeated 12

times. The supernatant was then centrifuged at 13,000 RPM for 20 minutes to remove cell debris. This was followed by another centrifugation step of the supernatant using an ultracentrifuge at 40,000 RPM for 20 minutes. The whole cell extract from 3 liters of yeast cell were then added to 500 μ L IgG Sepharose Fast Flow beads (GE Healthcare) for 3 hours at 4°C. The lysate was then allowed to drain by gravity flow in a 10 ml Poly-Prep chromatography column (BioRad). The beads were washed twice with TAP extraction buffer, and once with TEV cleavage buffer (20 mM HEPES pH 7.4, 10% glycerol, 100 mM NaCl, 0.1% Tween-20, 1 mM DTT) supplemented with protease inhibitors. Irc20 was then eluted from the IgG resin in 1 ml of the same buffer containing 300 units of TEV Protease and kept rotating overnight at 4°C. The flow-through containing Irc20 was then collected, washed with 3 ml of Calmodulin binding buffer (10 mM Tris HCl pH 8, 300 mM NaCl, 2 mM CaCl₂, 1 mM Mg acetate, 1 mM imidazole, 0.1% NP-40, 10% Glycerol, 0.5 mM DTT) supplemented with protease inhibitors, and added to 500 μ L of Calmodulin affinity resin (Stratagene) and rotated for 2 hours at 4°C. The beads were collected by centrifuging at 1,000 RPM, washed twice with 5 ml of the Calmodulin binding buffer, and twice with same buffer but containing 150 mM NaCl. The bound Irc20 was then eluted from Calmodulin beads by incubating the beads with 250 μ L of calmodulin elution buffer (10 mM Tris-HCl pH 8, 150 mM NaCl, 2 mM MgCl₂, 1 mM Immidazole, 2 mM EGTA, 0.1% NP-40, 10% Glycerol, 1 mM DTT) supplemented with protease inhibitors. Elution was done at 4°C for 7 minutes each time and the eluted Irc20 was collected by centrifuging at 1,000 RPM. This was repeated 5 times, then repeated with calmodulin elution buffer containing 500 mM

NaCl. The eluted fractions were finally pooled and concentrated using Amicon Ultra centrifugal filter units with a 30 kDa cutoff value. Protein purification and integrity was monitored by western blotting using an anti-CBP antibody (Millipore) and by silver staining. The concentration of Irc20 was calculated by western blotting, comparing Irc20 intensity with known amounts of recombinant Snf6 protein that had a C-terminal Calmodulin Binding Peptide tag using an anti-CBP antibody (Millipore). The steps of the TAP purification method are illustrated below in Figure 2.4.

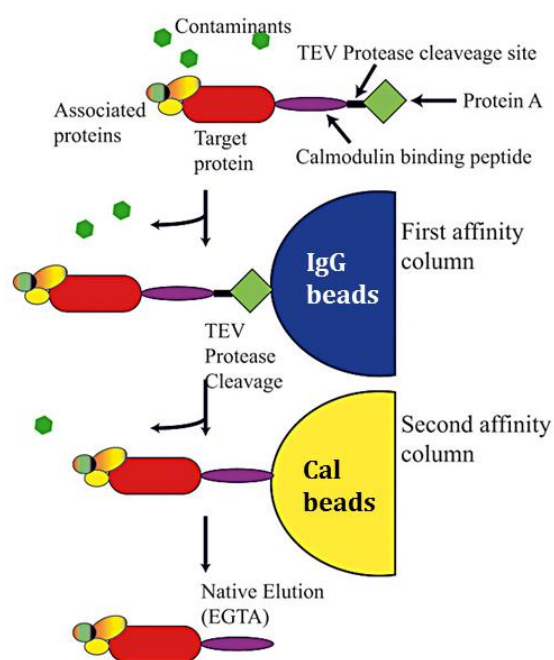


Figure 2.4: Tandem Affinity Purification (TAP) illustration.

Diagram illustrating Tandem affinity purification (TAP) adapted from Young 2012 (Young, Britton, & Robinson, 2012). The TAP tag consists of Calmodulin binding peptide (CBP) followed by a TEV cleavage site, then Protein A region. The first step of TAP purification involves incubating the cell lysates to IgG beads, to allow binding of the protein of interest with the beads using Protein A region. Washing removes contaminant proteins in the lysate. The bound protein is then eluted from IgG beads by cleaving with TEV protease. The eluted protein is bound to a second affinity bead, calmodulin beads, which interacts with the second tag on the protein, the CBP. Finally, the bound protein is eluted with EGTA which chelates Ca^{2+} , thus releasing the interaction between CBP and calmodulin.

2.2.2 Single affinity TAP purification

A single affinity bead (Calmodulin) was used to purify N-terminal TAP tagged Irc20 under its own promoter for analysis by size exclusion chromatography and mass spectrometry (ADJ5 for wild type Irc20 and ADJ47 for ubiquitin ligase mutant Irc20). The double affinity TAP purification was modified as follows: lysates from 6 liters of cultures were prepared as previously described in Section 2.1.1, supplemented with 2 mM CaCl₂, added to 500 µL of Calmodulin affinity resin (Stratagene) and rotated for 2 hours at 4°C. The beads were collected by centrifuging at 1,000 RPM, washed and the bound protein was eluted as previously described in Section 2.1.1. Protein purification and integrity was monitored by western blotting using anti-TAP antibody (Millipore) and by silver staining.

2.3 Purification of CBP-tagged Snf6 for quantification of purified proteins

The *SNF6* gene was amplified from yeast genomic DNA, and fused with a CBP tag using overlapping PCR. Primers used for amplification also contained 6XHis-tag to be used in purification, and NdeI and XhoI restriction enzyme cut sites. The amplified Snf6 tagged at the C-terminus with 6XHis-CBP tag was cloned into pET21b at NdeI and XhoI sites. *E. coli* strain BL21 was transformed with the plasmid and protein expression was induced with 1 mM IPTG. The expressed protein was purified under denaturing conditions in presence of 8 M Urea, using Ni-NTA beads which binds the 6XHis-tag on the Snf6. The protein was eluted with increasing amounts of imidazole. Protein levels were quantified by Bradford, and used as a standard for quantifying purified proteins using the CBP tag.

2.4 Size exclusion chromatography

A Superose 6 gel filtration column was pre-equilibrated with gel filtration buffer (50 mM Tris-HCl pH 7.5, 150 mM NaCl, 12.5 mM MgCl₂, 0.1% NP-40, 10% Glycerol). Gel filtration protein standards (Sigma MWGF1000) [thyroglobin (669 kDa), apoferritin (443 kDa), B-amylase (200 kDa), ADH (150 kDa), BSA (66 kDa), and carbonic anhydrase (29 kDa)] were injected to draw a standard curve. Single affinity (Calmodulin bead) purified Irc20 were injected on the column at a flow rate 0.2 ml/min and fractions of 0.5 ml collected. 50 µL of each fraction was separated on a 6% SDS-polyacrylamide gel and analyzed by western blotting using anti-CBP antibody.

2.5 Mass spectrometry analysis

Single affinity TAP purified Irc20 and *Irc20-C1239A* were treated with 0.1U Benzonase (Sigma) for 30 minutes at 37°C, to remove any co-purified DNA. The solution was brought to 400 µl with 100 mM Tris-HCl pH 8.5 and chilled. 100 µL of 100% trichloroacetic acid (TCA) was added and kept overnight at 4°C. Proteins were precipitated by centrifugation at 14,000 RPM for 30 minutes at 4°C, and washed twice with 500 µL ice-cold acetone then air-dried. Mass spectrometry analysis for TAP-Irc20 was done at the Stowers Institute for Medical Research, USA, whereas for TAP-Irc20-C1239A was done at the Taplin Mass Spectrometry Facility at Harvard Medical School, USA.

2.6 Immobilized template binding assay

A 2.5 kb fragment excised from plasmid pG5E4-5S that contains a dinucleosome length G5E4 fragment flanked on both sides by five 5S sequences was prepared as described (Hassan et al., 2002). The G5E4-5S fragment was end-labeled with biotin-14-dATP, gel purified, and reconstituted into a nucleosomal array by step dilution. Following reconstitution, the arrays were coupled to streptavidin Dynabeads (Dyna). 10 nM of Irc20 was added to 200 ng of the above template, in 20 μ L binding buffer and incubated for 1 hour at 30°C. The templates were then separated using a magnet, the supernatant was removed, and the beads were washed twice. The presence of Irc20 was determined by western blotting using the anti-CBP antibody.

2.7 SalI accessibility assay

The single Gal4-site probe (GUB) was generated by PCR using Cy5-end labelled primer, generating 5'-Cy5 labelled GUB fragment. This fragment was used as naked DNA or a reconstituted mononucleosome in this assay as described before. Irc20 was added to ~10 ng of this Cy5-GUB template in a binding buffer that contains (4 mM Tris-HCl pH 8, 5 mM DTT, 5 mM phenylmethylsulfonyl fluoride, 5% glycerol, 0.25 mg/ml bovine serum albumin, and 2 mM MgCl₂) in the presence or absence of 2 mM ATP. After incubation for 1 h at 30°C, the binding reactions were then treated with 10 units of SalI for 60 minutes at 37°C. 5X stop buffer (100 mM EDTA, 2.5% SDS, and 1 mg/ml proteinase K) was added to the reactions, and incubated at 50°C for 1 h. The samples were resolved on 8% acrylamide (29:1

acrylamide to bisacrylamide) 150 volts for 1 hour, and then visualized by fluorescent scanning on Typhoon FLA 9500.

2.8 ATP-hydrolysis assay

Analysis of the ATP-hydrolyzing ability of Irc20 was done using ADP-Glo™ Max Assay. Stock solutions of 1 mM ATP and ADP were prepared by diluting the Ultra Pure ATP and ADP supplied with the ADP-Glo MAX Assay kit (Promega) in 1x reaction buffer (20 mM Tris pH 8, 50 mM KCl, 5 mM MgCl₂, 5% Glycerol, 0.1 mg/ml BSA, 1 mM DTT, 10 ng/μL salmon sperm DNA). Mixtures of 5 μl of ATP (1 mM) and ADP were made in which the final ADP content varied from 0 to 20% (0, 25, 50, 100, 150 and 200 μM), which represents the percent conversion of ATP to ADP in the ATP hydrolysis experiments.

To measure the ATP consumption of Irc20 *in vitro*, 5 μl of reaction mixtures were prepared consisting of 25 or 50 nM protein or the ATPase mutant and 1x reaction buffer, followed by the addition of ATP to final concentration of 1 mM. For the no protein control, storage buffer was used at same volume of the protein. To each sample and standard, 5 μl of the ADP-Glo Reagent was added and incubated for 40 min, followed by the addition of 10 μl of ADP-Glo Max Detection Reagent and incubation for 1 hour. The luminescence was then measured using TECAN infinite M200 Pro. Standard curves (0, 25, 50, 100, 150, 200 and 250 μM) were created to correlate the ADP concentration with the luminescence. All reactions were carried out in duplicate.

2.9 Growth assay

Cells growing at log phase were normalized to an OD₆₀₀ of 0.3, serially diluted (1:10), and spotted, using a blotter, on YPD plates or YPD plates containing DNA damaging agents at concentrations specified in the figures. Plates were allowed to grow for 2-3 days at 30°C.

2.10 Rad52 foci detection

Exponentially growing cells were collected by spinning at 1,000 RPM for three minutes, and immobilized on a slide by resuspending the pelleted cells in minimal amount of water. Three to five independent cultures for each strain were visualized by fluorescent microscope Olympus BX51 fluorescent microscope at 100X magnification, and images were captured and analyzed. The number of cells with one or more foci compared to the total number of cells with visible nuclei in a field, were quantified. Values were compared by Student *t*-test for two-tailed unpaired samples of equal variance.

2.11 Co-immunoprecipitation

Total OD₆₀₀ of 80 of exponentially growing unfixed cells were pelleted, lysed in extraction buffer (50 mM HEPES pH 7.5, 150 mM NaCl, 10% Glycerol, 0.1% Tween) and cell lysates were quantified by Bradford (Biorad). 2.5 mg lysates were immunoprecipitated with 1.5 µg anti-Myc antibody (Sigma), rotated for 3 hours at 4°C followed by addition of 25 µl Protein G Dynabeads and rotating for 2 hours at 4°C. Beads were washed twice with extraction buffer, then resuspended in 25 µl 2X SDS loading dye (4% SDS, 20% glycerol, 10% 2-mercaptoethanol, 0.004%

bromophenol blue and 0.125 M Tris HCl pH 6.8), and loaded on SDS-PAGE followed by western blotting and probing with anti-Myc (Sigma) and anti-GFP (Abcam) antibodies.

2.12 ChIP at the HO cut site

Cells were grown overnight in YPD, subcultured in YEPLac grown to mid-OD₆₀₀ 0.3-0.4. Glucose was added to a fraction of the cells to repress HO, whereas galactose was added to the remainder of the cells to induce HO. Total OD₆₀₀ of 20 at 0, 2, 4, 6 and 8 hours after galactose addition (cells grown in the presence of glucose were collected at the 2-h time point), were fixed with 1% formaldehyde for 10 minutes at room temperature. Formaldehyde fixation is then quenched by adding 0.125M Glycine for 5 minutes. Cells were then pelleted, and washed with 20 ml of TBS buffer (50 mM Tris-HCl pH 7.5 and 150 mM NaCl). Pelleted cells are transferred to 2 ml screwcap tubes, resuspended in 1 ml FA Lysis Buffer (50 mM HEPES pH 7.5, 140 mM NaCl, 1 mM EDTA, 1% TritonX100, 0.1% sodium deoxycholate, 0.5 mM DTT supplemented with protease inhibitors) and bead beaten five times for 1 minute to extract cell lysate. Extracts are collected by making a hole at the bottom of the tube, placing it on a 15 ml tube, and spinned at 2,000 RPM for 2 minutes. Lysates were diluted to 1.4 ml with FA lysis buffer and sonicated in a chilled water bath using Diagenode sonicator at high power for 5 minutes (30 seconds on, 30 seconds off). Lysates were centrifuged at 14,000 RPM for 10 minutes at 4°C to remove cell debris and particles. Lysates were quantified by Bradford (Biorad). 0.5 mg lysates were diluted to 0.5 ml with FA lysis buffer, and immunoprecipitated using anti-Myc antibody (Sigma), by adding 2 µg antibody and

rotating for 3 hours at 4°C, followed by 30 µl washed Protein G Dynabeads for 2 hours at 4°C. 5% of each extract was not immunoprecipitated and served as input. Beads were washed with 1 ml FA lysis buffer, followed by 1 ml FA lysis buffer with 500 mM NaCl, followed by 1 ml Wash buffer (50 mM Tris-HCl pH 7.5, 250 mM LiCl, 1 mM EDTA, 0.1% NP-40, 0.1% Na deoxycholate), followed by a final wash with TE Buffer (10mM Tris-HCl pH 7.5, 1mM EDTA). DNA was then eluted from beads with 100 µl elution buffer containing (50mM Tris-HCl pH 7.5, 1mM EDTA, 1% SDS), incubating at 65°C for 10 minutes with shaking at 1,200 RPM. The elution was repeated and eluates pooled and decrosslinked together with the inputs overnight at 65°C. RNase was then added and incubated at 37°C for 30 minutes. DNA was then purified using Minelute reaction cleanup kit (Qiagen), and eluted in 20 µl. DNA was diluted five-fold, and 2 µl were used in 20 µl real time quantitative PCR reactions. Absolute-fold enrichment for Rad52–Myc at the HO DSB was calculated as follows: for each time point, the signal from a site near the HO DSB at the MAT locus was normalized to that from the non-cleaved *ACT1* locus in ChIP and input DNA samples. For each time point and site, the normalized ChIP signals were normalized to the normalized input DNA signals, because end resection can reduce the available DNA template. Finally, relative-fold enrichment was calculated by dividing the absolute-fold enrichment from induced cells to that of uninduced cells.

2.13 Measuring the presence of the endogenous 2-µm plasmid

Cells harboring the 2-µm plasmid were grown over night in YPD, then plated on YPD at a dilution that allows for single colonies to be picked. 8 colonies from each strain were analyzed by colony PCR using primers specific for 2-µm plasmid.

Colonies were resuspended in 30 μ l lyticase (50 U/ml) in 0.2 ml PCR tubes, and incubated at 37°C for 30 minutes, followed by 95°C for 10 minutes. 2 μ l of the lysed cells were analyzed by PCR using Taq polymerase in a 20 μ l reaction. 10 μ l were loaded on 1% Agarose gel and visualized by EtBr.

2.14 Curing yeast cells from the endogenous 2- μ m plasmid

The curing of 2- μ m plasmid from yeast cells was done as described by Tsalik and Gartenberg 1998 (Tsalik & Gartenberg, 1998). Cells were transformed with pBIS-GALkFLP(URA) (Addgene), which expresses a Flp ‘step-arrest’ mutant, *Flp H305L*, under *GALI*-promoter. This mutant carries out the first step of recombination, DNA cleavage, but fails to accomplish subsequent strand exchange and religation. This causes instability of the endogenous 2- μ m plasmid and its loss. After transformation and plating on SC-Ura (0.67% yeast nitrogen base without amino acids, 0.192% yeast synthetic drop-out medium supplements without uracil, 2% agar) with 2% glucose for selection, cells are streaked on SC-Ura media containing 2% galactose, to induce expression of the mutant Flp1. The removal of the pBIS-GALkFLP(URA) is then done by growing cells on 5-fluoroorotic acid (5-FOA) containing media.

2.15 2- μ m plasmid loss assay

pKAN4 (a kind gift from Melanie Dobson, Dalhousie University) is a modified form of the endogenous 2- μ m plasmid, which lacks the *FLP1* gene, and harbors a *KANMX4* selection marker which confers resistance to the antibiotic Geneticin. To monitor plasmid loss rates, [cir⁰] cells were transformed with pKAN4,

and selected for using Geneticin. Cells were then grown in liquid culture for 15 generations, followed by plating of equal amounts on YPD and YPD-Geneticin. Cells on genetecin plates were counted (cells harboring plasmid) and divided by cells on YPD plates (total number of cells). This gives the plasmid segregation efficiency and is analyzed for mutants and compared to WT strain.

2- μ m harboring *HIS3MX6* inserted downstream of the *STB* locus were used to analyze the plasmid segregation efficiency for plasmids harboring the *FLP1* gene. Similar to pKAN4, the plasmid segregation efficiency was calculated for Irc20 mutants and compared to WT strain.

2.16 Analyzing 2- μ m plasmid levels

Overnight cell cultures were pelleted and genomic DNA isolated using Wizard Genomic DNA purification kit (Promega), with the following modifications. DNA was precipitated in 100% ethanol and 0.3 M Na acetate. The pelleted DNA was resuspended in 500 μ l water, and quantified using a NanoDrop spectrophotometer (Thermo scientific). DNA was diluted to a concentration of 5 ng/ μ l and analyzed by quantitative real time PCR. Levels of 2- μ m plasmid were measured using a sequence from the Y subtelomeric element as the reference. Primers for measuring 2- μ m DNA and Y subtelomeric element are listed in the primer list. These two amplicons had virtually identical amplification efficiencies and gave the same relative values over a 100-fold dilution of the template DNA. qPCR was carried out with QuantStudio 7 Flex (Applied Biosystems) using SYBRTM green PCR master mix (Applied biosystems). Each reaction contained 10 μ l of SYBR Green Master Mix, 0.1 mM

forward and reverse primers, 10 ng genomic DNA, and distilled H₂O to a 20 µl final volume. PCR conditions were as follows: 1 cycle at 50°C for 2 minutes followed by 95°C for 10 minutes; and 40 cycles, each consisting of 95°C for 15 s, 60°C for 1 minute. The cycle number for the PCR product to reach preset threshold (CT number) was determined for two to three replicates for each DNA sample. The fold change of the 2-µm number compared to that of wild-type yeast DNA was calculated by $2^{-\Delta\Delta CT}$ methods. Values were compared by the Student *t* test.

2.17 Southern blotting for analyzing 2-µm species

15 µg of isolated DNA as described earlier in Section 2.16 and biontynylated lamda HindIII ladder were ran on 1.2% agarose gel in 1X TBE containing 0.75 µg/ml chloroquine at 3 V/cm for 22 hours at room temperature. The agarose gel was depurinated by incubating twice for 15 minutes in 0.25 M HCl, then denatured by incubating twice for 15 minutes in denaturation buffer (0.5 N NaOH, 1 M NaCl) and finally neutralized by incubating twice for 15 minutes in neutralization buffer (1 M Tris pH 7.5, 600 mM NaCl). DNA was then transferred to a positively charged nylon membrane overnight in 20X SSC (3 M NaCl, 0.3 Na citrate pH 7.0) by capillary transfer using a wick of Biorad filter paper (Brown, 1999). Membrane was crosslinked using UV, then hybridized with biotinylated probes designed to specifically detect the 2-µm plasmid in hybridization buffer (0.5 M Na₂PO₄ pH 7.2, 7% SDS, 1 mM EDTA) at 62°C overnight in hybridization oven. Membranes were washed twice for 15 minutes with 2X SSC, 0.1% SDS at 55°C followed by one wash with 1X SSC, 0.1% SDS at 55°C for 15 minutes. Detection of biotin labelled probe

was done using Thermo Scientific™ Pierce™ Chemiluminescent Nucleic Acid Detection Module as per the instructions provided with the kit.

2.18 Extraction of total cellular protein by TCA

Pellets from the yeast strains equivalent to an OD_{600} of 2.5-5 was collected by centrifugation, washed with 1 ml sterile water. Cells were then resuspended in cold (0.25 M NaOH/ 1% betamercaptoethanol) and incubated on ice for 10 minutes. 160 μ l of 50% TCA was then added and incubated for another 10 minutes on ice. Precipitated proteins were centrifuged at 14,000 RPM for 10 minutes, washed with cold acetone and air-dried for 10 minutes. Proteins were resuspended in 100 μ ls 2X SDS PAGE Loading Buffer, boiled for 5 minutes at 95°C, and centrifuged at 13,000 RPM for 5 minutes. 10-15 μ ls of supernatant are loaded on SDS-PAGE followed by western blotting.

2.19 Monitoring Flp1 levels

The *FLP1* gene was cloned into pRS416-Gal-RNQ1-YFP (Addgene) using XhoI and BamHI sites, to replace RNQ1 gene. The resulting vector expresses C-terminal YFP-tagged Flp1 under *GAL1*-promoter, in which expression is induced when cells are grown in galactose, and is repressed when glucose is added. This plasmid was transformed into WT [*cir*⁰] and Δ *irc20* [*cir*⁰] strains, and SC-Ura media was used for selection. Cells were grown overnight in SC-Ura broth, subcultured in the same media to get an exponentially growing culture. Cells were collected at 45, 90, 135 and 180 minutes, of total OD_{600} of 2.5 and whole cell extracts were prepared

by TCA method (Section 2.18). 10-15 μ ls of the whole cell extracts were loaded on 8% SDS-PAGE, and western blotting was done using anti-GFP antibody (Abcam).

Chapter 3: Results – Biochemical Characterization of Irc20

3.1 Overview

Despite implications for Irc20 in maintaining genome stability, little is known about its *in vitro* biochemical activities, especially relating to its ATPase domain. Sequence homology to the Snf2 catalytic domain of SWI/SNF chromatin remodeling complex had suggested chromatin remodeling activity for Irc20, but this was never tested. Here, we purified Irc20 from its native promoter, as well as from an inducible *GALI*-promoter to allow for high expression of the protein. Using the over-expressed purified protein, we tested its DNA and nucleosome binding activity, ATPase activity, and its ability to remodel a mononucleosomal template. We used the natively expressed purified protein to understand the interacting partners of Irc20 and whether it exists as a stable complex. Finally, we analyzed the co-purified proteins for wild type Irc20 and the ubiquitin ligase mutant *Irc20-C1239A* using mass spectrometry, in an attempt to understand specific involvement in cellular activities.

3.2 Purification and characterization of Irc20 protein

3.2.1 Irc20 is normally expressed in low amounts and shows promiscuous protein interactions

To better understand the function of the Irc20 protein and study its biochemical activities, we sought to purify Irc20 from *S. cerevisiae* using TAP purification method (Puig et al., 2001). A previous study on Irc20 had shown a loss of function phenotype when Irc20 was tagged on the more commonly used terminus, the C-terminus (Richardson et al., 2013). Therefore, to properly study the Irc20

biochemical activities, we tagged the protein with the TAP tag on the N-terminus using the *in vivo* site-specific mutagenesis system, *delitto perfetto* (Stuckey et al., 2011). This system leaves no marker gene thus does not interfere with the endogenous promoter of the gene. Irc20 purified from extracts of this strain as described in Section 2.2.1 was visualized by silver staining and western blotting following gel electrophoresis (Figure 3.1). Silver stained gels show multiple faint bands of sizes above and below the expected for Irc20, 180 KDa.

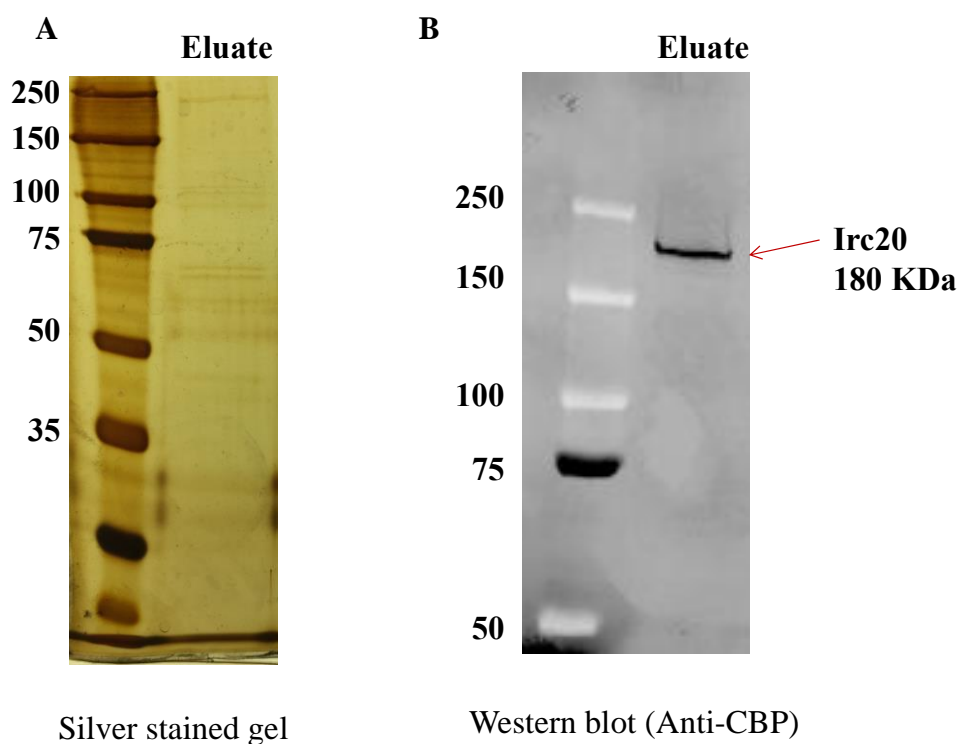


Figure 3.1: Purification of Irc20 under native expression conditions

A. TAP tagged Irc20 was purified from whole cell extracts using double affinity purification, and 10% of the elute was loaded on SDS-PAGE and stained with silver staining. B. 5% of eluted protein was loaded on SDS-PAGE and visualized by western blotting to visualize Irc20 using antibody against CBP part of the TAP tag.

Since the tandem purification steps in the TAP purification protocol are generally highly specific and do not commonly yield contaminants, we attempted to identify whether the co-purified proteins are possibly part of a large multi-subunit complex containing Irc20 as commonly seen with chromatin remodelers (Vignali, Hassan, Neely, & Workman, 2000). To investigate this, we subjected the single affinity TAP purified protein to size exclusion chromatography. Irc20 eluted in several fractions much higher than expected for its molecular weight, ranging from 200-600 KDa, suggesting that Irc20 does not exist in a stable complex of specific molecular weight (Figure 3.2B). Silver staining of these fractions showed several proteins interacting with Irc20 at these fractions (Figure 3.2C), suggesting that Irc20 is promiscuous in its interactions, where it interacts with several proteins forming different transient functional complexes.

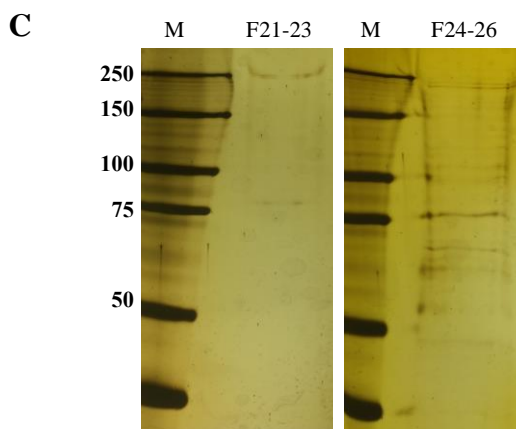
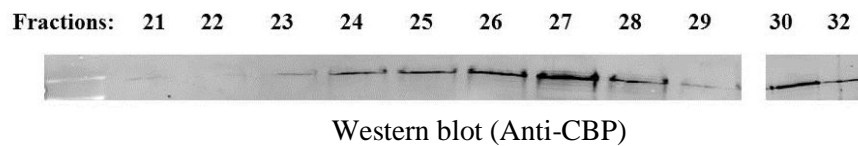
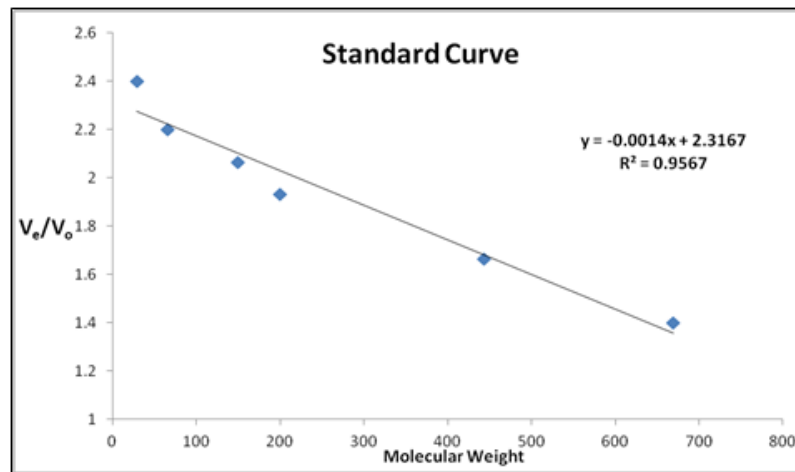
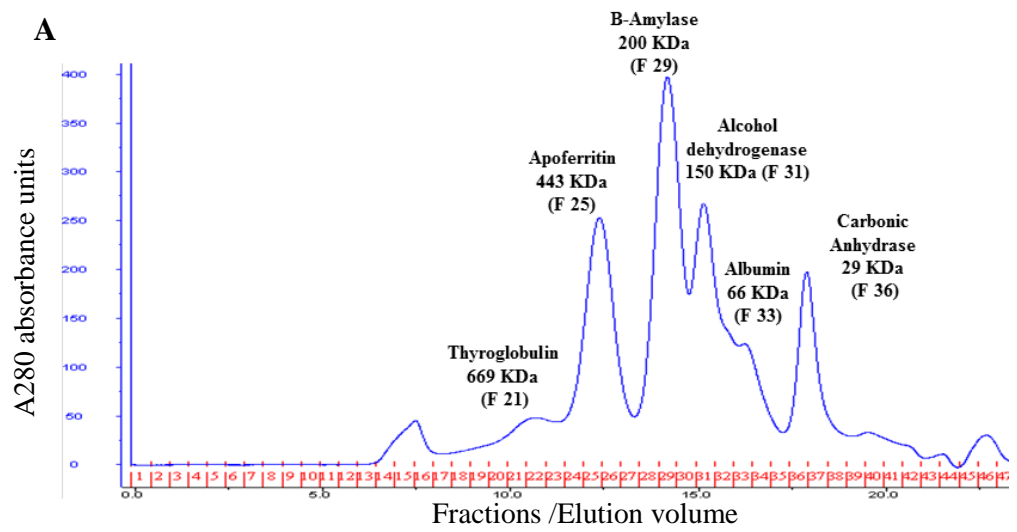


Figure 3.2: Size exclusion chromatography

A. Molecular weight protein standards run on Superose 6 gel filtration column were used to obtain a standard curve. B. Superose 6 Fractions eluted after injection of single affinity purified Irc20 were loaded on SDS-PAGE and detected by western blot with antibody against TAP tag. C. Silver staining of pooled fractions 21-23 and 24-26 showing multiple bands of interacting proteins.

We next attempted to identify these interacting proteins co-purifying with Irc20 using mass spectrometry analysis. Since ubiquitin ligase enzymes like Irc20 are known to interact only transiently with their substrates, using mutants in the ubiquitin ligase domains are frequently used when identifying substrates (Richardson et al., 2013; Rosenbaum et al., 2011), as this mutation causes the enzymes to be stuck on their substrates for longer time making capture of the interactions easier. Single affinity TAP purified wild type Irc20, and Irc20-C1239A mutant, which is mutated at the RING finger domain, were TCA precipitated and analyzed by mass spectrometry. Several proteins were specifically pulled down in Irc20 pull downs compared to untagged control. The top hits for each are listed in Table 3 and Table 4.

Several subunits of the septin ring complex, such as Cdc10, Cdc3, Cdc12, Cdc11 and Shs1 were pulled down specifically with the functional form of the Irc20 protein. This is in addition to Cdc48, which is an AAA-ATPase that works as a segregase to disassemble subunits containing poly-ubiquitylated substrates. As reported earlier, functional Irc20 is required for interaction with Cdc48 (Richardson et al., 2013). Additionally, Irc20 was found to interact with several subunits of the proteasomal system, both the 19S and the 20S subunits of the 26S proteasome. This is observed with both wild type Irc20 and the ubiquitin ligase mutant, reflecting its functional relevance, not a result of misfolding of Irc20 because of the introduced mutation. The interaction with the ubiquitin-proteasomal system is common for ubiquitin ligases where they primarily act to deliver their substrates to the

proteasome. Another prominent group of proteins pulled down with both forms of Irc20 are subunits of the Anaphase-Promoting Complex/Cyclosome (APC/C), an E3 ubiquitin ligase complex responsible for marking several cell cycle proteins for degradation by the 26S proteasome (Arnold, Hockner, & Seufert, 2015).

The previously reported role for Irc20 in transcriptional regulation is also demonstrable in its interactions with transcriptional factors. Irc20 interacts with several subunits of SWI/SNF remodeling complex, INO80, as well as several subunits of the mediator complex of RNA Polymerase II. Irc20 also interacts with several histone modifiers, such as subunits of Rpd3 histone deacetylase, and components of the NuA4 histone H4 acetyltransferase complex. Many transcriptional factors are found specifically bound to the ubiquitin ligase mutant such as Tra1, Swr1, Tfb2 and Taf4, and thus could be potential substrates for Irc20 and may be the way in which Irc20 regulates transcription. Specific interactions with these proteins by reciprocal co-immunoprecipitation need to be performed to confirm these interactions.

3.2.2 Purification of overexpressed Irc20 produces sufficient yield and purity

The presence of multiple protein bands and low yield of Irc20 prohibited the use of this purified protein in *in vitro* biochemical assays. To improve the yield, we attempted to increase the expression level of Irc20 by placing it under the *GALI*-promoter, which drives the expression of the protein to high levels when cells are grown in galactose (Figure 3.3A). Irc20 purified from extracts of this strain was visualized by silver staining and western blotting following gel electrophoresis

(Figure 3.3B). Silver staining of purified protein showed only one band corresponding to the size of Irc20, 180 KDa. The concentration of Irc20 was around 20 ng/ul, or 85 nM, when analyzed by western blot against a CBP-tagged quantified standard (CBP-Snf6). A TAP-tagged ATPase point mutant (K397A) was similarly purified and used as the negative control in the ATP-dependent assays. This yielded protein of around 150 nM.

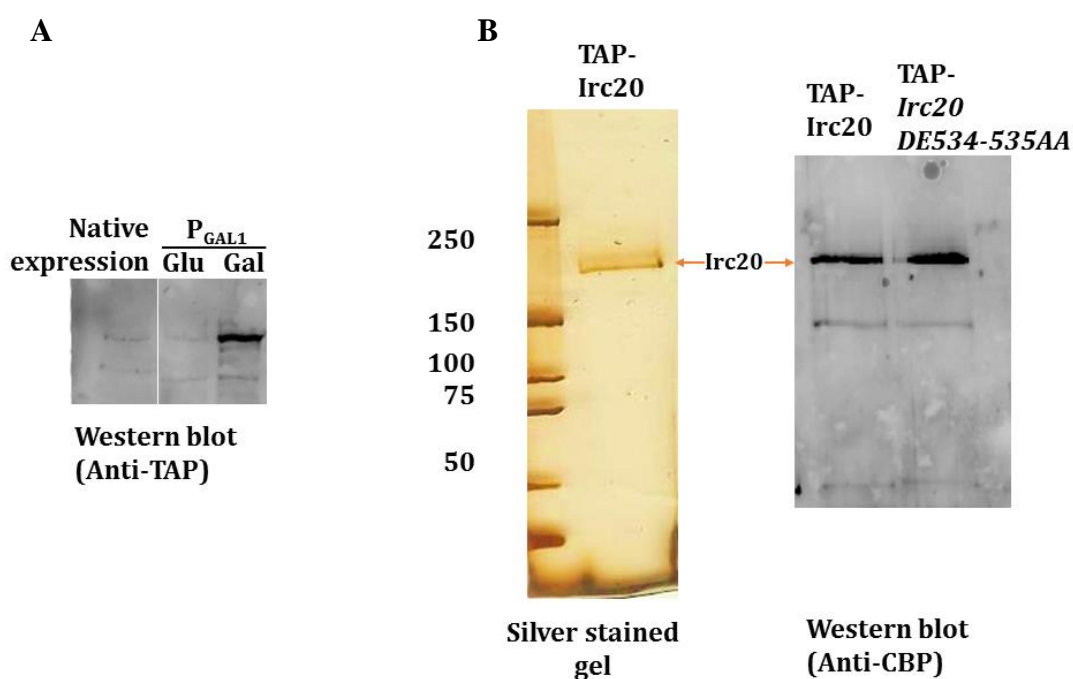


Figure 3.3: Overexpression and Purification of Irc20

A. *GAL1*-promoter was placed upstream N-terminal TAP-Irc20 and the difference in expression level between native and galactose induced expression is shown. B. Overexpressed TAP-Irc20 after purification was loaded on SDS-PAGE and checked for purity by silver staining. Purified wild type Irc20 and ATPase mutant Irc20K397A were normalized and loaded for western blot.

3.3 Irc20 shows DNA and nucleosome binding activities

In order to remodel chromatin, chromatin-remodeling complexes have to be able to recognize and bind to their substrate as a first step. Many chromatin-

remodeling complexes have also been shown to interact with DNA and histones. Cellular chromatin consists of arrays of nucleosomes rather than mononucleosomes. Therefore, we investigated the ability of Irc20 to bind chromatin using a DNA fragment of approximately 2.5 kb in length that was immobilized to paramagnetic beads either as free DNA or following chromatin assembly. We assembled nucleosomes onto the G5E4 DNA template using salt dilution. This DNA template which contains five Gal4-binding sites upstream of the adenovirus two E4 minimal promoter, flanked on both sides by five 5S rDNA nucleosome positioning sequences, was end-biotinylated, reconstituted, and immobilized onto streptavidin paramagnetic beads. After various incubations, the washed immobilized nucleosome arrays were assayed by western blots for the presence of the Irc20 using the anti-TAP antibody. Irc20 was found to be capable of binding to DNA and chromatin with comparable efficiency.

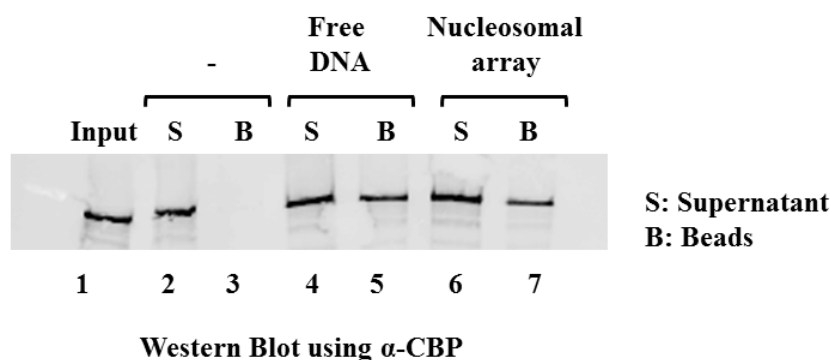


Figure 3.4: Irc20 shows DNA and nucleosome binding activities

Biotinylated G5E4 DNA and nucleosomal arrays were immobilized on streptavidin beads, and incubated with TAP-purified Irc20 for 1 hour at 30°C, then washed twice. Irc20 bound to the immobilized DNA was detected by loading the supernatant and beads on SDS-PAGE and visualized by western blotting using anti-CBP antibody. Lane 1 shows the amount of protein incubated with the beads in each condition (input). Lane 2 and 3 show Irc20 binding to beads without DNA. Lane 4 and 5 show Irc20 binding to DNA. Lane 6 and 7 show Irc20 binding to nucleosomal arrays.

3.4 Irc20 shows ATP hydrolyzing activity

Irc20 possesses an ATP hydrolyzing domain with SNF2 family homology. We tested whether TAP purified Irc20 hydrolyzes ATP using a luminescence based kit which detects ADP produced following ATP hydrolysis. Our results show that Irc20 is able to hydrolyze ATP, whereas a mutation in the Walker A motif (K397A) abolishes this activity (Figure 3.5).

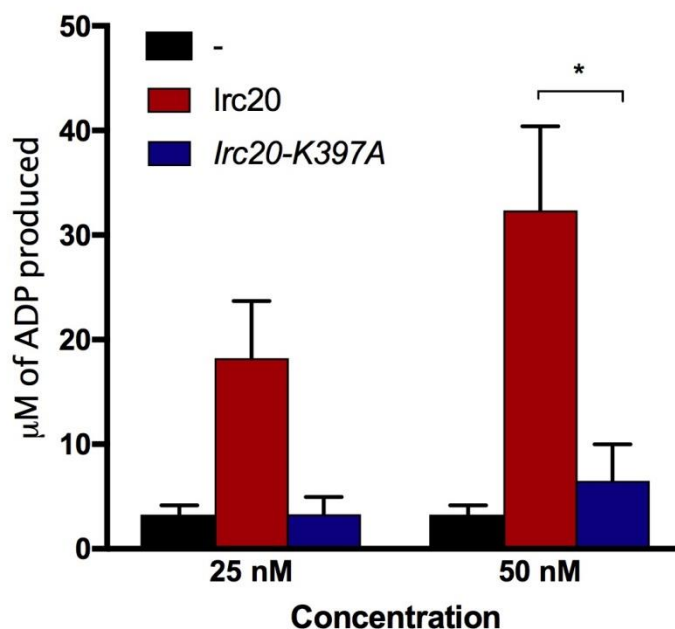


Figure 3.5: Irc20 hydrolyzes ATP

25 and 50 nM of Irc20 were incubated with 1 mM ATP in the presence of DNA for 30 minutes at 30°C. TAP-Irc20 was shown to hydrolyze ATP and produce 30 μ M ADP, whereas the ATPase mutant and no protein control did not show ADP production. Values are presented as Mean \pm SEM, and statistical significance was calculated using student *t*-test. Asterisk shows p value < 0.05 as compared to ATPase domain mutant.

A. GUB mononucleosomal template with SalI restriction site embedded within the nucleosome was used to test the ability of Irc20 to alter chromatin structure. B. Lane 1 shows the position of uncut GUB template, whereas 2 shows position of cut GUB fragment migrating faster. Lane 3 and 4 show the same but for mononucleosomal template. Lanes 5 and 6 show mononucleosomal template incubated with Irc20 for 1 hour at 30°C in the presence of 2 mM ATP, then SalI was added for 1 hour, to digest any altered chromatin by Irc20. Lane 7 is the same as lane 6, but without ATP.

3.6 Conclusion

Here, we report that Irc20 does not form a stable multi-subunit complex, but interacts with several proteins underlying its diverse roles in the cell. The low expression levels from its native promoter necessitated changing the promoter driving its expression to an inducible *GALI*-promoter for purification and subsequent *in vitro* assays. This allowed purification of Irc20 and the ATPase mutant primarily as single proteins. Biochemical characterization reveals that Irc20 has an ATP hydrolyzing activity in the presence of DNA. Irc20, however, does not show chromatin remodeling activity, unlike some other proteins in the Snf2 family.

Chapter 4: Results – Irc20 Recycles Rad52 from DSB Sites during Recombination

4.1 Overview

Several studies implicate Irc20 in facilitating DNA recombinational repair (Alvaro et al., 2007; Miura et al., 2012). Loss of the Irc20 gene causes *increased recombination centers*, hence its name. Even though loss of Irc20 does not show sensitivities to any DNA damaging agents, it was reported that in absence of Irc20, there is less synthesis dependent strand annealing (SDSA), less precise end joining, less gene conversion with short tracts of cross overs, but more gene conversion involving longer tracts of cross overs (Miura et al., 2012). To understand the molecular mechanisms of the role of Irc20 in DNA repair, we analyzed the recombination centers in point mutants of Irc20 in its ATPase and ubiquitin ligase domains. We also tested whether Irc20 physically interacts with Rad52, thereby possibly affecting Rad52 activity at repair foci. Finally, using an inducible DSB at a specific locus using the HO-endonuclease system, we measured recruitment levels of Rad52 by ChIP in the presence and absence of Irc20.

4.2 Both the ATPase and the ubiquitin ligase mutants of Irc20 show increased spontaneous Rad52 foci under non-damaging conditions

In response to DNA damage, proteins involved in HR re-localize into discrete subnuclear foci (Alvaro et al., 2007). Fluorescently tagged Rad52, the major recombinase in homologous recombination, allows monitoring the dynamics of these repair foci. Irc20 was originally identified in a screen of gene deletions causing increased spontaneous Rad52 foci, without affecting the overall recombination

outcome (Alvaro et al., 2007). We sought to identify the activity of Irc20 required for the induction of increased spontaneous Rad52 foci. To do this, we tagged Rad52 with GFPEnvy tag, in strains lacking *IRC20* gene, or having point mutations in the ATPase domain (*DE534-535AA*) or the ubiquitin ligase RING finger domain (*C1239A*). We examined exponentially growing cultures of each strain using a fluorescent microscope, and measured the number of cells having GFP foci per total number of cells per field.

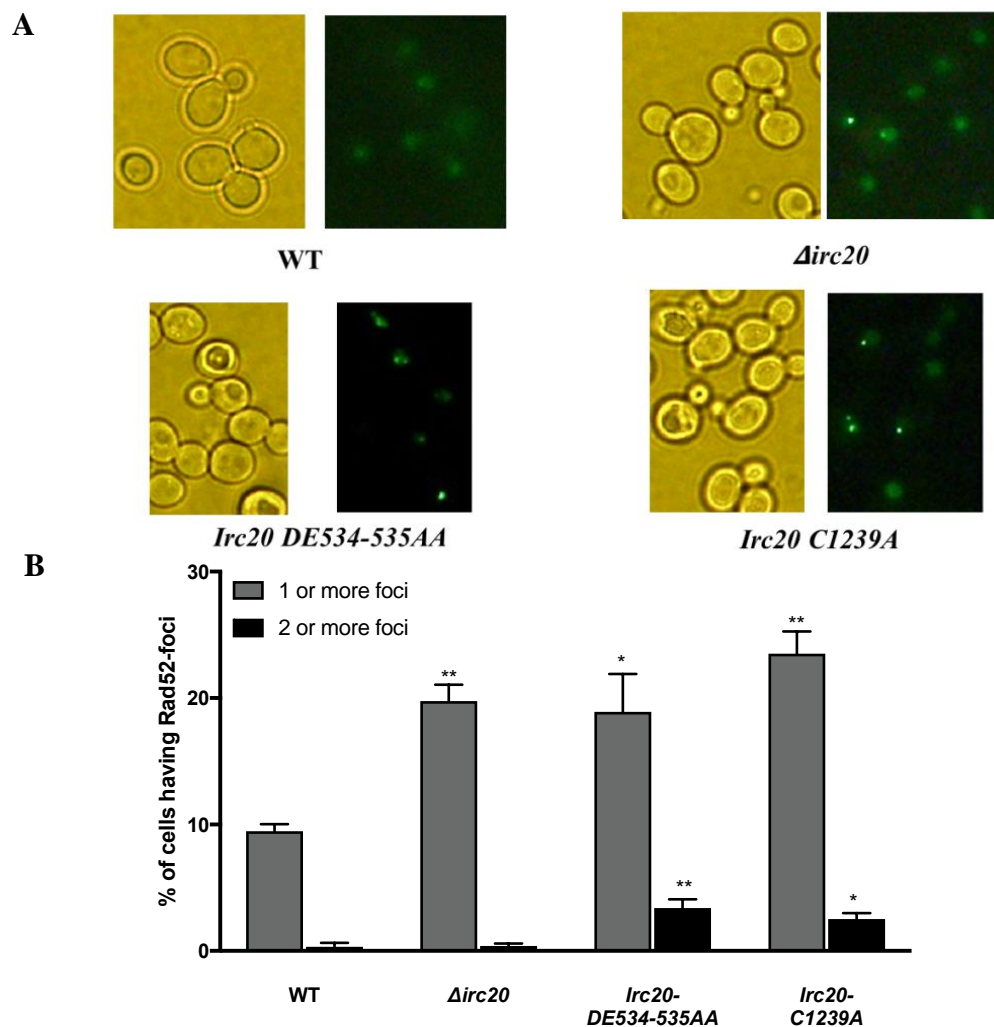


Figure 4.1: Increased Rad52 foci in both ATPase and ubiquitin ligase mutants of Irc20

A. Strains having null or point mutations in *irc20* were tagged with a GFP-tag at the C-terminus of Rad52, and visualized with fluorescent microscopy. $\Delta irc20$, *Irc20-DE534-535AA*, and *Irc20-C1239A* mutants show increased incidence of Rad52 foci. *Irc20* point mutants also show higher number of cells harboring two or more foci per nucleus. B. Foci were counted and quantified for each of the mutant strains. Cells having two or more foci per nucleus were counted separately. Values were analyzed by student *t*-test. One asterisk shows p value<0.05, two asterisks shows p value <0.01, as compared to WT. n=300-500 cells per strain.

Our results show that in wild type cells, around 8% of the cells exhibit visible recombination foci, whereas in $\Delta irc20$ mutant, as previously reported, around 20% of the cells exhibit foci (Figure 4.1). This increased incidence of recombination foci was also observed for point mutants in both the ATPase (K397A) and ubiquitin ligase domains (C1239A), 18% and 22%, respectively (Figure 4.1). Additionally, we observed a marked increase in cells exhibiting more than one foci per cell, which was negligible in wild type cells, but increased five-folds when point mutations in *Irc20* were introduced. These results show that both the ATP-hydrolyzing and ubiquitin ligase activities of *Irc20* are important in regulating spontaneous Rad52 foci generation.

4.3 *Irc20* deletion does not show sensitivities to DNA damaging agents and does not genetically interact with other repair factors

Even though there is an observed increase in recombination centers in the absence of *Irc20*, $\Delta irc20$ do not show any phenotypes or sensitivity to DNA damaging agents (Miura et al., 2012; Richardson et al., 2013). This suggests that *Irc20* works in a non-essential secondary pathway in homologous recombination repair. Genetic assays are commonly used to identify the specific role of a particular protein in DNA repair. These assays utilize double mutations in genes to elucidate common or redundant pathways in which proteins are involved. If a double mutation

causes increased sensitivity to a particular DNA damaging agent, this indicates that these two genes act in parallel to repair the damage induced by this agent. If a double mutation is epistatic to either single mutation, this indicates that they are acting in the same repair pathway. If one mutation rescues the sensitivity of the other, this suggests that both genes are in the same pathway, with one acting upstream of the other.

Using this kind of genetic assay, Miura *et al.* (2012) showed that $\Delta irc20$ rescues the DNA damage sensitivities observed in $\Delta mre11$ mutants (Miura *et al.*, 2012). They used this to conclude that Irc20 works upstream of Mre11 in homologous recombination repair to facilitate its action as a nuclease. While it was suggested that their results are due to the helicase activity of Irc20 (Miura *et al.*, 2012), the involvement of the ubiquitin ligase activity cannot be excluded. To identify the activity of Irc20 responsible for this potential function, we sought to delete *mre11* gene in strains having point mutations in each of the functional domains of Irc20. We used serial dilutions of exponentially growing cells and spotted them on YPD with and without DNA damaging agents and allowed them to grow for 2-3 days. To our surprise, a double mutant of $\Delta irc20$ and $\Delta mre11$ was as sick as $\Delta mre11$, unlike the previously reported result of synthetic rescue (Figure 4.2A). We suspected that the difference in strain background to be the reason for this difference in phenotype observed in our study perhaps because we were using primarily the BY4741 yeast strain background while Miura *et al.* (2012) used the W303 background. However, when we repeated the phenotype with the W303 strain background, we were still not able to observe $\Delta irc20$ rescuing the DNA

damage sensitivities of *Amre11* mutants. Therefore, it is likely that in the construction of double mutants by Miura *et al.* (2012) the *Amre11* cassette would have replaced the *Airc20* cassette, resulting in a single mutant of *irc20*.

We utilized a similar genetic assay to investigate other pathways by which Irc20 could mediate its recombinational role. We, however, did not observe any positive or negative genetic interactions for Irc20 with other repair genes tested such as Rad6, Rad5, Rad18, Srs2, Rad52, and Rad27. The growth assays for Rad6 and Rad18 is shown in Figure 4.2B.

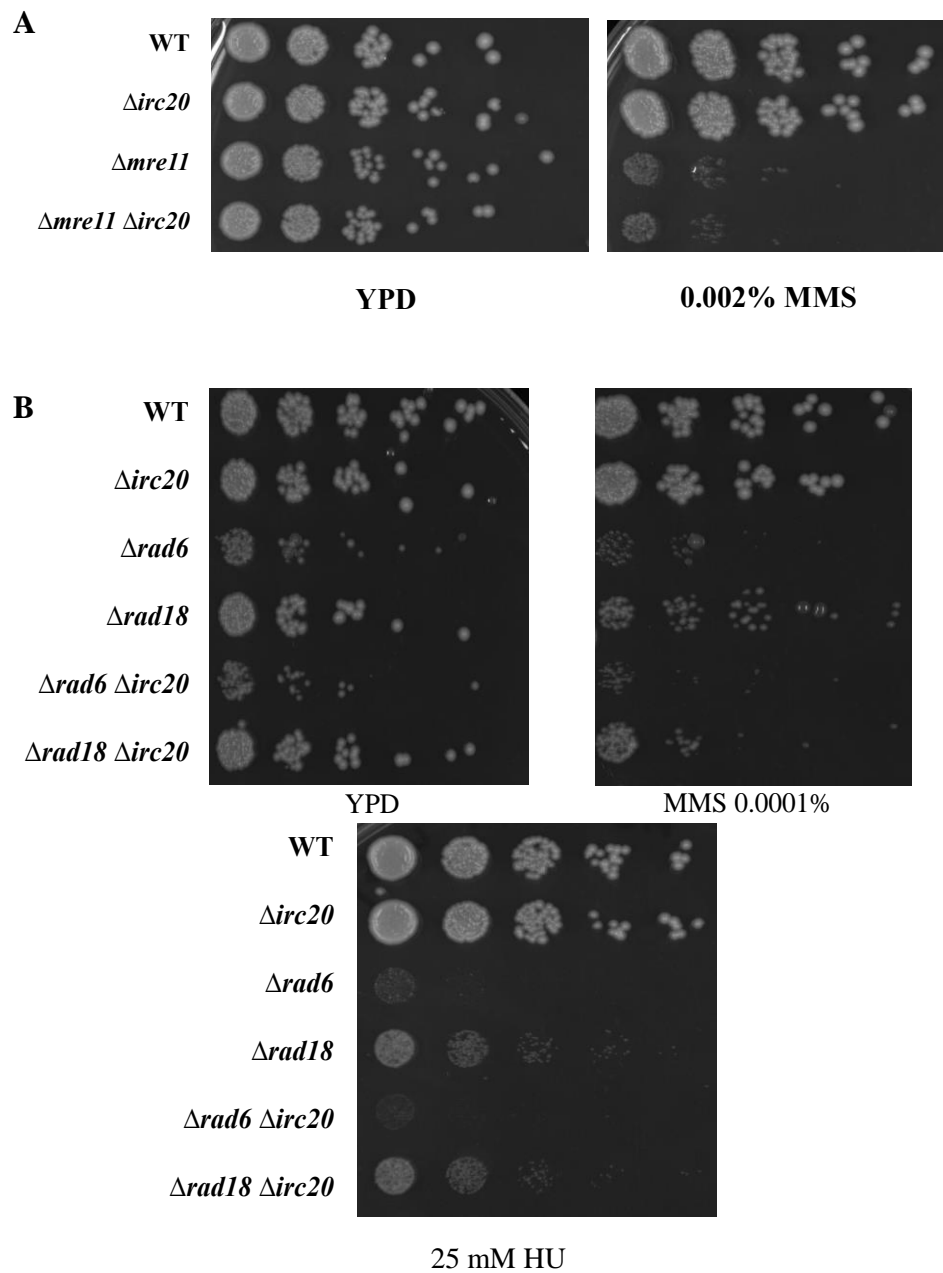


Figure 4.2: Irc20 does not show synthetic rescue with Mre11 or display genetic interactions with other DNA repair factors

Serial dilutions of exponentially growing cells were spotted on YPD with and without DNA damaging agents. A. Double mutant of $\Delta irc20$ and $\Delta mre11$ was equally sick as $\Delta mre11$ when cells were spotted on YPD media containing 0.002% MMS. B. Similar genetic assays were done using $\Delta rad6$ and $\Delta rad18$ and no positive or negative genetic interactions were observed when cells were spotted on YPD containing MMS or hydroxyurea.

4.4 Irc20 interacts with Rad52

The earlier report had only implicated Irc20 as a helicase working upstream of Mre11 facilitating its nuclease activity (Miura et al., 2012). Since genetic interaction with Mre11 was now questionable, and since we observed increased Rad52 foci in the ubiquitin ligase mutant, we sought to investigate the functional and physical relationship between Irc20 and Rad52. We suspected that Irc20 may play a dual role using both its ATPase and ubiquitin ligase domains to direct the HR pathways to SDSA and shorter tract gene conversion events. As E3 ubiquitin ligases ligate ubiquitin moieties to proteins to facilitate primarily their proteolytic degradation, we tested whether Rad52 could be a substrate for Irc20. Towards this, we tested the possible physical interaction between Irc20 and Rad52 using co-immunoprecipitation experiments. This was done by tagging Irc20 with the Myc-tag in a strain where Rad52 was tagged with GFPEnvy. Pull downs were done using anti-Myc antibody and the IP was probed for Rad52 interaction using anti-GFP antibody (Figure 4.3). Our results show a weak but visible interaction, characteristic of interactions between ubiquitin ligases and their substrates.

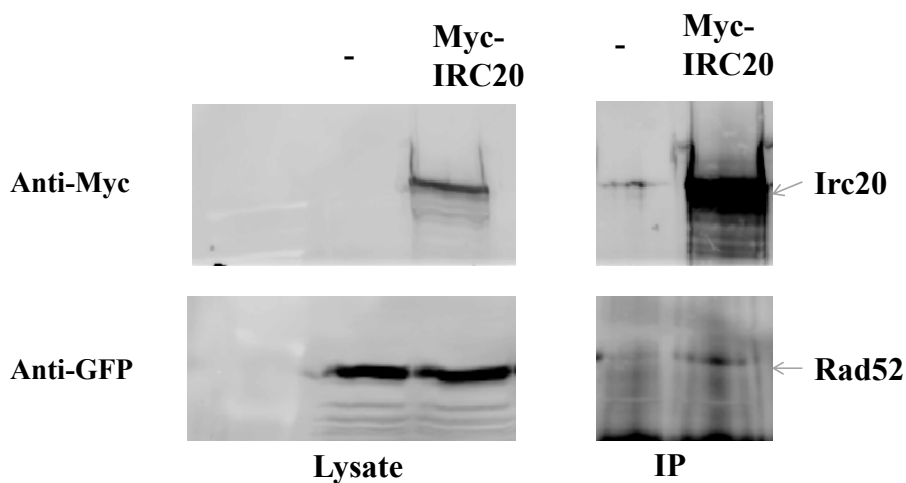


Figure 4.3: Irc20 physically interacts with Rad52 weakly

Co-immunoprecipitation shows weak immunoprecipitation of GFP-Rad52 with 13Myc-tagged Irc20 pulled down using anti-myc antibody on Protein G Dynabeads. IP samples were loaded on SDS-PAGE. Upper panel shows blot probed with anti-Myc to detect pulled down Irc20. Lower panel shows blot probed with anti-GFP to detect Rad52 interaction with Irc20.

4.5 Irc20 facilitates the removal of Rad52 during DSB repair

We next attempted to understand how the absence of Irc20 affects Rad52 recruitment and dynamics at a specific inducible DSB site by *HO endonuclease*. We utilized a well-standardized system for monitoring the dynamics of recruitment of repair factors at a specific DSB (Bennett, Papamichos-Chronakis, & Peterson, 2013; Eapen, Sugawara, Tsabar, Wu, & Haber, 2012). This system uses the *HO endonuclease*, which introduces a cut at the MAT locus on chromosome III during mating type switching. The *HO endonuclease* in this assay is placed under the *GALI*-promoter, thus it is repressed in the presence of glucose, and only induced in the presence of galactose. Additionally, the donor sequences for the MAT locus, the

HMR and HML, are deleted, in order to delay the repair process for easier monitoring of the dynamics of protein recruitment to DSB site.

We tagged Rad52 with 13Myc-tag in the JKM139 strain, which has the *HO endonuclease* gene under the *GALI*-promoter. Rad52 recruitment to regions around DSB at 0.18 kb, and 2.1 kb to the right of the break (distal from centromere), was monitored using chromatin immunoprecipitation experiments (ChIP) and quantified by real time PCR using region specific primers (Figure 4.4). For each time point, the signal from a site near the HO DSB at the MAT locus is normalized to that from the non-cleaved *ACT1* locus in ChIP and input DNA samples. For each time point and site, the ChIP signals are normalized to the input DNA signals, because DNA end resection can reduce the available DNA template. Finally, relative-fold enrichment was calculated by dividing the absolute-fold enrichment from induced cells to that of un-induced cells.

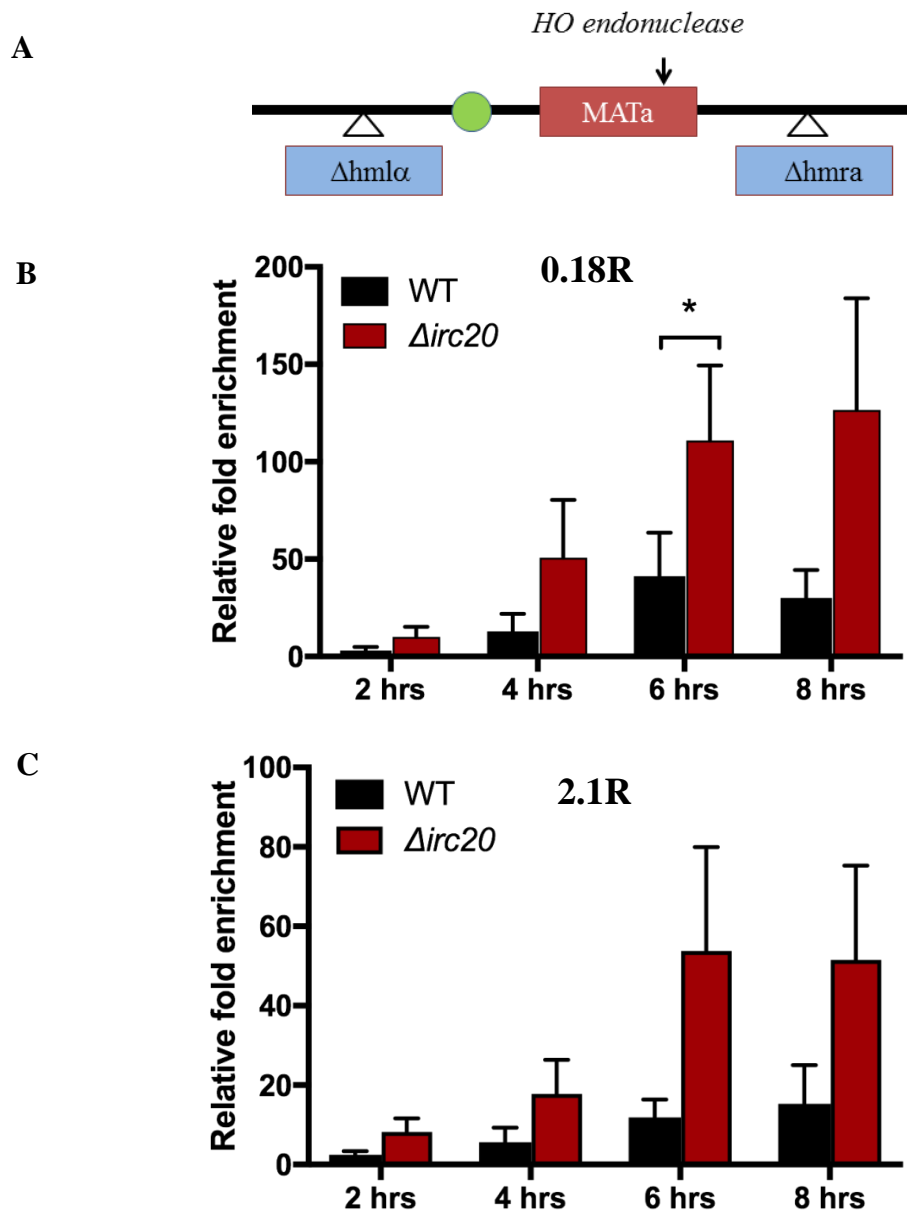


Figure 4.4: Irc20 controls levels of Rad52 at an induced DSB

A. Diagram illustrating HO endonuclease introducing a cut at MAT locus during mating type switching. B and C. Chromatin Immunoprecipitation for 13Myc-Rad52 using anti-myc antibody immobilized on protein G Dynabeads, in the presence and absence of Irc20. Two regions were checked, 0.18 kb (Panel A) and 2.1 kb (Panel B) distal to centromere. Absolute-fold enrichment for Rad52-Myc at the HO DSB was calculated as follows: for each time point, the signal from the indicated site near the HO DSB at the MAT locus was normalized to that from the non-cleaved *ACT1* locus in ChIP and input DNA samples. For each time point and site, the ChIP signals were normalized to the input DNA signals. Finally, relative-fold enrichment was calculated by dividing the absolute-fold enrichment from induced cells to that of un-induced cells. The results of three independent experiments were used. Values are presented as Mean \pm SEM. One asterisk shows p value <0.05

For both 0.18 kb and 2.1 kb regions, Rad52 enrichment was increased in the $\Delta irc20$ mutant compared to the wild type control. The relative-fold enrichment of Rad52 at 0.18R peaks at around 40-fold at 6 hours after DSB induction, whereas in $\Delta irc20$ it reaches 100-fold at 6 hours and peaks at 120-fold at 8 hours after DSB induction. At 2.1R, the relative-fold enrichment peaks at around 20-folds at 8 hours after DSB induction, whereas in $\Delta irc20$ mutants the relative-fold enrichment reaches 50-folds after 6 hours following DSB induction. As can be observed in (Figure 4.4), at all-time points and regions tested, $\Delta irc20$ mutants showed 2 to 3-fold higher relative enrichment compared to the wild-type strain. These results suggest that Irc20 promotes the removal of Rad52 during DSB repair.

4.6 Conclusion

To better understand the role of Irc20 in controlling spontaneous Rad52 foci formation, we dissected the Irc20 functions by introducing point mutations in both its functional domains. We observed higher incidence of foci in mutants of both functional domains, and a marked increase in cells harboring two or more foci per cell, which is normally negligible in wild-type cells. We also used genetic assays to probe Irc20 function, but were not able to reproduce an earlier report by Miura *et al.*, and did not find significant genetic interactions to conclude any particular pathway involvement. Moreover, we tested interactions between Irc20 and Rad52, and observed physical interaction in the absence of DNA damage. It would be interesting to test the physical interaction of Irc20 with Rad52 in the presence of damaging agents. We, finally, measured recruitment kinetics of Rad52 to a specific induced DSB in the presence and absence of Irc20 and observed higher relative enrichment

levels of Rad52 in $\Delta irc20$ mutants at all-time points and regions tested. Altogether, these results suggest a role for Irc20 as a regulator of Rad52 enrichment at DSBs either to control recombination, or possibly to recycle Rad52 and allow for subsequent repair events thus facilitating homologous recombination.

Chapter 5: Results – Irc20 Regulates 2- μ m Plasmid Levels

5.1 Overview

The 2- μ m yeast endogenous plasmid is tightly regulated to be maintained at 40-60 copies per cell. The control of copy number and the partitioning of the 2- μ m plasmid is regulated by SUMO and ubiquitin modifications mediated by the cellular machinery. During the course of our study, we noticed the spontaneous generation of strains lacking the endogenous 2- μ m plasmid [*cir*⁰] when *IRC20* is deleted or when point mutations are introduced into the ATPase or the ubiquitin ligase domain. This prompted us to examine the potential role that Irc20 plays in the 2- μ m plasmid stability and copy number control. Towards this, we measured the 2- μ m plasmid presence in several strains having null or point mutations in *IRC20*. We also analyzed the 2- μ m plasmid stability using two modified 2- μ m plasmids harboring selection markers, differing in the presence or absence of *FLP1*. To examine the role of Irc20 in the 2- μ m plasmid copy number control, we measured the 2- μ m plasmid levels in *irc20* mutant strains. Moreover, we studied the forms in which the 2- μ m plasmid exists in Irc20 mutant strain by Southern blot. Finally, we investigated the role of Irc20 in regulating the levels of tagged-Flp1 expressed from a repressible promoter.

5.2 Mutations in *IRC20* gene occasionally generate [*cir*⁰] strains

At several points during our study, we observed the generation of strains lacking the 2- μ m plasmid, which normally has a loss rate of 10^{-5} - 10^{-4} per cell division. This prompted us to study how frequent this phenomenon may be. To do

this, we used [cir⁺] strains grown overnight in YPD, then plated them to analyze single colonies. Eight single colonies for WT, *Δirc20*, *Irc20-DE534-535AA*, and *Irc20-C1239A* were analyzed for the presence of the 2- μ plasmid using colony PCR using primers specific for the 2- μ plasmid sequence. We observed the occasional loss of the plasmid when *irc20* is deleted or in a strain where the ubiquitin ligase activity of Irc20 was abrogated (Figure 5.1). 1-2 colonies in 8 colonies tested did not harbor the generally highly stable 2- μ plasmid in the *Δirc20* strain and the Irc20 ubiquitin ligase mutant.

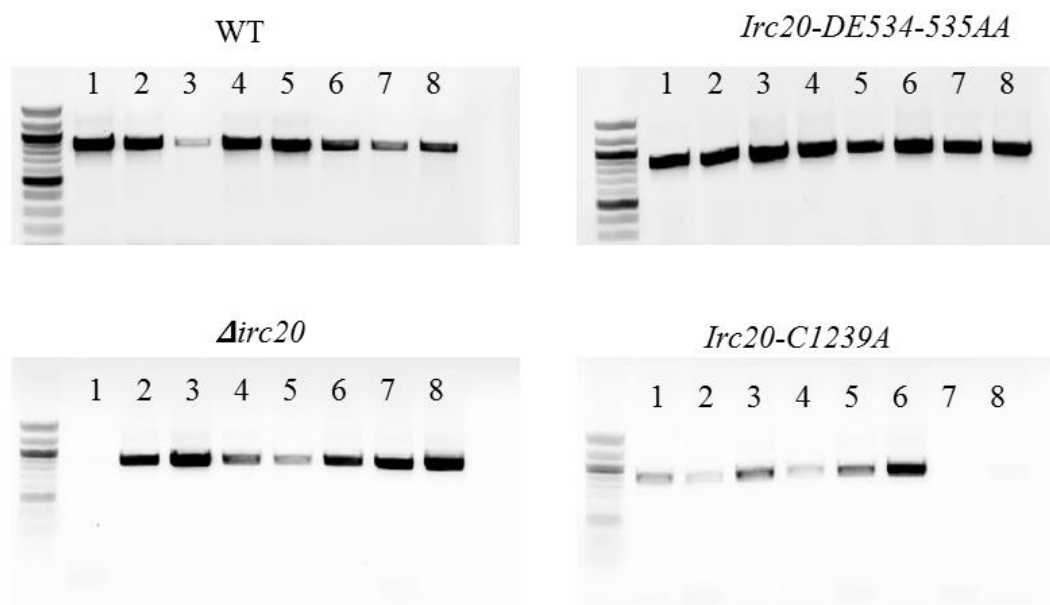


Figure 5.1: Absence of Irc20 ubiquitin ligase activity leads to the occasional loss of the endogenous 2- μ plasmid

Eight single colonies from WT, *Δirc20*, *Irc20-DE534-535AA* and *Irc20 C1239A* were analyzed by colony PCR to detect the presence of the endogenous 2- μ plasmid after overnight growth. Occasional loss of the endogenous 2- μ plasmid was observed (1 in 8 for *Δirc20* and 2 in 8 for *Irc20-C1239A*).

5.3 The loss of 2- μ m plasmids does not occur if plasmids do not harbor the Flp1 gene

We suspected a role involving the partitioning system of the endogenous 2- μ m plasmid comprising of Rep1, Rep2, and the partitioning locus *STB* (Ahn et al., 1997). We used a KanMX4 tagged 2- μ m plasmid (pKAN4) as a measure of endogenous 2- μ m plasmid stability. To determine the rate of pKAN4 loss, yeast transformants were initially grown in YPD medium containing the antibiotic Geneticin to select for retention of the plasmid. The proportion of plasmid-containing cells was then determined after 15 generations of growth in medium that did not select for the retention of the plasmid (YPD), by comparing plating efficiency on solid YPD medium containing or lacking Geneticin. We used *Arsc2* mutant as a positive control for this experiment as it is known to have lower plasmid retention rates owing to the role of RSC2 in 2- μ m plasmid partitioning (Pinder et al., 2013; Wong et al., 2002).

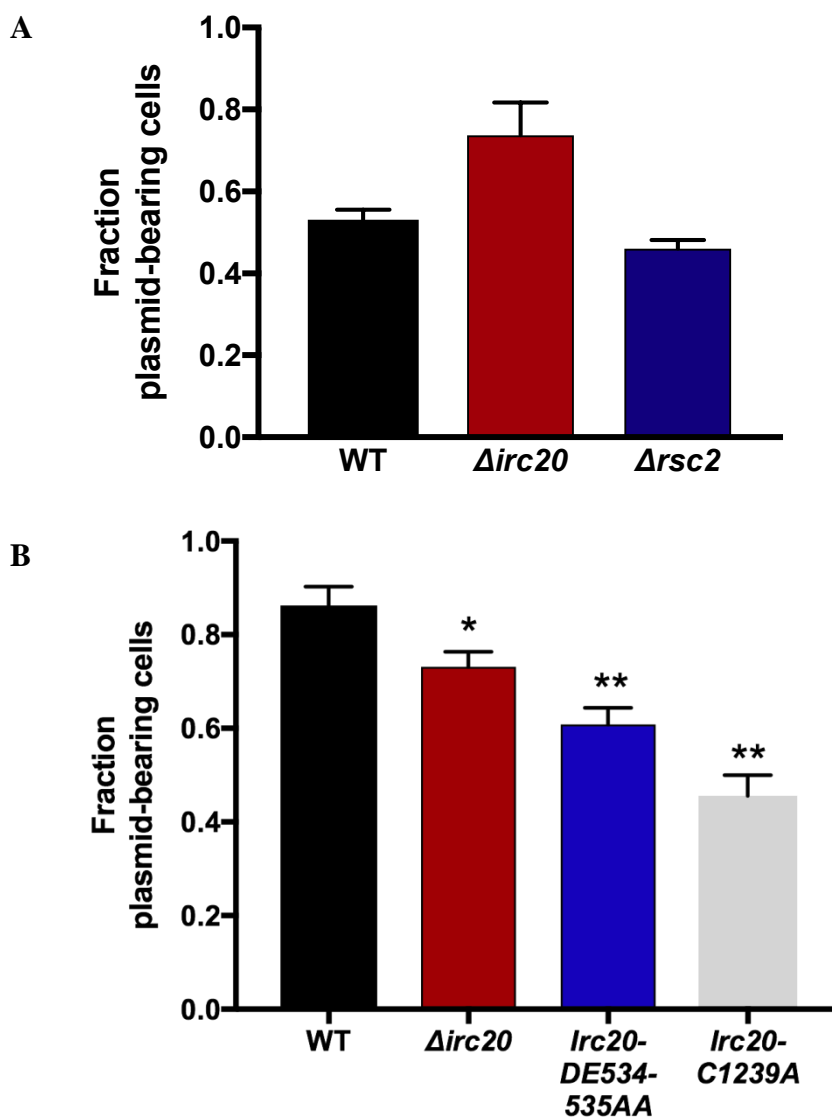


Figure 5.2: $\Delta irc20$ mutant only show loss in 2- μ m stability if the 2- μ m plasmid harbors a *Flp1* gene

The fraction of plasmid bearing cells were calculated by counting the number of colonies on selection plates (Geneticin or SD-His) compared to the number of colonies on non-selective plate (YPD) in three different independent cultures of each strain. A. Plasmid segregation efficiency was calculated for pKAN4, a modified form of the 2- μ m plasmid where *FLP1* gene is absent, and *KANMX6* is inserted to allow for selection. B. Plasmid segregation efficiency was calculated for p2 μ m-His3MX6-STB, a modified form of the 2- μ m plasmid where a *HIS3MX6* is inserted downstream of the *STB* locus to allow for selection. Values are presented as Mean \pm SEM. One asterisk shows pvalue<0.05, two asterisks shows pvalue <0.01, as compared to WT.

To our surprise, the stability of the pKAN4 plasmid was not reduced in the *Δirc20* strain, but rather, it showed higher stability (Figure 5.2A). A *Δrsc2* mutant, however, showed less pKAN4 plasmid stability, at a similar level to a previous report (Pinder et al., 2013). This led us to suspect a role involving the Flp1 gene since pKAN4 differs from the endogenous 2- μ m plasmid in that it lacks *FLP1*.

To reconcile the discrepancies in the 2- μ m plasmid segregation efficiency, we constructed a new 2- μ m plasmid harboring a *HIS3MX6* cassette (which allows the cells to grow on media lacking Histidine) inserted downstream the *STB* locus. To determine the rate of p2 μ m-His3MX6-STB loss, yeast transformants were initially grown in SD-His medium to select for the retention of the plasmid. The proportion of plasmid-containing cells was then determined after 15 generations of growth in medium that did not select for the retention of the plasmid (YPD), by comparing the plating efficiency on solid YPD versus SD-His media. Using this construct, we were able to detect lower plasmid segregation efficiency in *irc20* mutant strains as compared to WT (Figure 5.2B). The 2- μ m plasmid segregation efficiency is lower when cells harbor point mutations in either the ATPase or the ubiquitin ligase domain of Irc20, than when the *IRC20* gene is deleted. The maximum reduction in plasmid segregation efficiency is seen in the ubiquitin ligase mutant (*Irc20-C1239A*), where the fraction of cells bearing the plasmid reached 0.5 as compared to WT where it was 0.85. It is worth-noting that the pKAN4 and the p2 μ m-His3MX6-STB differ in the plasmid background, where pKAN4 contains bacterial maintenance sequences and the p2 μ m-His3MX6-STB does not. This accounts for the difference in

plasmid segregation efficiencies between both in WT strains, as introduction of DNA sequences in the endogenous 2- μ m plasmid is known to affect its stability.

5.4 The 2- μ m plasmid copy numbers are elevated in *Irc20* null mutant but not in point mutants

We next attempted to measure the 2- μ m plasmid levels in [*cir*⁺] strains, expecting to see lower levels of the 2- μ m plasmid reflecting the loss of 2- μ m plasmid in a subpopulation of cells while exponentially growing, as observed earlier. We measured the levels of the 2- μ m plasmid by isolating DNA from wild-type and *irc20* null and point mutant strains, and quantified by real time PCR using 2- μ m specific primers normalized to a genomic control region.

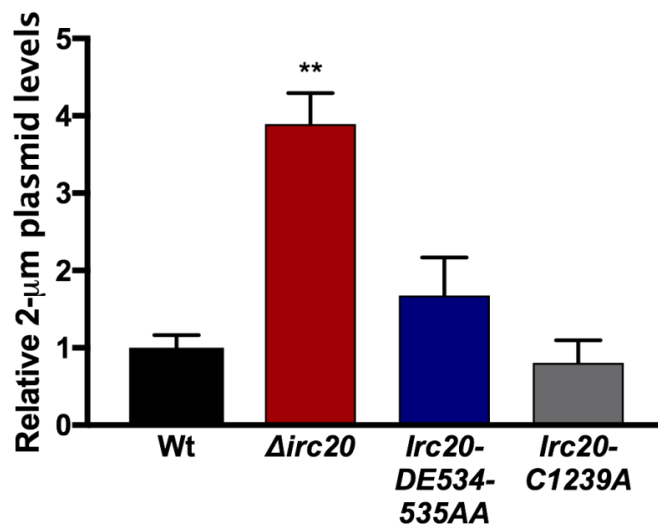


Figure 5.3: Elevated 2- μ m plasmid levels are observed in Δ *irc20*, but not in point mutants

The levels of the endogenous 2- μ m plasmid in null and point mutants of *irc20* were measured by real time PCR, using primers specific for the 2- μ m plasmid relative to Y-subtelomeric regions. A Δ *irc20* mutant showed 3 to 4-fold higher levels of the 2- μ m plasmid, whereas point mutants in the ATPase and ubiquitin ligase domains of *Irc20* showed normal levels. Three to six independent cultures were analyzed. Statistical significance was calculated by two-tailed Student *t*-test for unpaired samples. Two asterisks show *p*value <0.01.

Surprisingly, a *Δirc20* mutant showed three to four-fold higher 2- μ m plasmid levels (Figure 5.3). Even though elevated 2- μ m levels is commonly seen in SUMO and ubiquitin pathway mutants, it was unexpected to observe the same in *Δirc20* mutant since a *Δirc20* mutant does not show cold sensitivities and nibbled colony appearance as that observed in strains accumulating higher 2- μ m plasmid levels. We also, measured the 2- μ m levels in point mutants of Irc20 in its functional domains. Neither the ATPase domain mutant nor the ubiquitin ligase domain mutant showed elevated 2- μ m plasmid levels (Figure 5.3), this can be attributed to the more pronounced loss of the 2- μ m plasmid in these mutants as observed by the plasmid loss assay.

5.5 The elevation in 2- μ m plasmid copy number in Irc20 null mutant is dependent on HR

The elevation of the 2- μ m plasmid in several SUMO pathway mutants, such as *Δsiz1Δsiz2*, and STUbLs, such as *Δslx5* and *Δslx8*, have already been reported and is considered to be responsible for the sickness observed in these strains, such as the nibbled colony appearance and cold sensitivities (Chen et al., 2005). This elevated 2- μ m plasmid copy number, and associated sickness were found to be dependent on HR repair factors such as Rad52, Mre11 and Rad59 (Xiong et al., 2009). This was also shown to be dependent on the hyperactivity of Flp1, resulting in hyper-recombination and accumulation of aberrant high molecular weight structures of the 2- μ m plasmid that are toxic to the cell (Xiong et al., 2009). Even though we had not observed sensitivities in the *Δirc20* mutant, we still tested whether the elevation of 2-

μm levels was dependent on the HR pathway. For this, we checked the 2- μm plasmid levels in $\Delta\text{irc}20\Delta\text{rad}52$ and in the $\Delta\text{irc}20\Delta\text{mre}11$ double mutants.

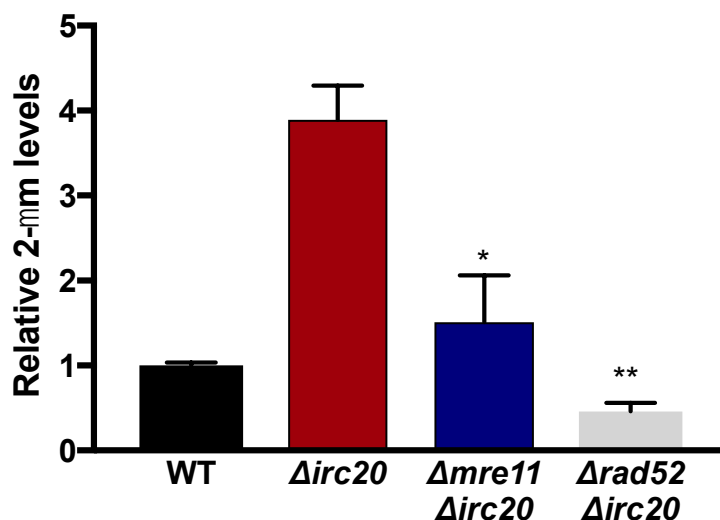


Figure 5.4: The hyper-amplification of the 2- μm plasmid in $\Delta\text{irc}20$ mutants is dependent on HR factors

The levels of 2- μm plasmids in $\Delta\text{irc}20$, $\Delta\text{mre}11\Delta\text{irc}20$ and $\Delta\text{rad}52\Delta\text{irc}20$ mutants were measured by real time PCR using primers specific to 2- μm plasmid DNA sequence and quantified relative to Y-subtelomeric regions. Double mutants of *irc20* with HR repair factors significantly reduces the 2- μm plasmid levels compared to a single $\Delta\text{irc}20$ mutant. Three to four independent cultures were analyzed. Statistical significance was calculated by two-tailed Student *t*-test for unpaired samples. One asterisk shows *p*value <0.05 and two asterisks show *p*value <0.01.

We observed a significant reduction in the 2- μm levels when loss of the *IRC20* gene was coupled with loss in HR factors, such as Mre11 and Rad52 (in $\Delta\text{mre}11\Delta\text{irc}20$ and $\Delta\text{rad}52\Delta\text{irc}20$ double mutants). The reduction was more pronounced in double mutants with *RAD52*, possibly reflecting some residual homologous recombination events occurring in the absence of Mre11. These results indicate that the amplification of the 2- μm copy number in $\Delta\text{irc}20$ mutant is due to improperly regulated HR events.

5.6 The *Irc20* null mutant and the ATPase domain mutant both show production of a high molecular weight form of the 2- μ m plasmid

SUMO pathway mutants were shown to have an aggregated form of the hyperamplified 2- μ m plasmid underlying the sensitivities observed (Xiong et al., 2009). We investigated the form in which the 2- μ m plasmids predominantly exist in the Δ *irc20* mutant by southern blotting using uncut DNA isolated from the WT and the *irc20* mutants. The DNA was probed with biotinylated oligos specific to the 2- μ m sequence. Both the ATPase domain and ubiquitin ligase domain mutants were analyzed, but we later realized that the ubiquitin ligase mutant had lost the 2- μ m plasmid, and thus the 2- μ m plasmid form in this mutant was not detected in this experiment (see Figure 5.5, last lane).

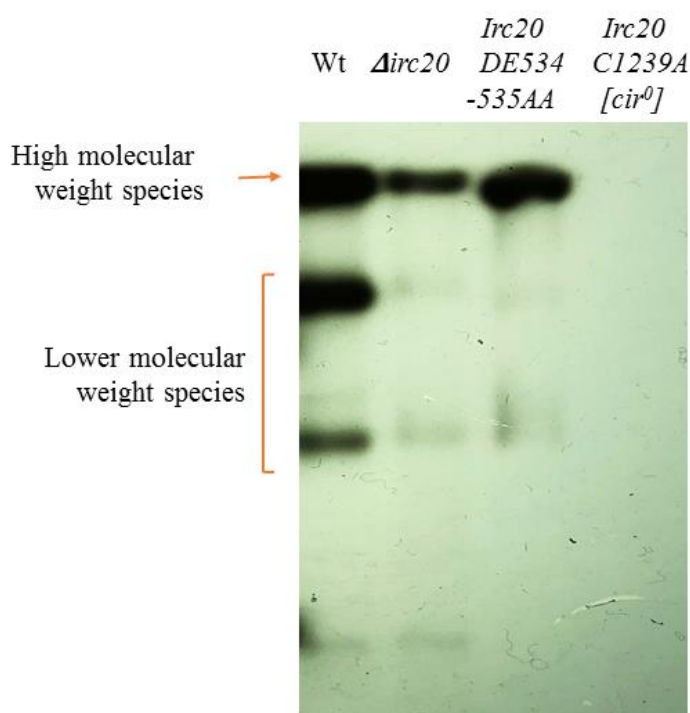


Figure 5.5: Formation of high molecular weight forms of 2- μ m in Δ *irc20* and ATPase domain mutant *Irc20*-DE534-535AA

DNA isolated from WT, $\Delta irc20$ and *Irc20-DE534-535AA* mutants were run on 1% agarose gel with 0.75 $\mu\text{g/ml}$ chloroquine in 1XTBE at 3 V/cm for 21 hours. The DNA was transferred to nylon membrane overnight, and the membrane was probed with biotinylated probes specific to 2- μm sequence. The hybridized probes were then visualized using Thermo Scientific™ Pierce™ Chemiluminescent Nucleic Acid Detection Module which uses streptavidin bound horse radish peroxidase and visualized by chemiluminescence. The first lane shows DNA from a WT strain, 2- μm exists in several forms, possibly of different linking numbers, and unresolved concatemers. DNA from $\Delta irc20$ and *Irc20-DE534-535AA* shows the 2- μm plasmid predominantly existing as high molecular forms, possibly as unresolved concatemers owing to Irc20's role in HR.

High molecular weight forms of the 2- μm were found to be the predominant species in the $\Delta irc20$ and ATPase domain mutants (*irc20-DE534-535AA*), as opposed to wild type strains which show multiple forms, reflecting the multiple concatamer forms that exist during copy number amplification of the plasmid. Despite the normal levels of the 2- μm plasmid in the ATPase domain mutant, the high molecular weight form was still the predominant form present. Therefore, it is possible to envisage two separate roles for Irc20 leading to hyper-amplification and the resolution of the concatamer forms of the 2- μm plasmid in yeast.

5.7 Irc20 controls copy number amplification of the 2- μm plasmid by regulating the Flp1 protein levels in the cell

Since Flp1 is the enzyme responsible for amplifying the copy number of 2- μm plasmid in case of mis-segregation, we tested whether Irc20 could be regulating the Flp1 levels in the cell. To test this, the FLP1 gene was cloned into a centromeric plasmid (pRS416), under the *GALI*-promoter with a YFP-tag at the C-terminus. This plasmid was transformed into WT and an $\Delta irc20$ mutant, and grown in raffinose overnight. To induce expression, the cells were grown for 6 hours in galactose, then transferred to glucose-containing medium, to switch off expression, and monitor the degradation of Flp1 in the presence or absence of Irc20. This *GALI*-promoter system

allows for shutting off expression, to monitor the existing levels of a protein without interference from newly expressed ones.

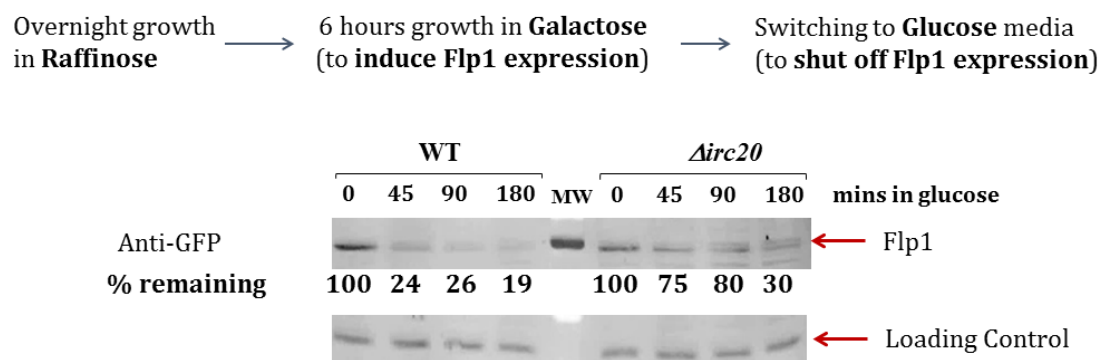


Figure 5.6: Irc20 regulates Flp1 levels

WT and an $\Delta irc20$ mutant were transformed with a centromeric plasmid (pRS416) expressing GFP-tagged Flp1 under *GALI*-promoter. Cells were grown for 6 hours in 2% galactose to induce expression of Flp1, then transferred to glucose media to monitor the degradation of Flp1 in presence or absence of Irc20. Cells were pelleted at 45, 90, and 180 minutes. Whole cell extracts were prepared, run on SDS-PAGE, and Flp1 levels were monitored by western blotting using anti-GFP antibody.

We observed higher stability and less degradation of Flp1 in cells lacking Irc20 ($\Delta irc20$ mutant). The levels of Flp1 reduced to 26% by 90 minutes in wild-type cells following switching to glucose media, whereas it remained at 75-80% levels in the $\Delta irc20$. This suggests that the increased copy number of the 2- μ m plasmid in $\Delta irc20$ cells could be, at least partly, due to increased Flp1 levels.

5.8 Conclusion

We identified a novel role for Irc20 in regulating the 2- μ m plasmid levels. We discovered that the $\Delta irc20$ mutant show higher 2- μ m levels associated with decreased 2- μ m stability in a manner dependent on HR. We also observed that the 2-

μ m plasmids in the $\Delta irc20$ mutant as well as the ATPase domain mutant predominantly exist in high molecular weight forms. Finally, we observed less degradation of Flp1, which is responsible for initiating the 2- μ m plasmid copy number amplification in $\Delta irc20$ mutant compared to the wild-type.

Chapter 6: Discussion and Future Prospectives

6.1 Irc20 is an ATPase that does not alter the chromatin structure

The *S. cerevisiae* protein Irc20 is classified as a helicase-like protein from the SF2 superfamily of helicases (Flaus et al., 2006). Within this superfamily, helicases are divided based on sequence homologies into several families, and proteins with homology to the Snf2p were grouped into the Snf2 family. Further grouping divides the Snf2-family proteins into 24 subfamilies, with Irc20 belonging to the SHPRH subfamily. The SHPRH subfamily, as well as the Rad5/Rad16, and Ris1 subfamilies are unique in that they possess a RING domain characteristic of RING-type E3 ubiquitin ligases. Although being classified into the Snf2 family based on sequence homology to the catalytic subunit of the SWI/SNF chromatin remodeler, Snf2, only some of the families have members that can alter DNA-histone interactions and thus chromatin structure (Becker & Horz, 2002). Most of the remaining family members utilize the energy produced by ATP hydrolysis to instead translocate on DNA (Van Komen, Petukhova, Sigurdsson, Stratton, & Sung, 2000), or alter DNA contacts with proteins other than histones (Auble et al., 1994).

E3 ubiquitin ligases play roles in diverse processes through regulating protein levels and activities. Out of the 100 E3 ubiquitin ligases in yeast, and the 600 in humans, very few combine an ATP hydrolyzing domain with the RING domain. These include the yeast proteins, Rad5, Rad16, and Uls1 (Ris1), and the human proteins, SHPRH, HLTF, and TTF2. The role of the ATP hydrolysis in ubiquitin ligation, or how these two functions are interrelated is still not well understood for

most of them. ATP hydrolysis could perhaps assist in presenting the substrate for ubiquitin ligation or translocating the protein post-modification.

Irc20 was shown to possess E3 ubiquitin ligase activity, and mutations in both its ATPase and ubiquitin ligase domains results in a loss of function phenotype (Richardson et al., 2013). Here, we show that Irc20 can hydrolyze ATP in the presence of DNA, and that a point mutation in the Walker A motif (K397A) abolishes this activity (Figure 3.5). We also show that Irc20 interacts with DNA and with nucleosomal arrays (Figure 3.4), but does not remodel the nucleosome structure (Figure 3.6). It thus remains to be identified what the energy of ATP hydrolysis in Irc20 is used for.

6.2 Irc20 interacts with multiple proteins in diverse pathways

The reported functions of Irc20 in DNA repair and transcription regulation, prompted us to identify the potential interactions of Irc20 with other proteins using mass spectrometry to understand its possible ubiquitylation substrates. Richardson *et al.* (2013) have previously studied Irc20 interactions by mass spectrometry analysis (Richardson et al., 2013), however, in that experiment, Irc20 was overexpressed. In fact, as the *bur-* and *spt-* phenotypes of Irc20 are observed only when it is overexpressed (Richardson et al., 2013), it would be likely that the interactions of the overexpressed protein do not reflect interactions at its native expression levels.

To this end, we did mass spectrometry analysis on two levels. The first was to identify general interacting partners of Irc20. This was done by single affinity pull down of the protein, followed by gel filtration chromatography to separate larger and

smaller complexes and measure the size of a potential Irc20 complex. We did not observe major differences in the protein composition between fractions, again reflecting the lack of stable interactions. Irc20, however, was shown to interact with several proteins of multi-subunit complexes, such as septin ring proteins, APC/C complex, and the SWI/SNF remodeling complex. This is in addition to several subunits of the ubiquitin-proteasome, as expected for an ubiquitin ligase. The reported interaction between overexpressed Irc20 and Cdc48 seems to be physiologically relevant even under native expression levels, as Cdc48 is efficiently pulled down in our experiment as well.

Identifying substrates of ubiquitin ligases has historically been a difficult process. This is because interactions between them are transient, therefore hard to capture. A point mutation introduced in the RING domain of Irc20 presumably collapses the globular structure of the RING domain, prohibiting its interaction with the E2 enzyme, thus prolonging its interaction with the substrate and hence easing its detection. Thus, a second mass spectrometry analysis was done using the Irc20-C1239A ubiquitin ligase mutant, this time to specifically identify potential substrates. Some transcription factors are specifically pulled down only in the ubiquitin ligase mutant such as Tra1, Swr1, Tfb2, and Taf4. It would be interesting to test if these proteins are *in vivo* substrates of Irc20. We, however, did not detect any preferentially pulled down Smt3, as reported by Richardson *et al.* (2013), even though we have also observed significantly higher SUMOylation of Irc20-C1239A (data not presented in this thesis). This could be because of the rapid loss of the

SUMO modifications during sample preparation for mass spectrometry, that could be retained under the fixation conditions used by Richardson *et al.* (2013).

The results of the mass spectrometry analysis were not pursued/analyzed further because none of the identified proteins fit with the overall aim of the thesis, which was to study the role of Irc20 in DNA repair. Nonetheless, it would provide leads for future experiments and studies in investigating potential substrates of Irc20.

6.3 The role of Irc20 in HR

Irc20 was identified in a screen of gene deletions causing increased recombination centers monitored by the accumulation of GFP-tagged Rad52 (Alvaro *et al.*, 2007). This screen revealed proteins involved in several different pathways, and whose deletion affected recombination either directly or indirectly. This included proteins involved in transcription regulation, DNA repair, and replication as well as proteins with unknown functions such as Irc20, and thus were labelled IRCs for increased recombination centers. Our results show that regulating the formation of these spontaneous recombination foci require both activities of Irc20, the ATPase and the ubiquitin ligase. We showed that introducing a single point mutation in either domain increases foci to the same level as observed in the $\Delta irc20$ mutant. Since mutations in diverse pathways cause a similar hyper-recombination phenotype, the molecular mechanism of how Irc20 functions required further investigation.

Using recombination assays, Miura *et al.* (2012) showed direct involvement of Irc20 in the SDSA pathway of HR repair. This study showed that in the absence of Irc20, there is less SDSA and more imprecise end joining. They also showed that

even though there was less overall gene conversion events in the absence of Irc20, there was more cross overs involving longer tracts of DNA. Using genetic interaction assays with other genes involved in HR, they showed that Irc20 rescued sensitivities observed in $\Delta mre11$ mutant, and that it works in the same pathway as Srs2, to promote the SDSA pathway of HR (Miura et al., 2012). With these findings, they suggested that Irc20 works at an early step during HR during D-loop formation, to drive the entire HR process to favor SDSA. They also suggested that Irc20 acts as a helicase working before the Mre11 nuclease, possibly to make the DNA an appropriate substrate for Mre11.

We, however, did not observe the synthetic rescue phenotype that Miura *et al.* (2012) reported, and we believe this is because the deletion cassettes used to introduce gene deletions share significant homology, and thus frequently replace each other in case of double mutants. Indeed, the $\Delta mre11\Delta irc20$ gives complete synthetic rescue similar to the phenotype of $\Delta irc20$. It is therefore possible that Miura *et al.* (2012) are looking at a single $\Delta irc20$ mutation and not a double mutant. This, however, does not exclude the role of Irc20 in facilitating recombination, but most likely through a different mechanism than was suggested by these authors.

We tested whether perhaps Irc20 works on the level of Rad52 recruitment or retention on the DNA. Using co-immunoprecipitation assays, we showed physical interaction between Irc20 and Rad52 under non-damaging conditions. To understand the functional significance of this interaction, we tested the recruitment of Rad52 to DSBs in the presence and absence of Irc20. We hypothesized that decreased recruitment of Rad52 in the absence of Irc20 would reflect delayed repair due to

insufficient levels of Rad52 to drive the subsequent steps of recombination and would explain the reduced recombination seen in $\Delta irc20$ mutants. Increased levels would explain more retention of Rad52 around DSBs, which although reflects ongoing repair, but untimely removal of Rad52 would delay the overall HR repair process. Indeed, we observed 2 to 3-fold increase in the relative enrichment of Rad52 at a single induced DSB site as monitored by ChIP using primers around the DSB. This, together with the observations by Miura *et al.* (2012) regarding recombination outcomes in the absence of Irc20, points to a function for Irc20 where it promotes HR repair through facilitating the timely removal or recycling of Rad52 at DSB sites. The increased retention of Rad52 in $\Delta irc20$ would lead to less efficient overall recombination, whether by SDSA or gene conversion by cross overs as observed by Miura *et al.* (2012). It would also explain the increased longer tract crossovers, as delayed repair through retained Rad52 would cause excessive action by the nucleases responsible for DNA end resection at DSBs. This would expose longer tracts of ssDNA and thus may lead to longer tract crossovers.

The SIMs in Irc20 may also orchestrate its interaction with Rad52. Irc20 was shown to contain at least two SIMs, and to interact with SUMO *in vivo* (Richardson *et al.*, 2013). Rad52 is known to be SUMOylated when bound to DNA, and this SUMOylation plays both pro- and anti-recombination roles. The pro-recombination role of SUMO-Rad52 could perhaps be explained by facilitating its interaction with Rad51. This pro-recombination role is particularly visible at high levels of DNA damage, as cells expressing non-SUMOylatable Rad52 are sensitive to high levels of DNA damage but not to a single induced DSB (Ohuchi *et al.*, 2008). SUMOylation

of Rad52 also makes it a target for Slx5-Slx8 mediated proteolytic degradation (Xie et al., 2007) as well as allows its interaction with Cdc48-Ufd1 segregase (Bergink et al., 2013), thus could also lead to reduced recombination. We suggest that Irc20 acts in regulating Rad52 levels at DSBs. Our results suggest a scenario in which Irc20 interacts with Rad52 at DSBs, after Rad52 is SUMOylated, through Irc20 SIMs. This interaction would then facilitate the removal of Rad52 after it assists in loading Rad51 on ssDNA. The subsequent steps of HR would proceed as normal, since Rad52 is required at the initial stages of HR. Under non-damaging conditions, Rad52 accumulation on ssDNA tracts left behind replication forks could also be substrates for Irc20 removal, thus explaining the increased Rad52 foci observed in $\Delta irc20$ mutants.

6.4 Irc20 and Cdc48, opposing or similar roles?

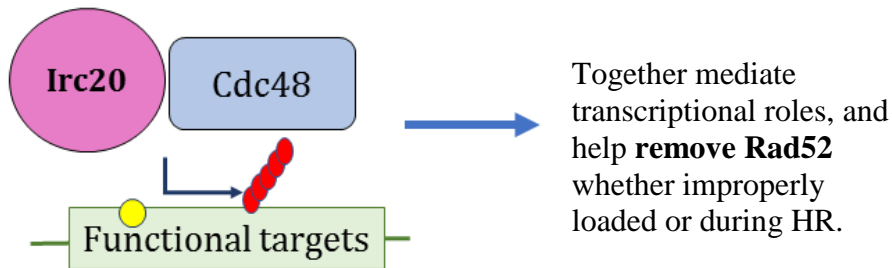
Richardson *et al.* (2013) had suggested opposing roles for Irc20 and Cdc48 in transcription regulation. They observed that overexpressing Irc20 leads to a similar phenotype as a loss-of-function mutation in Cdc48, the *bur-* phenotype. The mutation in Cdc48 that leads to this *bur-* phenotype, (*R369K*), impairs Cdc48 ability to bind ubiquitin chains (Q. Wang et al., 2005), without affecting the overall function of Cdc48. They also show that the overexpression of Irc20 does not reflect a dominant negative mechanism, as the *bur-* phenotype requires functional forms of Irc20 to be overexpressed (Richardson et al., 2013). The opposing roles of Irc20 and Cdc48, despite their direct interaction, suggested that one inhibits the other. Either Cdc48 normally inhibits Irc20 role in transcription activation, so high levels of Irc20 would overwhelm Cdc48's ability to repress Irc20 function, and thus transcription

would be activated. Alternatively, Irc20 is the inhibitor of Cdc48, which would function to inhibit transcription, so overexpressing Irc20 would show the overall transcription activating *bur-* phenotype observed.

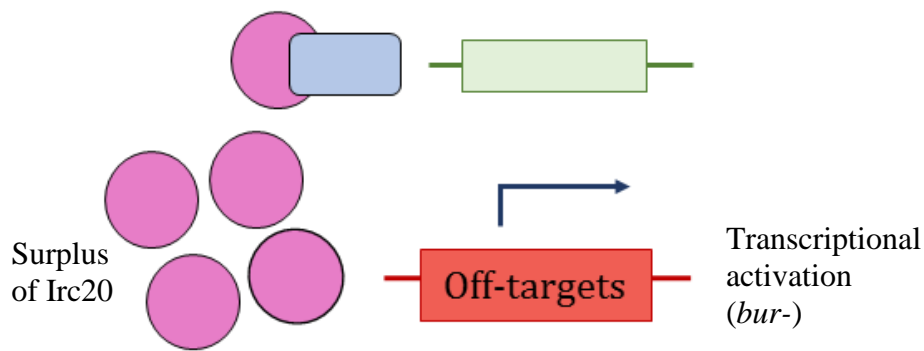
We have also observed physical interaction between Irc20 and Cdc48, even under native expression levels of Irc20, thus confirming the functional relevance of their interaction at physiological levels. However, we show a role for Irc20 similar to that of Cdc48 in regulating Rad52 accumulation on DNA. Cdc48 was shown to curb the superfluous accumulation of Rad52 and Rad51 on DNA when recombination is not needed, similar to what we observed for Irc20. We, thus, suggest that while interaction between Irc20 and Cdc48 occurs regardless of the expression levels of Irc20, the outcome depends on Irc20 levels. We hypothesize a model in which at the normal low physiological levels of Irc20, it is predominantly coupled with Cdc48. In case of HR, Irc20 catalyzes the formation of poly-ubiquitin chains on Rad52, or other recombination factors, and this poly-ubiquitin chain would cause the retention of Cdc48 facilitating its segregase activity.

Under overexpression conditions, however, Irc20 may interact with other proteins such as transcription factors as Irc20 levels would now exceed those of Cdc48, mediating the transcriptional phenotype (*bur-*) observed. The Cdc48 mutation (*R369K*), would mimic an overexpression of Irc20 phenotype as it would affect the retention of Cdc48 at its functional sites and thus Irc20 would similarly be available for interacting with other proteins leading to the *bur-* phenotype even at native expression levels.

A Normal expression levels



B Overexpression of Irc20



C *cdc48-R369K*

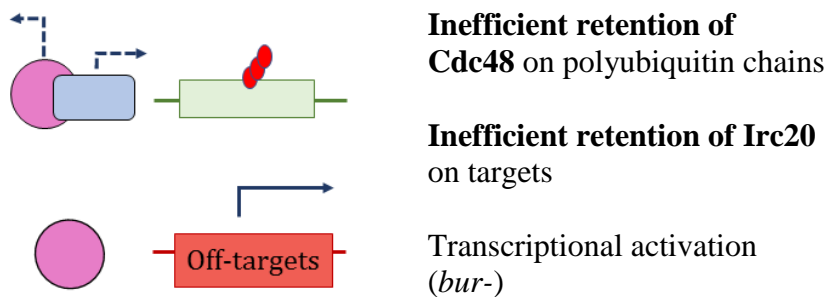


Figure 6.1: A model for the functional interaction between Irc20 and Cdc48

A. In normal low physiological levels, Irc20 is predominantly coupled with Cdc48. In case of HR, Irc20 catalyzes the formation of poly-ubiquitin chains on Rad52, or other recombination factors, and this poly-ubiquitin chain would cause the retention of Cdc48 facilitating its segregase activity. B. Under overexpression conditions, however, Irc20 may interact with other proteins such as transcription factors as Irc20 levels would now exceed those of Cdc48, mediating the transcriptional phenotype (*bur-*) observed. C. The Cdc48 mutation *R369K*, would mimic an overexpression of Irc20 phenotype as it would affect the retention of Cdc48 at its functional sites and thus Irc20 would similarly be available for interacting with other proteins leading to the *bur-* phenotype even at native expression levels.

Irc20, although does not show chromatin remodeling activity, shares several features common for Snf2 family members. Irc20 shows ATP hydrolysis activity in the presence of DNA as well as DNA and nucleosome binding activity. This suggests Irc20 may be utilizing the energy generated from ATP hydrolysis to translocate along DNA, similar to chromatin remodelers, but instead of loosening contacts of histone proteins with DNA, Irc20 may function to loosen the contacts of other DNA binding proteins to DNA. It is thus plausible to suggest that the role of Irc20 in conjunction with the Cdc48 segregase complex is to loosen the interaction between the proteins to be segregated with DNA.

6.5 The role of Irc20 in regulating the 2- μ m plasmid levels

During the course of our study, we observed the occasional generation of [cir⁰] strains, even though the 2- μ m plasmid is normally highly stable and propagates at levels similar to chromosomes. This prompted us to study the role of Irc20 in 2- μ m plasmid regulation. Despite our observations of higher frequency of endogenous 2- μ m plasmid loss, when using a plasmid designed to study 2- μ m plasmid stability, pKAN4, we were not able to observe the same. The pKAN4 plasmid differs from the endogenous 2- μ m plasmid in that it lacks the *FLP1*. This is useful when studying partitioning as having a functional *FLP1* obscures plasmid mis-segregation defects by correcting decreases in copy number. The discrepancy indicated that Irc20 might regulate the 2- μ m plasmid stability through a mechanism involving Flp1.

To understand the role of Irc20 in relation to Flp1, we measured endogenous 2- μ m levels in the Δ *irc20* mutant. We observed three to four-folds higher 2- μ m

levels in $\Delta irc20$ mutant compared to the wild type strain. This was surprising as we had not observed any cold sensitivities, nibbled colony appearance, or heterogenous looking colonies as that observed with SUMO and ubiquitin pathway mutants that have elevated 2- μ m plasmid levels. However, this can be attributed to the fact that the increase in 2- μ m plasmid copy number observed in $\Delta irc20$ mutant (3 to 4-folds) is not as high as that in other SUMO pathway mutants (10 to 30-folds) (Xiong et al., 2009). A similar modest increase in copy number without significant growth sensitivities was previously reported for the ubiquitin conjugating enzyme Ubc4 (Sleep et al., 2001), thus perhaps Irc20 and Ubc4 together constitute a secondary pathway for 2- μ m plasmid copy number control.

We also show that the elevated 2- μ m plasmid levels observed in the $\Delta irc20$ null mutant depends on HR factors, and is thus a product of hyper-recombination. In the $\Delta irc20$ mutant, the 2- μ m plasmid predominantly exists as a higher molecular weight form as shown by Southern blotting (Figure 5.5). This likely reflects concatamer forms that are unresolved into monomeric forms (Figure 1.5C) in the absence of Irc20. This high molecular weight form is also the predominant species in the *Irc20-DE534-535AA* ATPase domain mutant (Figure 5.5), even though the 2- μ m levels are not elevated in this mutant. This suggests that the regulation of copy number and concatamer resolution are two separate functions of Irc20. We also monitored the Flp1 levels after expressing a YFP-tagged form from a repressible promoter and observing levels remaining at different time points after shutting off expression. We observed higher levels of Flp1 in strains lacking Irc20 (Figure 5.6).

This suggests that Irc20 normally regulates Flp1 levels, thereby controlling the amplification of the 2- μ m plasmid copy number.

Overall, we hypothesize that Irc20 regulates the 2- μ m plasmid levels through two mechanisms. The first is by directly regulating Flp1 levels, possibly by assisting its degradation. This would be most likely through its ubiquitin ligase activity, although Flp1 levels still need to be tested in the ubiquitin ligase mutant. The other mechanism is through the role of Irc20 in regulating HR. In the absence of Irc20, increased retention of Rad52 on 2- μ m plasmids that are undergoing Flp1-induced copy number amplification elicited by random mis-segregation events, would lead to delayed resolution and accumulation of these unresolved species. If this is combined with increased Flp1 levels, it would cause both elevated copy number and high molecular weight forms as observed in the Δ *irc20* mutant. If the Flp1 levels are not elevated, which we expect to be the case in the ATPase mutant, only the resolution of the 2- μ m plasmid forms would be impaired, but copy number would not be elevated. The lack of increased copy number in *Irc20-C1239A*, can be explained by the rapid loss of the 2- μ m plasmid in this mutant that would be reflected in a growing culture as an average of normal 2- μ m copy number.

We could not help but notice that the same mutation that causes the *bur-* phenotype in Cdc48 (*cdc48-R369K*), shows cold sensitivities, a characteristic feature of elevated 2- μ m plasmid levels, even though the overall function of Cdc48 is not affected. Therefore, it would be interesting to test if the *cdc48-R369K* mutant shows elevated 2- μ m plasmid levels similar to Irc20.

Overall, Irc20 appears as a new regulator of HR repair with a prominent role in regulating 2- μ m plasmid levels. SUMO and ubiquitin pathway enzymes are becoming increasingly appreciated as molecular fine-tuners of enzyme activities and the role we report here for Irc20 adds to importance of these enzymes. How Irc20 utilizes both its ATPase and ubiquitin ligase activities to accomplish this is still not known and would present interesting questions to be pursued in the future.

References

- Acharya, N., Johnson, R. E., Prakash, S., & Prakash, L. (2006). Complex formation with Rev1 enhances the proficiency of *Saccharomyces cerevisiae* DNA polymerase zeta for mismatch extension and for extension opposite from DNA lesions. *Mol Cell Biol*, *26*(24), 9555-9563. doi:10.1128/mcb.01671-06
- Ahn, Y. T., Wu, X. L., Biswal, S., Velmurugan, S., Volkert, F. C., & Jayaram, M. (1997). The 2microm-plasmid-encoded Rep1 and Rep2 proteins interact with each other and colocalize to the *Saccharomyces cerevisiae* nucleus. *J Bacteriol*, *179*(23), 7497-7506.
- Alseth, I., Eide, L., Pirovano, M., Rognes, T., Seeberg, E., & Bjoras, M. (1999). The *Saccharomyces cerevisiae* homologues of endonuclease III from *Escherichia coli*, Ntg1 and Ntg2, are both required for efficient repair of spontaneous and induced oxidative DNA damage in yeast. *Mol Cell Biol*, *19*(5), 3779-3787.
- Altmannova, V., Eckert-Boulet, N., Arneric, M., Kolesar, P., Chaloupkova, R., Damborsky, J., . . . Krejci, L. (2010). Rad52 SUMOylation affects the efficiency of the DNA repair. *Nucleic Acids Res*, *38*(14), 4708-4721. doi:10.1093/nar/gkq195
- Alvaro, D., Lisby, M., & Rothstein, R. (2007). Genome-wide analysis of Rad52 foci reveals diverse mechanisms impacting recombination. *PLoS Genet*, *3*(12), e228. doi:10.1371/journal.pgen.0030228
- Amerik, A. Y., Li, S. J., & Hochstrasser, M. (2000). Analysis of the deubiquitinating enzymes of the yeast *Saccharomyces cerevisiae*. *Biol Chem*, *381*(9-10), 981-992. doi:10.1515/bc.2000.121
- Amerik, A. Y., Nowak, J., Swaminathan, S., & Hochstrasser, M. (2000). The Doa4 deubiquitinating enzyme is functionally linked to the vacuolar protein-sorting and endocytic pathways. *Mol Biol Cell*, *11*(10), 3365-3380.
- Antony, E., Tomko, E. J., Xiao, Q., Krejci, L., Lohman, T. M., & Ellenberger, T. (2009). Srs2 disassembles Rad51 filaments by a protein-protein interaction triggering ATP turnover and dissociation of Rad51 from DNA. *Mol Cell*, *35*(1), 105-115. doi:10.1016/j.molcel.2009.05.026
- Armstrong, A. A., Mohideen, F., & Lima, C. D. (2012). Recognition of SUMO-modified PCNA requires tandem receptor motifs in Srs2. *Nature*, *483*(7387), 59-63. doi:10.1038/nature10883

- Arnold, L., Hockner, S., & Seufert, W. (2015). Insights into the cellular mechanism of the yeast ubiquitin ligase APC/C-Cdh1 from the analysis of in vivo degrons. *Mol Biol Cell*, *26*(5), 843-858. doi:10.1091/mbc.E14-09-1342
- Auble, D. T., Hansen, K. E., Mueller, C. G., Lane, W. S., Thorner, J., & Hahn, S. (1994). Mot1, a global repressor of RNA polymerase II transcription, inhibits TBP binding to DNA by an ATP-dependent mechanism. *Genes Dev*, *8*(16), 1920-1934.
- Balakirev, M. Y., Mullally, J. E., Favier, A., Assard, N., Sulpice, E., Lindsey, D. F., . . . Wilkinson, K. D. (2015). Wss1 metalloprotease partners with Cdc48/Doa1 in processing genotoxic SUMO conjugates. *Elife*, *4*. doi:10.7554/eLife.06763
- Bang, D. D., Verhage, R., Goosen, N., Brouwer, J., & van de Putte, P. (1992). Molecular cloning of RAD16, a gene involved in differential repair in *Saccharomyces cerevisiae*. *Nucleic Acids Res*, *20*(15), 3925-3931.
- Bartek, J., & Lukas, J. (2007). DNA damage checkpoints: from initiation to recovery or adaptation. *Curr Opin Cell Biol*, *19*(2), 238-245. doi:10.1016/j.ceb.2007.02.009
- Becker, P. B., & Horz, W. (2002). ATP-dependent nucleosome remodeling. *Annu Rev Biochem*, *71*, 247-273. doi:10.1146/annurev.biochem.71.110601.135400
- Belle, A., Tanay, A., Bitincka, L., Shamir, R., & O'Shea, E. K. (2006). Quantification of protein half-lives in the budding yeast proteome. *Proc Natl Acad Sci U S A*, *103*(35), 13004-13009. doi:10.1073/pnas.0605420103
- Bennett, G., Papamichos-Chronakis, M., & Peterson, C. L. (2013). DNA repair choice defines a common pathway for recruitment of chromatin regulators. *Nat Commun*, *4*, 2084. doi:10.1038/ncomms3084
- Bergink, S., Ammon, T., Kern, M., Schermelleh, L., Leonhardt, H., & Jentsch, S. (2013). Role of Cdc48/p97 as a SUMO-targeted segregase curbing Rad51-Rad52 interaction. *Nat Cell Biol*, *15*(5), 526-532. doi:10.1038/ncb2729
- Bermudez-Lopez, M., Ceschia, A., de Piccoli, G., Colomina, N., Pasero, P., Aragon, L., & Torres-Rosell, J. (2010). The Smc5/6 complex is required for dissolution of DNA-mediated sister chromatid linkages. *Nucleic Acids Res*, *38*(19), 6502-6512. doi:10.1093/nar/gkq546
- Bermudez-Lopez, M., Pocino-Merino, I., Sanchez, H., Bueno, A., Guasch, C., Almedawar, S., . . . Torres-Rosell, J. (2015). ATPase-dependent control of

- the Mms21 SUMO ligase during DNA repair. *PLoS Biol*, 13(3), e1002089. doi:10.1371/journal.pbio.1002089
- Bertolaet, B. L., Clarke, D. J., Wolff, M., Watson, M. H., Henze, M., Divita, G., & Reed, S. I. (2001). UBA domains of DNA damage-inducible proteins interact with ubiquitin. *Nat Struct Biol*, 8(5), 417-422. doi:10.1038/87575
- Blastyak, A., Pinter, L., Unk, I., Prakash, L., Prakash, S., & Haracska, L. (2007). Yeast Rad5 protein required for postreplication repair has a DNA helicase activity specific for replication fork regression. *Mol Cell*, 28(1), 167-175. doi:10.1016/j.molcel.2007.07.030
- Bohm, S., Mihalevic, M. J., Casal, M. A., & Bernstein, K. A. (2015). Disruption of SUMO-targeted ubiquitin ligases Slx5-Slx8/RNF4 alters RecQ-like helicase Sgs1/BLM localization in yeast and human cells. *DNA Repair (Amst)*, 26, 1-14. doi:10.1016/j.dnarep.2014.12.004
- Bologna, S., Altmannova, V., Valtorta, E., Koenig, C., Liberali, P., Gentili, C., . . . Ferrari, S. (2015). Sumoylation regulates EXO1 stability and processing of DNA damage. *Cell Cycle*, 14(15), 2439-2450. doi:10.1080/15384101.2015.1060381
- Botchan, M. (2004). Hitchhiking without covalent integration. *Cell*, 117(3), 280-281.
- Bowen, N. J., Fujita, N., Kajita, M., & Wade, P. A. (2004). Mi-2/NuRD: multiple complexes for many purposes. *Biochim Biophys Acta*, 1677(1-3), 52-57. doi:10.1016/j.bbaexp.2003.10.010
- Boyer, L. A., Latek, R. R., & Peterson, C. L. (2004). The SANT domain: a unique histone-tail-binding module? *Nat Rev Mol Cell Biol*, 5(2), 158-163. doi:10.1038/nrm1314
- Branzei, D. (2011). Ubiquitin family modifications and template switching. *FEBS Lett*, 585(18), 2810-2817. doi:10.1016/j.febslet.2011.04.053
- Branzei, D., Sollier, J., Liberi, G., Zhao, X., Maeda, D., Seki, M., . . . Foiani, M. (2006). Ubc9- and mms21-mediated sumoylation counteracts recombinogenic events at damaged replication forks. *Cell*, 127(3), 509-522. doi:10.1016/j.cell.2006.08.050
- Branzei, D., Vanoli, F., & Foiani, M. (2008). SUMOylation regulates Rad18-mediated template switch. *Nature*, 456(7224), 915-920. doi:10.1038/nature07587

- Briggs, S. D., Xiao, T., Sun, Z. W., Caldwell, J. A., Shabanowitz, J., Hunt, D. F., . . . Strahl, B. D. (2002). Gene silencing: trans-histone regulatory pathway in chromatin. *Nature*, *418*(6897), 498. doi:10.1038/nature00970
- Brown, T. (1999). Analysis of DNA sequences by blotting and hybridization. In *Current Protocols in Molecular Biology* (pp. 2.9.1-2.9.20): John Wiley & Sons.
- Burgess, R. C., Rahman, S., Lisby, M., Rothstein, R., & Zhao, X. (2007). The Slx5-Slx8 complex affects sumoylation of DNA repair proteins and negatively regulates recombination. *Mol Cell Biol*, *27*(17), 6153-6162. doi:10.1128/mcb.00787-07
- Buser, R., Kellner, V., Melnik, A., Wilson-Zbinden, C., Schellhaas, R., Kastner, L., . . . Peter, M. (2016). The Replisome-Coupled E3 Ubiquitin Ligase Rtt101Mms22 Counteracts Mrc1 Function to Tolerate Genotoxic Stress. *PLoS Genet*, *12*(2), e1005843. doi:10.1371/journal.pgen.1005843
- Bylebyl, G. R., Belichenko, I., & Johnson, E. S. (2003). The SUMO isopeptidase Ulp2 prevents accumulation of SUMO chains in yeast. *J Biol Chem*, *278*(45), 44113-44120. doi:10.1074/jbc.M308357200
- Cairns, B. R., Lorch, Y., Li, Y., Zhang, M., Lacomis, L., Erdjument-Bromage, H., . . . Kornberg, R. D. (1996). RSC, an essential, abundant chromatin-remodeling complex. *Cell*, *87*(7), 1249-1260.
- Cal-Bakowska, M., Litwin, I., Bocer, T., Wysocki, R., & Dziadkowiec, D. (2011). The Swi2-Snf2-like protein Uls1 is involved in replication stress response. *Nucleic Acids Res*, *39*(20), 8765-8777. doi:10.1093/nar/gkr587
- Chai, B., Huang, J., Cairns, B. R., & Laurent, B. C. (2005). Distinct roles for the RSC and Swi/Snf ATP-dependent chromatin remodelers in DNA double-strand break repair. *Genes Dev*, *19*(14), 1656-1661. doi:10.1101/gad.1273105
- Chavez, A., George, V., Agrawal, V., & Johnson, F. B. (2010). Sumoylation and the structural maintenance of chromosomes (Smc) 5/6 complex slow senescence through recombination intermediate resolution. *J Biol Chem*, *285*(16), 11922-11930. doi:10.1074/jbc.M109.041277
- Chen, X. L., Reindle, A., & Johnson, E. S. (2005). Misregulation of 2 microm circle copy number in a SUMO pathway mutant. *Mol Cell Biol*, *25*(10), 4311-4320. doi:10.1128/mcb.25.10.4311-4320.2005

- Chernova, T. A., Allen, K. D., Wesoloski, L. M., Shanks, J. R., Chernoff, Y. O., & Wilkinson, K. D. (2003). Pleiotropic effects of Ubp6 loss on drug sensitivities and yeast prion are due to depletion of the free ubiquitin pool. *J Biol Chem*, *278*(52), 52102-52115. doi:10.1074/jbc.M310283200
- Choi, K., Batke, S., Szakal, B., Lowther, J., Hao, F., Sarangi, P., . . . Zhao, X. (2015). Concerted and differential actions of two enzymatic domains underlie Rad5 contributions to DNA damage tolerance. *Nucleic Acids Res*, *43*(5), 2666-2677. doi:10.1093/nar/gkv004
- Choi, K., Szakal, B., Chen, Y. H., Branzei, D., & Zhao, X. (2010). The Smc5/6 complex and Esc2 influence multiple replication-associated recombination processes in *Saccharomyces cerevisiae*. *Mol Biol Cell*, *21*(13), 2306-2314. doi:10.1091/mbc.E10-01-0050
- Chung, I., & Zhao, X. (2015). DNA break-induced sumoylation is enabled by collaboration between a SUMO ligase and the ssDNA-binding complex RPA. *Genes Dev*, *29*(15), 1593-1598. doi:10.1101/gad.265058.115
- Clapier, C. R., & Cairns, B. R. (2009). The biology of chromatin remodeling complexes. *Annu Rev Biochem*, *78*, 273-304. doi:10.1146/annurev.biochem.77.062706.153223
- Cleaver, J. E. (1972). Xeroderma pigmentosum: variants with normal DNA repair and normal sensitivity to ultraviolet light. *J Invest Dermatol*, *58*(3), 124-128.
- Clemenson, C., & Marsolier-Kergoat, M. C. (2009). DNA damage checkpoint inactivation: adaptation and recovery. *DNA Repair (Amst)*, *8*(9), 1101-1109. doi:10.1016/j.dnarep.2009.04.008
- Cremona, C. A., Sarangi, P., Yang, Y., Hang, L. E., Rahman, S., & Zhao, X. (2012). Extensive DNA damage-induced sumoylation contributes to replication and repair and acts in addition to the mecl1 checkpoint. *Mol Cell*, *45*(3), 422-432. doi:10.1016/j.molcel.2011.11.028
- Cui, H., Ghosh, S. K., & Jayaram, M. (2009). The selfish yeast plasmid uses the nuclear motor Kip1p but not Cin8p for its localization and equal segregation. *J Cell Biol*, *185*(2), 251-264. doi:10.1083/jcb.200810130
- Daele, D. L., Ferrari, E., Longerich, S., Zheng, X. F., Xue, X., Branzei, D., . . . Myung, K. (2012). Rad5-dependent DNA repair functions of the *Saccharomyces cerevisiae* FANCM protein homolog Mph1. *J Biol Chem*, *287*(32), 26563-26575. doi:10.1074/jbc.M112.369918

- Dae, D. L., & Myung, K. (2012). Fanconi-like crosslink repair in yeast. In *Genome Integr* (Vol. 3, pp. 7). England.
- Danielsen, J. R., Povlsen, L. K., Villumsen, B. H., Streicher, W., Nilsson, J., Wikstrom, M., . . . Mailand, N. (2012). DNA damage-inducible SUMOylation of HERC2 promotes RNF8 binding via a novel SUMO-binding Zinc finger. *J Cell Biol*, *197*(2), 179-187. doi:10.1083/jcb.201106152
- Das-Bradoo, S., Nguyen, H. D., Wood, J. L., Ricke, R. M., Haworth, J. C., & Bielinsky, A. K. (2010). Defects in DNA ligase I trigger PCNA ubiquitylation at Lys 107. *Nat Cell Biol*, *12*(1), 74-79; sup pp 71-20. doi:10.1038/ncb2007
- Davies, A. A., Huttner, D., Daigaku, Y., Chen, S., & Ulrich, H. D. (2008). Activation of ubiquitin-dependent DNA damage bypass is mediated by replication protein a. *Mol Cell*, *29*(5), 625-636. doi:10.1016/j.molcel.2007.12.016
- Dhont, L., Mascaux, C., & Belayew, A. (2016). The helicase-like transcription factor (HLTF) in cancer: loss of function or oncomorphic conversion of a tumor suppressor? *Cell Mol Life Sci*, *73*(1), 129-147. doi:10.1007/s00018-015-2060-6
- Ding, H., Descheemaeker, K., Marynen, P., Nelles, L., Carvalho, T., Carmo-Fonseca, M., . . . Belayew, A. (1996). Characterization of a helicase-like transcription factor involved in the expression of the human plasminogen activator inhibitor-1 gene. *DNA Cell Biol*, *15*(6), 429-442. doi:10.1089/dna.1996.15.429
- Dobson, M. J., Pickett, A. J., Velmurugan, S., Pinder, J. B., Barrett, L. A., Jayaram, M., & Chew, J. S. (2005). The 2 microm plasmid causes cell death in *Saccharomyces cerevisiae* with a mutation in Ulp1 protease. *Mol Cell Biol*, *25*(10), 4299-4310. doi:10.1128/mcb.25.10.4299-4310.2005
- Eapen, V. V., Sugawara, N., Tsabar, M., Wu, W. H., & Haber, J. E. (2012). The *Saccharomyces cerevisiae* chromatin remodeler Fun30 regulates DNA end resection and checkpoint deactivation. *Mol Cell Biol*, *32*(22), 4727-4740. doi:10.1128/mcb.00566-12
- Elmore, Z. C., Donaher, M., Matson, B. C., Murphy, H., Westerbeck, J. W., & Kerscher, O. (2011). Sumo-dependent substrate targeting of the SUMO protease Ulp1. *BMC Biol*, *9*, 74. doi:10.1186/1741-7007-9-74

- Ferreira, H. C., Luke, B., Schober, H., Kalck, V., Lingner, J., & Gasser, S. M. (2011). The PIAS homologue Siz2 regulates perinuclear telomere position and telomerase activity in budding yeast. *Nat Cell Biol*, *13*(7), 867-874. doi:10.1038/ncb2263
- Finley, D., Bartel, B., & Varshavsky, A. (1989). The tails of ubiquitin precursors are ribosomal proteins whose fusion to ubiquitin facilitates ribosome biogenesis. *Nature*, *338*(6214), 394-401. doi:10.1038/338394a0
- Finley, D., Ozkaynak, E., & Varshavsky, A. (1987). The yeast polyubiquitin gene is essential for resistance to high temperatures, starvation, and other stresses. *Cell*, *48*(6), 1035-1046.
- Finley, D., Ulrich, H. D., Sommer, T., & Kaiser, P. (2012). The ubiquitin-proteasome system of *Saccharomyces cerevisiae*. *Genetics*, *192*(2), 319-360. doi:10.1534/genetics.112.140467
- Flanagan, J. F., & Peterson, C. L. (1999). A role for the yeast SWI/SNF complex in DNA replication. *Nucleic Acids Res*, *27*(9), 2022-2028.
- Flaus, A., Martin, D. M., Barton, G. J., & Owen-Hughes, T. (2006). Identification of multiple distinct Snf2 subfamilies with conserved structural motifs. *Nucleic Acids Res*, *34*(10), 2887-2905. doi:10.1093/nar/gkl295
- Friedl, A. A., Liefshitz, B., Steinlauf, R., & Kupiec, M. (2001). Deletion of the SRS2 gene suppresses elevated recombination and DNA damage sensitivity in rad5 and rad18 mutants of *Saccharomyces cerevisiae*. *Mutat Res*, *486*(2), 137-146.
- Futcher, A. B. (1986). Copy number amplification of the 2 micron circle plasmid of *Saccharomyces cerevisiae*. *J Theor Biol*, *119*(2), 197-204.
- Futcher, A. B., & Cox, B. S. (1983). Maintenance of the 2 microns circle plasmid in populations of *Saccharomyces cerevisiae*.
- Game, J. C., & Chernikova, S. B. (2009). The role of RAD6 in recombinational repair, checkpoints and meiosis via histone modification. *DNA Repair (Amst)*, *8*(4), 470-482. doi:10.1016/j.dnarep.2009.01.007
- Game, J. C., Williamson, M. S., Spicakova, T., & Brown, J. M. (2006). The RAD6/BRE1 histone modification pathway in *Saccharomyces* confers radiation resistance through a RAD51-dependent process that is independent of RAD18. *Genetics*, *173*(4), 1951-1968. doi:10.1534/genetics.106.057794

- Gardner, J. M., Smoyer, C. J., Stensrud, E. S., Alexander, R., Gogol, M., Wiegraebe, W., & Jaspersen, S. L. (2011). Targeting of the SUN protein Mps3 to the inner nuclear membrane by the histone variant H2A.Z. *J Cell Biol*, *193*(3), 489-507. doi:10.1083/jcb.201011017
- Gazy, I., & Kupiec, M. (2012). The importance of being modified: PCNA modification and DNA damage response. *Cell Cycle*, *11*(14), 2620-2623. doi:10.4161/cc.20626
- Ghosh, S. K., Hajra, S., & Jayaram, M. (2007). Faithful segregation of the multicopy yeast plasmid through cohesin-mediated recognition of sisters. *Proc Natl Acad Sci U S A*, *104*(32), 13034-13039. doi:10.1073/pnas.0702996104
- Giannattasio, M., Lazzaro, F., Plevani, P., & Muzi-Falconi, M. (2005). The DNA damage checkpoint response requires histone H2B ubiquitination by Rad6-Bre1 and H3 methylation by Dot1. *J Biol Chem*, *280*(11), 9879-9886. doi:10.1074/jbc.M414453200
- Gillette, T. G., Yu, S., Zhou, Z., Waters, R., Johnston, S. A., & Reed, S. H. (2006). Distinct functions of the ubiquitin-proteasome pathway influence nucleotide excision repair. *Embo j*, *25*(11), 2529-2538. doi:10.1038/sj.emboj.7601120
- Gillies, J., Hickey, C. M., Su, D., Wu, Z., Peng, J., & Hochstrasser, M. (2016). SUMO Pathway Modulation of Regulatory Protein Binding at the Ribosomal DNA Locus in *Saccharomyces cerevisiae*. *Genetics*. doi:10.1534/genetics.116.187252
- Gomez-Llorente, Y., Malik, R., Jain, R., Choudhury, J. R., Johnson, R. E., Prakash, L., . . . Aggarwal, A. K. (2013). The architecture of yeast DNA polymerase zeta. *Cell Rep*, *5*(1), 79-86. doi:10.1016/j.celrep.2013.08.046
- Grandin, N., & Charbonneau, M. (2008). Protection against chromosome degradation at the telomeres. *Biochimie*, *90*(1), 41-59. doi:10.1016/j.biochi.2007.07.008
- Grenon, M., Costelloe, T., Jimeno, S., O'Shaughnessy, A., Fitzgerald, J., Zgheib, O., . . . Lowndes, N. F. (2007). Docking onto chromatin via the *Saccharomyces cerevisiae* Rad9 Tudor domain. *Yeast*, *24*(2), 105-119. doi:10.1002/yea.1441
- Griffiths, L. M., Swartzlander, D., Meadows, K. L., Wilkinson, K. D., Corbett, A. H., & Doetsch, P. W. (2009). Dynamic compartmentalization of base excision repair proteins in response to nuclear and mitochondrial oxidative stress. *Mol Cell Biol*, *29*(3), 794-807. doi:10.1128/mcb.01357-08

- Guzder, S. N., Habraken, Y., Sung, P., Prakash, L., & Prakash, S. (1995). Reconstitution of yeast nucleotide excision repair with purified Rad proteins, replication protein A, and transcription factor TFIIH. *J Biol Chem*, *270*(22), 12973-12976.
- Guzder, S. N., Sung, P., Prakash, L., & Prakash, S. (1998). The DNA-dependent ATPase activity of yeast nucleotide excision repair factor 4 and its role in DNA damage recognition. *J Biol Chem*, *273*(11), 6292-6296.
- Han, J., Zhang, H., Wang, Z., Zhou, H., & Zhang, Z. (2013). A Cul4 E3 ubiquitin ligase regulates histone hand-off during nucleosome assembly. *Cell*, *155*(4), 817-829. doi:10.1016/j.cell.2013.10.014
- Hang, L. E., Liu, X., Cheung, I., Yang, Y., & Zhao, X. (2011). SUMOylation regulates telomere length homeostasis by targeting Cdc13. *Nat Struct Mol Biol*, *18*(8), 920-926. doi:10.1038/nsmb.2100
- Hang, L. E., Lopez, C. R., Liu, X., Williams, J. M., Chung, I., Wei, L., . . . Zhao, X. (2014). Regulation of Ku-DNA association by Yku70 C-terminal tail and SUMO modification. *J Biol Chem*, *289*(15), 10308-10317. doi:10.1074/jbc.M113.526178
- Hang, L. E., Peng, J., Tan, W., Szakal, B., Menolfi, D., Sheng, Z., . . . Zhao, X. (2015). Rtt107 Is a Multi-functional Scaffold Supporting Replication Progression with Partner SUMO and Ubiquitin Ligases. *Mol Cell*, *60*(2), 268-279. doi:10.1016/j.molcel.2015.08.023
- Hanna, J., Leggett, D. S., & Finley, D. (2003). Ubiquitin depletion as a key mediator of toxicity by translational inhibitors. *Mol Cell Biol*, *23*(24), 9251-9261.
- Harreman, M., Taschner, M., Sigurdsson, S., Anindya, R., Reid, J., Somesh, B., . . . Svejstrup, J. Q. (2009). Distinct ubiquitin ligases act sequentially for RNA polymerase II polyubiquitylation. *Proc Natl Acad Sci U S A*, *106*(49), 20705-20710. doi:10.1073/pnas.0907052106
- Hassan, A. H., Prochasson, P., Neely, K. E., Galasinski, S. C., Chandy, M., Carrozza, M. J., & Workman, J. L. (2002). Function and selectivity of bromodomains in anchoring chromatin-modifying complexes to promoter nucleosomes. *Cell*, *111*(3), 369-379.
- Hay, R. T. (2005). SUMO: a history of modification. *Mol Cell*, *18*(1), 1-12. doi:10.1016/j.molcel.2005.03.012

- Hay, R. T. (2013). Decoding the SUMO signal. *Biochem Soc Trans*, *41*(2), 463-473. doi:10.1042/bst20130015
- Hibi, K., Kodera, Y., Ito, K., Akiyama, S., & Nakao, A. (2005). Aberrant methylation of HLTF, SOCS-1, and CDH13 genes is shown in colorectal cancers without lymph node metastasis. *Dis Colon Rectum*, *48*(6), 1282-1286. doi:10.1007/s10350-004-0947-7
- Hibi, K., Nakayama, H., Kanyama, Y., Kodera, Y., Ito, K., Akiyama, S., & Nakao, A. (2003). Methylation pattern of HLTF gene in digestive tract cancers. *Int J Cancer*, *104*(4), 433-436. doi:10.1002/ijc.10985
- Hickey, C. M., Wilson, N. R., & Hochstrasser, M. (2012). Function and regulation of SUMO proteases. *Nat Rev Mol Cell Biol*, *13*(12), 755-766. doi:10.1038/nrm3478
- Hishida, T., Hirade, Y., Haruta, N., Kubota, Y., & Iwasaki, H. (2010). Srs2 plays a critical role in reversible G2 arrest upon chronic and low doses of UV irradiation via two distinct homologous recombination-dependent mechanisms in postreplication repair-deficient cells. *Mol Cell Biol*, *30*(20), 4840-4850. doi:10.1128/mcb.00453-10
- Hoegge, C., Pfander, B., Moldovan, G. L., Pyrowolakis, G., & Jentsch, S. (2002). RAD6-dependent DNA repair is linked to modification of PCNA by ubiquitin and SUMO. *Nature*, *419*(6903), 135-141. doi:10.1038/nature00991
- Holm, C. (1982). Clonal lethality caused by the yeast plasmid 2 mu DNA. *Cell*, *29*(2), 585-594.
- Horigome, C., Bustard, D. E., Marcomini, I., Delgosaie, N., Tsai-Pflugfelder, M., Cobb, J. A., & Gasser, S. M. (2016). PolySUMOylation by Siz2 and Mms21 triggers relocation of DNA breaks to nuclear pores through the Slx5/Slx8 STUbL. *Genes Dev*. doi:10.1101/gad.277665.116
- Huang, C. C., Chang, K. M., Cui, H., & Jayaram, M. (2011). Histone H3-variant Cse4-induced positive DNA supercoiling in the yeast plasmid has implications for a plasmid origin of a chromosome centromere. *Proc Natl Acad Sci U S A*, *108*(33), 13671-13676. doi:10.1073/pnas.1101944108
- Huang, C. C., Hajra, S., Ghosh, S. K., & Jayaram, M. (2011). Cse4 (CenH3) association with the *Saccharomyces cerevisiae* plasmid partitioning locus in its native and chromosomally integrated states: implications in centromere evolution. *Mol Cell Biol*, *31*(5), 1030-1040. doi:10.1128/mcb.01191-10

- Huang, J., Liang, B., Qiu, J., & Laurent, B. C. (2005). ATP-dependent chromatin-remodeling complexes in DNA double-strand break repair: remodeling, pairing and (re)pairing. *Cell Cycle*, *4*(12), 1713-1715.
- Huertas, D., Sendra, R., & Munoz, P. (2009). Chromatin dynamics coupled to DNA repair. *Epigenetics*, *4*(1), 31-42.
- Hwang, C. S., Shemorry, A., Auerbach, D., & Varshavsky, A. (2010). The N-end rule pathway is mediated by a complex of the RING-type Ubr1 and HECT-type Ufd4 ubiquitin ligases. *Nat Cell Biol*, *12*(12), 1177-1185. doi:10.1038/ncb2121
- Ii, T., Mullen, J. R., Slagle, C. E., & Brill, S. J. (2007). Stimulation of in vitro sumoylation by Slx5-Slx8: evidence for a functional interaction with the SUMO pathway. *DNA Repair (Amst)*, *6*(11), 1679-1691. doi:10.1016/j.dnarep.2007.06.004
- Ira, G., Malkova, A., Liberi, G., Foiani, M., & Haber, J. E. (2003). Srs2 and Sgs1-Top3 suppress crossovers during double-strand break repair in yeast. *Cell*, *115*(4), 401-411.
- Iyer, L. M., Koonin, E. V., & Aravind, L. (2004). Novel predicted peptidases with a potential role in the ubiquitin signaling pathway. *Cell Cycle*, *3*(11), 1440-1450.
- Jalal, D., Chalissery, J., & Hassan, A. H. (2017). Genome maintenance in *Saccharomyces cerevisiae*: the role of SUMO and SUMO-targeted ubiquitin ligases. *Nucleic Acids Res*, *45*(5), 2242-2261. doi:10.1093/nar/gkw1369
- Jarosch, E., Taxis, C., Volkwein, C., Bordallo, J., Finley, D., Wolf, D. H., & Sommer, T. (2002). Protein dislocation from the ER requires polyubiquitination and the AAA-ATPase Cdc48. *Nat Cell Biol*, *4*(2), 134-139. doi:10.1038/ncb746
- Johnson, E. S., & Gupta, A. A. (2001). An E3-like factor that promotes SUMO conjugation to the yeast septins. *Cell*, *106*(6), 735-744.
- Johnson, E. S., Schwienhorst, I., Dohmen, R. J., & Blobel, G. (1997). The ubiquitin-like protein Smt3p is activated for conjugation to other proteins by an Aos1p/Uba2p heterodimer. *Embo j*, *16*(18), 5509-5519. doi:10.1093/emboj/16.18.5509

- Kalocsay, M., Hiller, N. J., & Jentsch, S. (2009). Chromosome-wide Rad51 spreading and SUMO-H2A.Z-dependent chromosome fixation in response to a persistent DNA double-strand break. *Mol Cell*, *33*(3), 335-343. doi:10.1016/j.molcel.2009.01.016
- Karras, G. I., & Jentsch, S. (2010). The RAD6 DNA damage tolerance pathway operates uncoupled from the replication fork and is functional beyond S phase. *Cell*, *141*(2), 255-267. doi:10.1016/j.cell.2010.02.028
- Kats, E. S., Enserink, J. M., Martinez, S., & Kolodner, R. D. (2009). The *Saccharomyces cerevisiae* Rad6 postreplication repair and Siz1/Srs2 homologous recombination-inhibiting pathways process DNA damage that arises in *asf1* mutants. *Mol Cell Biol*, *29*(19), 5226-5237. doi:10.1128/mcb.00894-09
- Kerscher, O., Felberbaum, R., & Hochstrasser, M. (2006). Modification of proteins by ubiquitin and ubiquitin-like proteins. *Annu Rev Cell Dev Biol*, *22*, 159-180. doi:10.1146/annurev.cellbio.22.010605.093503
- Khadaroo, B., Teixeira, M. T., Luciano, P., Eckert-Boulet, N., Germann, S. M., Simon, M. N., . . . Lisby, M. (2009). The DNA damage response at eroded telomeres and tethering to the nuclear pore complex. *Nat Cell Biol*, *11*(8), 980-987. doi:10.1038/ncb1910
- Kirkin, V., & Dikic, I. (2007). Role of ubiquitin- and Ubl-binding proteins in cell signaling. *Curr Opin Cell Biol*, *19*(2), 199-205. doi:10.1016/j.ceb.2007.02.002
- Klochender-Yeivin, A., Picarsky, E., & Yaniv, M. (2006). Increased DNA damage sensitivity and apoptosis in cells lacking the Snf5/Ini1 subunit of the SWI/SNF chromatin remodeling complex. *Mol Cell Biol*, *26*(7), 2661-2674. doi:10.1128/mcb.26.7.2661-2674.2006
- Kochenova, O. V., Soshkina, J. V., Stepchenkova, E. I., Inge-Vechtomov, S. G., & Shcherbakova, P. V. (2011). Participation of translesion synthesis DNA polymerases in the maintenance of chromosome integrity in yeast *Saccharomyces cerevisiae*. *Biochemistry (Mosc)*, *76*(1), 49-60.
- Koegl, M., Hoppe, T., Schlenker, S., Ulrich, H. D., Mayer, T. U., & Jentsch, S. (1999). A novel ubiquitination factor, E4, is involved in multiubiquitin chain assembly. *Cell*, *96*(5), 635-644.

- Kolesar, P., Altmannova, V., Silva, S., Lisby, M., & Krejci, L. (2016). Pro-recombination role of Srs2 requires SUMO but is independent of PCNA interaction. *J Biol Chem*. doi:10.1074/jbc.M115.685891
- Kolesar, P., Sarangi, P., Altmannova, V., Zhao, X., & Krejci, L. (2012). Dual roles of the SUMO-interacting motif in the regulation of Srs2 sumoylation. *Nucleic Acids Res*, *40*(16), 7831-7843. doi:10.1093/nar/gks484
- Komander, D., & Rape, M. (2012). The ubiquitin code. *Annu Rev Biochem*, *81*, 203-229. doi:10.1146/annurev-biochem-060310-170328
- Kramarz, K., Litwin, I., Cal-Bakowska, M., Szakal, B., Branzei, D., Wysocki, R., & Dziadkowiec, D. (2014). Swi2/Snf2-like protein Uls1 functions in the Sgs1-dependent pathway of maintenance of rDNA stability and alleviation of replication stress. *DNA Repair (Amst)*, *21*, 24-35. doi:10.1016/j.dnarep.2014.05.008
- Krejci, L., Altmannova, V., Spirek, M., & Zhao, X. (2012). Homologous recombination and its regulation. *Nucleic Acids Res*, *40*(13), 5795-5818. doi:10.1093/nar/gks270
- Kuang, L., Kou, H., Xie, Z., Zhou, Y., Feng, X., Wang, L., & Wang, Z. (2013). A non-catalytic function of Rev1 in translesion DNA synthesis and mutagenesis is mediated by its stable interaction with Rad5. *DNA Repair (Amst)*, *12*(1), 27-37. doi:10.1016/j.dnarep.2012.10.003
- Kubota, T., Nishimura, K., Kanemaki, M. T., & Donaldson, A. D. (2013). The Elg1 replication factor C-like complex functions in PCNA unloading during DNA replication. *Mol Cell*, *50*(2), 273-280. doi:10.1016/j.molcel.2013.02.012
- Langst, G., Bonte, E. J., Corona, D. F., & Becker, P. B. (1999). Nucleosome movement by CHRAC and ISWI without disruption or trans-displacement of the histone octamer. *Cell*, *97*(7), 843-852.
- Laurent, B. C., Treich, I., & Carlson, M. (1993). Role of yeast SNF and SWI proteins in transcriptional activation. *Cold Spring Harb Symp Quant Biol*, *58*, 257-263.
- Lee, D., An, J., Park, Y. U., Liaw, H., Woodgate, R., Park, J. H., & Myung, K. (2017). SHPRH regulates rRNA transcription by recognizing the histone code in an mTOR-dependent manner. *Proc Natl Acad Sci U S A*, *114*(17), E3424-e3433. doi:10.1073/pnas.1701978114

- Lescasse, R., Pobiega, S., Callebaut, I., & Marcand, S. (2013). End-joining inhibition at telomeres requires the translocase and polySUMO-dependent ubiquitin ligase Uls1. *Embo j*, 32(6), 805-815. doi:10.1038/emboj.2013.24
- Li, S. J., & Hochstrasser, M. (2000). The yeast ULP2 (SMT4) gene encodes a novel protease specific for the ubiquitin-like Smt3 protein. *Mol Cell Biol*, 20(7), 2367-2377.
- Lin, J. R., Zeman, M. K., Chen, J. Y., Yee, M. C., & Cimprich, K. A. (2011). SHPRH and HLTF act in a damage-specific manner to coordinate different forms of postreplication repair and prevent mutagenesis. *Mol Cell*, 42(2), 237-249. doi:10.1016/j.molcel.2011.02.026
- Lindroos, H. B., Strom, L., Itoh, T., Katou, Y., Shirahige, K., & Sjogren, C. (2006). Chromosomal association of the Smc5/6 complex reveals that it functions in differently regulated pathways. *Mol Cell*, 22(6), 755-767. doi:10.1016/j.molcel.2006.05.014
- Liu, Y. T., Chang, K. M., Ma, C. H., & Jayaram, M. (2016). Replication-dependent and independent mechanisms for the chromosome-coupled persistence of a selfish genome. *Nucleic Acids Res*, 44(17), 8302-8323. doi:10.1093/nar/gkw694
- Liu, Y. T., Ma, C. H., & Jayaram, M. (2013). Co-segregation of yeast plasmid sisters under monopolin-directed mitosis suggests association of plasmid sisters with sister chromatids. *Nucleic Acids Res*, 41(7), 4144-4158. doi:10.1093/nar/gkt096
- Longtine, M. S., McKenzie, A., 3rd, Demarini, D. J., Shah, N. G., Wach, A., Brachat, A., . . . Pringle, J. R. (1998). Additional modules for versatile and economical PCR-based gene deletion and modification in *Saccharomyces cerevisiae*. *Yeast*, 14(10), 953-961. doi:10.1002/(sici)1097-0061(199807)14:10<953::aid-yea293>3.0.co;2-u
- Lu, C. Y., Tsai, C. H., Brill, S. J., & Teng, S. C. (2010). Sumoylation of the BLM ortholog, Sgs1, promotes telomere-telomere recombination in budding yeast. *Nucleic Acids Res*, 38(2), 488-498. doi:10.1093/nar/gkp1008
- Luo, H., & Kausch, A. P. (2002). Application of FLP/FRT site-specific DNA recombination system in plants. *Genet Eng (N Y)*, 24, 1-16.

- Lusser, A., Urwin, D. L., & Kadonaga, J. T. (2005). Distinct activities of CHD1 and ACF in ATP-dependent chromatin assembly. *Nat Struct Mol Biol*, *12*(2), 160-166. doi:10.1038/nsmb884
- Ma, C. H., Cui, H., Hajra, S., Rowley, P. A., Fekete, C., Sarkeshik, A., . . . Jayaram, M. (2013). Temporal sequence and cell cycle cues in the assembly of host factors at the yeast 2 micron plasmid partitioning locus. *Nucleic Acids Res*, *41*(4), 2340-2353. doi:10.1093/nar/gks1338
- Marechal, A., & Zou, L. (2015). RPA-coated single-stranded DNA as a platform for post-translational modifications in the DNA damage response. *Cell Res*, *25*(1), 9-23. doi:10.1038/cr.2014.147
- McGrath, J. P., Jentsch, S., & Varshavsky, A. (1991). UBA 1: an essential yeast gene encoding ubiquitin-activating enzyme. *Embo j*, *10*(1), 227-236.
- McIntyre, J., & Woodgate, R. (2015). Regulation of translesion DNA synthesis: Posttranslational modification of lysine residues in key proteins. *DNA Repair (Amst)*, *29*, 166-179. doi:10.1016/j.dnarep.2015.02.011
- Mehta, S., Yang, X. M., Chan, C. S., Dobson, M. J., Jayaram, M., & Velmurugan, S. (2002). The 2 micron plasmid purloins the yeast cohesin complex: a mechanism for coupling plasmid partitioning and chromosome segregation? *J Cell Biol*, *158*(4), 625-637. doi:10.1083/jcb.200204136
- Miura, T., Shibata, T., & Kusano, K. (2013). Putative antirecombinase Srs2 DNA helicase promotes noncrossover homologous recombination avoiding loss of heterozygosity. *Proc Natl Acad Sci U S A*, *110*(40), 16067-16072. doi:10.1073/pnas.1303111110
- Miura, T., Yamana, Y., Usui, T., Ogawa, H. I., Yamamoto, M. T., & Kusano, K. (2012). Homologous recombination via synthesis-dependent strand annealing in yeast requires the Irc20 and Srs2 DNA helicases. *Genetics*, *191*(1), 65-78. doi:10.1534/genetics.112.139105
- Moinova, H. R., Chen, W. D., Shen, L., Smiraglia, D., Olechnowicz, J., Ravi, L., . . . Markowitz, S. D. (2002). HLTF gene silencing in human colon cancer. *Proc Natl Acad Sci U S A*, *99*(7), 4562-4567. doi:10.1073/pnas.062459899
- Moldovan, G. L., Pfander, B., & Jentsch, S. (2006). PCNA controls establishment of sister chromatid cohesion during S phase. *Mol Cell*, *23*(5), 723-732. doi:10.1016/j.molcel.2006.07.007

- Morrison, A. J., Highland, J., Krogan, N. J., Arbel-Eden, A., Greenblatt, J. F., Haber, J. E., & Shen, X. (2004). INO80 and gamma-H2AX interaction links ATP-dependent chromatin remodeling to DNA damage repair. *Cell*, *119*(6), 767-775. doi:10.1016/j.cell.2004.11.037
- Motegi, A., Liaw, H. J., Lee, K. Y., Roest, H. P., Maas, A., Wu, X., . . . Myung, K. (2008). Polyubiquitination of proliferating cell nuclear antigen by HLTF and SHPRH prevents genomic instability from stalled replication forks. *Proc Natl Acad Sci U S A*, *105*(34), 12411-12416. doi:10.1073/pnas.0805685105
- Mueller, J. P., & Smerdon, M. J. (1995). Repair of plasmid and genomic DNA in a rad7 delta mutant of yeast. *Nucleic Acids Res*, *23*(17), 3457-3464.
- Mullen, J. R., & Brill, S. J. (2008). Activation of the Slx5-Slx8 ubiquitin ligase by poly-small ubiquitin-like modifier conjugates. *J Biol Chem*, *283*(29), 19912-19921. doi:10.1074/jbc.M802690200
- Mullen, J. R., Kaliraman, V., Ibrahim, S. S., & Brill, S. J. (2001). Requirement for three novel protein complexes in the absence of the Sgs1 DNA helicase in *Saccharomyces cerevisiae*. *Genetics*, *157*(1), 103-118.
- Muller, S., Hoegel, C., Pyrowolakis, G., & Jentsch, S. (2001). SUMO, ubiquitin's mysterious cousin. *Nat Rev Mol Cell Biol*, *2*(3), 202-210. doi:10.1038/35056591
- Murray, J. A., Scarpa, M., Rossi, N., & Cesareni, G. (1987). Antagonistic controls regulate copy number of the yeast 2 mu plasmid. *Embo j*, *6*(13), 4205-4212.
- Ng, H. H., Xu, R. M., Zhang, Y., & Struhl, K. (2002). Ubiquitination of histone H2B by Rad6 is required for efficient Dot1-mediated methylation of histone H3 lysine 79. *J Biol Chem*, *277*(38), 34655-34657. doi:10.1074/jbc.C200433200
- Nguyen, H. D., Becker, J., Thu, Y. M., Costanzo, M., Koch, E. N., Smith, S., . . . Bielinsky, A. K. (2013). Unligated Okazaki Fragments Induce PCNA Ubiquitination and a Requirement for Rad59-Dependent Replication Fork Progression. *PLoS One*, *8*(6), e66379. doi:10.1371/journal.pone.0066379
- Noel, J. F., & Wellinger, R. J. (2011). Abrupt telomere losses and reduced end-resection can explain accelerated senescence of Smc5/6 mutants lacking telomerase. *DNA Repair (Amst)*, *10*(3), 271-282. doi:10.1016/j.dnarep.2010.11.010

- Ohuchi, T., Seki, M., Branzei, D., Maeda, D., Ui, A., Ogiwara, H., . . . Enomoto, T. (2008). Rad52 sumoylation and its involvement in the efficient induction of homologous recombination. *DNA Repair (Amst)*, 7(6), 879-889. doi:10.1016/j.dnarep.2008.02.005
- Ortolan, T. G., Chen, L., Tongaonkar, P., & Madura, K. (2004). Rad23 stabilizes Rad4 from degradation by the Ub/proteasome pathway. *Nucleic Acids Res*, 32(22), 6490-6500. doi:10.1093/nar/gkh987
- Oza, P., Jaspersen, S. L., Miele, A., Dekker, J., & Peterson, C. L. (2009). Mechanisms that regulate localization of a DNA double-strand break to the nuclear periphery. *Genes Dev*, 23(8), 912-927. doi:10.1101/gad.1782209
- Oza, P., & Peterson, C. L. (2010). Opening the DNA repair toolbox: localization of DNA double strand breaks to the nuclear periphery. *Cell Cycle*, 9(1), 43-49.
- Ozkaynak, E., Finley, D., & Varshavsky, A. (1984). The yeast ubiquitin gene: head-to-tail repeats encoding a polyubiquitin precursor protein. *Nature*, 312(5995), 663-666.
- Pabla, R., Rozario, D., & Siede, W. (2008). Regulation of *Saccharomyces cerevisiae* DNA polymerase eta transcript and protein. *Radiat Environ Biophys*, 47(1), 157-168. doi:10.1007/s00411-007-0132-1
- Pages, V., Bresson, A., Acharya, N., Prakash, S., Fuchs, R. P., & Prakash, L. (2008). Requirement of Rad5 for DNA polymerase zeta-dependent translesion synthesis in *Saccharomyces cerevisiae*. *Genetics*, 180(1), 73-82. doi:10.1534/genetics.108.091066
- Palancade, B., Liu, X., Garcia-Rubio, M., Aguilera, A., Zhao, X., & Doye, V. (2007). Nucleoporins prevent DNA damage accumulation by modulating Ulp1-dependent sumoylation processes. *Mol Biol Cell*, 18(8), 2912-2923. doi:10.1091/mbc.E07-02-0123
- Panse, V. G., Kuster, B., Gerstberger, T., & Hurt, E. (2003). Unconventional tethering of Ulp1 to the transport channel of the nuclear pore complex by karyopherins. *Nat Cell Biol*, 5(1), 21-27. doi:10.1038/ncb893
- Parker, J. L., Bielen, A. B., Dikic, I., & Ulrich, H. D. (2007). Contributions of ubiquitin- and PCNA-binding domains to the activity of Polymerase eta in *Saccharomyces cerevisiae*. *Nucleic Acids Res*, 35(3), 881-889. doi:10.1093/nar/gkl1102

- Parker, J. L., Bucceri, A., Davies, A. A., Heidrich, K., Windecker, H., & Ulrich, H. D. (2008). SUMO modification of PCNA is controlled by DNA. *Embo j*, 27(18), 2422-2431. doi:10.1038/emboj.2008.162
- Parnas, O., Zipin-Roitman, A., Pfander, B., Liefshitz, B., Mazor, Y., Ben-Aroya, S., . . . Kupiec, M. (2010). Elg1, an alternative subunit of the RFC clamp loader, preferentially interacts with SUMOylated PCNA. *Embo j*, 29(15), 2611-2622. doi:10.1038/emboj.2010.128
- Pebernard, S., Schaffer, L., Campbell, D., Head, S. R., & Boddy, M. N. (2008). Localization of Smc5/6 to centromeres and telomeres requires heterochromatin and SUMO, respectively. *Embo j*, 27(22), 3011-3023. doi:10.1038/emboj.2008.220
- Peng, J., Schwartz, D., Elias, J. E., Thoreen, C. C., Cheng, D., Marsischky, G., . . . Gygi, S. P. (2003). A proteomics approach to understanding protein ubiquitination. *Nat Biotechnol*, 21(8), 921-926. doi:10.1038/nbt849
- Petroski, M. D., & Deshaies, R. J. (2005). Function and regulation of cullin-RING ubiquitin ligases. *Nat Rev Mol Cell Biol*, 6(1), 9-20. doi:10.1038/nrm1547
- Pfander, B., Moldovan, G. L., Sacher, M., Hoege, C., & Jentsch, S. (2005). SUMO-modified PCNA recruits Srs2 to prevent recombination during S phase. *Nature*, 436(7049), 428-433. doi:10.1038/nature03665
- Pickart, C. M. (2000). Ubiquitin in chains. *Trends Biochem Sci*, 25(11), 544-548.
- Pinder, J. B., McQuaid, M. E., & Dobson, M. J. (2013). Deficient sumoylation of yeast 2-micron plasmid proteins Rep1 and Rep2 associated with their loss from the plasmid-partitioning locus and impaired plasmid inheritance. *PLoS One*, 8(3), e60384. doi:10.1371/journal.pone.0060384
- Pommier, Y., Barcelo, J. M., Rao, V. A., Sordet, O., Jobson, A. G., Thibaut, L., . . . Redon, C. (2006). Repair of topoisomerase I-mediated DNA damage. *Prog Nucleic Acid Res Mol Biol*, 81, 179-229. doi:10.1016/s0079-6603(06)81005-6
- Prajapati, H. K., Rizvi, S. M., Rathore, I., & Ghosh, S. K. (2017). Microtubule-associated proteins, Bik1 and Bim1, are required for faithful partitioning of the endogenous 2 micron plasmids in budding yeast. *Mol Microbiol*, 103(6), 1046-1064. doi:10.1111/mmi.13608

- Prakash, S., Johnson, R. E., & Prakash, L. (2005). Eukaryotic translesion synthesis DNA polymerases: specificity of structure and function. *Annu Rev Biochem*, *74*, 317-353. doi:10.1146/annurev.biochem.74.082803.133250
- Prakash, S., Sung, P., & Prakash, L. (1993). DNA repair genes and proteins of *Saccharomyces cerevisiae*. *Annu Rev Genet*, *27*, 33-70. doi:10.1146/annurev.ge.27.120193.000341
- Psakhye, I., & Jentsch, S. (2012). Protein group modification and synergy in the SUMO pathway as exemplified in DNA repair. *Cell*, *151*(4), 807-820. doi:10.1016/j.cell.2012.10.021
- Puig, O., Caspary, F., Rigaut, G., Rutz, B., Bouveret, E., Bragado-Nilsson, E., . . . Seraphin, B. (2001). The tandem affinity purification (TAP) method: a general procedure of protein complex purification. *Methods*, *24*(3), 218-229. doi:10.1006/meth.2001.1183
- Qu, Y., Gharbi, N., Yuan, X., Olsen, J. R., Blicher, P., Dalhus, B., . . . Ke, X. (2016). Axitinib blocks Wnt/beta-catenin signaling and directs asymmetric cell division in cancer. *Proc Natl Acad Sci U S A*, *113*(33), 9339-9344. doi:10.1073/pnas.1604520113
- Qu, Y., Kalland, K. H., & Ke, X. (2017). Small molecule induces Wnt asymmetry in cancer. *Cell Cycle*, *16*(2), 141-142. doi:10.1080/15384101.2016.1235850
- Raasi, S., & Pickart, C. M. (2003). Rad23 ubiquitin-associated domains (UBA) inhibit 26 S proteasome-catalyzed proteolysis by sequestering lysine 48-linked polyubiquitin chains. *J Biol Chem*, *278*(11), 8951-8959.
- Rabinovich, E., Kerem, A., Frohlich, K. U., Diamant, N., & Bar-Nun, S. (2002). AAA-ATPase p97/Cdc48p, a cytosolic chaperone required for endoplasmic reticulum-associated protein degradation. *Mol Cell Biol*, *22*(2), 626-634.
- Ramsey, K. L., Smith, J. J., Dasgupta, A., Maqani, N., Grant, P., & Auble, D. T. (2004). The NEF4 complex regulates Rad4 levels and utilizes Snf2/Swi2-related ATPase activity for nucleotide excision repair. *Mol Cell Biol*, *24*(14), 6362-6378. doi:10.1128/mcb.24.14.6362-6378.2004
- Rape, M., Hoppe, T., Gorr, I., Kalocay, M., Richly, H., & Jentsch, S. (2001). Mobilization of processed, membrane-tethered SPT23 transcription factor by CDC48(UFD1/NPL4), a ubiquitin-selective chaperone. *Cell*, *107*(5), 667-677.

- Reed, S. H., & Gillette, T. G. (2007). Nucleotide excision repair and the ubiquitin proteasome pathway--do all roads lead to Rome? *DNA Repair (Amst)*, 6(2), 149-156. doi:10.1016/j.dnarep.2006.10.026
- Reyes-Turcu, F. E., Ventii, K. H., & Wilkinson, K. D. (2009). Regulation and cellular roles of ubiquitin-specific deubiquitinating enzymes. *Annu Rev Biochem*, 78, 363-397. doi:10.1146/annurev.biochem.78.082307.091526
- Richardson, A., Gardner, R. G., & Prelich, G. (2013). Physical and Genetic Associations of the Irc20 Ubiquitin Ligase with Cdc48 and SUMO. *PLoS One*, 8(10), e76424. doi:10.1371/journal.pone.0076424
- Rosenbaum, J. C., Fredrickson, E. K., Oeser, M. L., Garrett-Engele, C. M., Locke, M. N., Richardson, L. A., . . . Gardner, R. G. (2011). Disorder targets misorder in nuclear quality control degradation: a disordered ubiquitin ligase directly recognizes its misfolded substrates. *Mol Cell*, 41(1), 93-106. doi:10.1016/j.molcel.2010.12.004
- Russell, S. J., Reed, S. H., Huang, W., Friedberg, E. C., & Johnston, S. A. (1999). The 19S regulatory complex of the proteasome functions independently of proteolysis in nucleotide excision repair. *Mol Cell*, 3(6), 687-695.
- Sacher, M., Pfander, B., Hoegge, C., & Jentsch, S. (2006). Control of Rad52 recombination activity by double-strand break-induced SUMO modification. *Nat Cell Biol*, 8(11), 1284-1290. doi:10.1038/ncb1488
- Sarangi, P., Bartosova, Z., Altmannova, V., Holland, C., Chavdarova, M., Lee, S. E., . . . Zhao, X. (2014). Sumoylation of the Rad1 nuclease promotes DNA repair and regulates its DNA association. *Nucleic Acids Res*, 42(10), 6393-6404. doi:10.1093/nar/gku300
- Sau, S., Liu, Y. T., Ma, C. H., & Jayaram, M. (2015). Stable persistence of the yeast plasmid by hitchhiking on chromosomes during vegetative and germ-line divisions of host cells. *Mob Genet Elements*, 5(2), 1-8. doi:10.1080/2159256x.2015.1031359
- Schauber, C., Chen, L., Tongaonkar, P., Vega, I., Lambertson, D., Potts, W., & Madura, K. (1998). Rad23 links DNA repair to the ubiquitin/proteasome pathway. *Nature*, 391(6668), 715-718. doi:10.1038/35661
- Scheffner, M., Nuber, U., & Huibregtse, J. M. (1995). Protein ubiquitination involving an E1-E2-E3 enzyme ubiquitin thioester cascade. *Nature*, 373(6509), 81-83. doi:10.1038/373081a0

- Schober, H., Ferreira, H., Kalck, V., Gehlen, L. R., & Gasser, S. M. (2009). Yeast telomerase and the SUN domain protein Mps3 anchor telomeres and repress subtelomeric recombination. *Genes Dev*, 23(8), 928-938. doi:10.1101/gad.1787509
- Schweizer, H. P. (2003). Applications of the *Saccharomyces cerevisiae* Flp-FRT system in bacterial genetics. *J Mol Microbiol Biotechnol*, 5(2), 67-77. doi:10.1159/000069976
- Shah, P. P., Zheng, X., Epshtein, A., Carey, J. N., Bishop, D. K., & Klein, H. L. (2010). Swi2/Snf2-related translocases prevent accumulation of toxic Rad51 complexes during mitotic growth. *Mol Cell*, 39(6), 862-872. doi:10.1016/j.molcel.2010.08.028
- Shcherbik, N., & Haines, D. S. (2007). Cdc48p(Npl4p/Ufd1p) binds and segregates membrane-anchored/tethered complexes via a polyubiquitin signal present on the anchors. *Mol Cell*, 25(3), 385-397. doi:10.1016/j.molcel.2007.01.024
- Shiratori, A., Shibata, T., Arisawa, M., Hanaoka, F., Murakami, Y., & Eki, T. (1999). Systematic identification, classification, and characterization of the open reading frames which encode novel helicase-related proteins in *Saccharomyces cerevisiae* by gene disruption and Northern analysis. *Yeast*, 15(3), 219-253. doi:10.1002/(sici)1097-0061(199902)15:3<219::aid-yea349>3.0.co;2-3
- Silver, H. R., Nissley, J. A., Reed, S. H., Hou, Y. M., & Johnson, E. S. (2011). A role for SUMO in nucleotide excision repair. *DNA Repair (Amst)*, 10(12), 1243-1251. doi:10.1016/j.dnarep.2011.09.013
- Sleep, D., Finnis, C., Turner, A., & Evans, L. (2001). Yeast 2 microm plasmid copy number is elevated by a mutation in the nuclear gene UBC4. *Yeast*, 18(5), 403-421. doi:10.1002/yea.679
- Som, T., Armstrong, K. A., Volkert, F. C., & Broach, J. R. (1988). Autoregulation of 2 micron circle gene expression provides a model for maintenance of stable plasmid copy levels. *Cell*, 52(1), 27-37.
- Song, J., Durrin, L. K., Wilkinson, T. A., Krontiris, T. G., & Chen, Y. (2004). Identification of a SUMO-binding motif that recognizes SUMO-modified proteins. *Proc Natl Acad Sci U S A*, 101(40), 14373-14378. doi:10.1073/pnas.0403498101

- Sood, R., Makalowska, I., Galdzicki, M., Hu, P., Eddings, E., Robbins, C. M., . . . Trent, J. M. (2003). Cloning and characterization of a novel gene, SHPRH, encoding a conserved putative protein with SNF2/helicase and PHD-finger domains from the 6q24 region. *Genomics*, 82(2), 153-161.
- Sriramachandran, A. M., & Dohmen, R. J. (2014). SUMO-targeted ubiquitin ligases. *Biochim Biophys Acta*, 1843(1), 75-85. doi:10.1016/j.bbamcr.2013.08.022
- Stephan, A. K., Kliszczak, M., & Morrison, C. G. (2011). The Nse2/Mms21 SUMO ligase of the Smc5/6 complex in the maintenance of genome stability. *FEBS Lett*, 585(18), 2907-2913. doi:10.1016/j.febslet.2011.04.067
- Stingele, J., Schwarz, M. S., Bloemeke, N., Wolf, P. G., & Jentsch, S. (2014). A DNA-dependent protease involved in DNA-protein crosslink repair. *Cell*, 158(2), 327-338. doi:10.1016/j.cell.2014.04.053
- Stricklett, P. K., Nelson, R. D., & Kohan, D. E. (1999). The Cre/loxP system and gene targeting in the kidney. *Am J Physiol*, 276(5 Pt 2), F651-657.
- Strope, P. K., Kozmin, S. G., Skelly, D. A., Magwene, P. M., Dietrich, F. S., & McCusker, J. H. (2015). 2mu plasmid in *Saccharomyces* species and in *Saccharomyces cerevisiae*. *FEMS Yeast Res*, 15(8). doi:10.1093/femsyr/fov090
- Stuckey, S., Mukherjee, K., & Storici, F. (2011). In vivo site-specific mutagenesis and gene collage using the delitto perfetto system in yeast *Saccharomyces cerevisiae*. *Methods Mol Biol*, 745, 173-191. doi:10.1007/978-1-61779-129-1_11
- Su, X. A., Dion, V., Gasser, S. M., & Freudenreich, C. H. (2015). Regulation of recombination at yeast nuclear pores controls repair and triplet repeat stability. *Genes Dev*, 29(10), 1006-1017. doi:10.1101/gad.256404.114
- Takahashi, Y., Dulev, S., Liu, X., Hiller, N. J., Zhao, X., & Strunnikov, A. (2008). Cooperation of sumoylated chromosomal proteins in rDNA maintenance. *PLoS Genet*, 4(10), e1000215. doi:10.1371/journal.pgen.1000215
- Takahashi, Y., & Strunnikov, A. (2008). In vivo modeling of polysumoylation uncovers targeting of Topoisomerase II to the nucleolus via optimal level of SUMO modification. *Chromosoma*, 117(2), 189-198. doi:10.1007/s00412-007-0137-1

- Tan, W., Wang, Z., & Prelich, G. (2013). Physical and Genetic Interactions Between Uls1 and the Slx5-Slx8 SUMO-Targeted Ubiquitin Ligase. *G3 (Bethesda)*. doi:10.1534/g3.113.005827
- Tatham, M. H., Geoffroy, M. C., Shen, L., Plechanovova, A., Hattersley, N., Jaffray, E. G., . . . Hay, R. T. (2008). RNF4 is a poly-SUMO-specific E3 ubiquitin ligase required for arsenic-induced PML degradation. *Nat Cell Biol*, 10(5), 538-546. doi:10.1038/ncb1716
- Terleth, C., Schenk, P., Poot, R., Brouwer, J., & van de Putte, P. (1990). Differential repair of UV damage in rad mutants of *Saccharomyces cerevisiae*: a possible function of G2 arrest upon UV irradiation. *Mol Cell Biol*, 10(9), 4678-4684.
- Theodosiou, N. A., & Xu, T. (1998). Use of FLP/FRT system to study *Drosophila* development. *Methods*, 14(4), 355-365. doi:10.1006/meth.1998.0591
- Tomi, N. S., Davari, K., Grotzky, D., Loos, F., Bottcher, K., Frankenberger, S., & Jungnickel, B. (2014). Analysis of SHPRH functions in DNA repair and immunoglobulin diversification. *DNA Repair (Amst)*, 24, 63-72. doi:10.1016/j.dnarep.2014.09.010
- Torres-Ramos, C. A., Prakash, S., & Prakash, L. (2002). Requirement of RAD5 and MMS2 for postreplication repair of UV-damaged DNA in *Saccharomyces cerevisiae*. *Mol Cell Biol*, 22(7), 2419-2426.
- Torres-Rosell, J., Machin, F., Farmer, S., Jarmuz, A., Eydmann, T., Dalgaard, J. Z., & Aragon, L. (2005). SMC5 and SMC6 genes are required for the segregation of repetitive chromosome regions. *Nat Cell Biol*, 7(4), 412-419. doi:10.1038/ncb1239
- Torres-Rosell, J., Sunjevaric, I., De Piccoli, G., Sacher, M., Eckert-Boulet, N., Reid, R., . . . Lisby, M. (2007). The Smc5-Smc6 complex and SUMO modification of Rad52 regulates recombinational repair at the ribosomal gene locus. *Nat Cell Biol*, 9(8), 923-931. doi:10.1038/ncb1619
- Tsalik, E. L., & Gartenberg, M. R. (1998). Curing *Saccharomyces cerevisiae* of the 2 micron plasmid by targeted DNA damage. *Yeast*, 14(9), 847-852. doi:10.1002/(sici)1097-0061(19980630)14:9<847::aid-yea285>3.0.co;2-9
- Tsutakawa, S. E., Yan, C., Xu, X., Weinacht, C. P., Freudenthal, B. D., Yang, K., . . . Ivanov, I. (2015). Structurally distinct ubiquitin- and sumo-modified PCNA: implications for their distinct roles in the DNA damage response. *Structure*, 23(4), 724-733. doi:10.1016/j.str.2015.02.008

- Ulrich, H. D. (2002). Degradation or maintenance: actions of the ubiquitin system on eukaryotic chromatin. *Eukaryot Cell*, 1(1), 1-10.
- Ulrich, H. D. (2009a). Regulating post-translational modifications of the eukaryotic replication clamp PCNA. *DNA Repair (Amst)*, 8(4), 461-469. doi:10.1016/j.dnarep.2009.01.006
- Ulrich, H. D. (2009b). The SUMO system: an overview. *Methods Mol Biol*, 497, 3-16. doi:10.1007/978-1-59745-566-4_1
- Uzunova, K., Gottsche, K., Miteva, M., Weisshaar, S. R., Glanemann, C., Schnellhardt, M., . . . Dohmen, R. J. (2007). Ubiquitin-dependent proteolytic control of SUMO conjugates. *J Biol Chem*, 282(47), 34167-34175. doi:10.1074/jbc.M706505200
- Van Komen, S., Petukhova, G., Sigurdsson, S., Stratton, S., & Sung, P. (2000). Superhelicity-driven homologous DNA pairing by yeast recombination factors Rad51 and Rad54. *Mol Cell*, 6(3), 563-572.
- Verhage, R., Zeeman, A. M., de Groot, N., Gleig, F., Bang, D. D., van de Putte, P., & Brouwer, J. (1994). The RAD7 and RAD16 genes, which are essential for pyrimidine dimer removal from the silent mating type loci, are also required for repair of the nontranscribed strand of an active gene in *Saccharomyces cerevisiae*. *Mol Cell Biol*, 14(9), 6135-6142.
- Verma, R., Oania, R., Fang, R., Smith, G. T., & Deshaies, R. J. (2011). Cdc48/p97 mediates UV-dependent turnover of RNA Pol II. *Mol Cell*, 41(1), 82-92. doi:10.1016/j.molcel.2010.12.017
- Vigasova, D., Sarangi, P., Kolesar, P., Vlasakova, D., Slezakova, Z., Altmannova, V., . . . Krejci, L. (2013). Lif1 SUMOylation and its role in non-homologous end-joining. *Nucleic Acids Res*, 41(10), 5341-5353. doi:10.1093/nar/gkt236
- Vignali, M., Hassan, A. H., Neely, K. E., & Workman, J. L. (2000). ATP-dependent chromatin-remodeling complexes. *Mol Cell Biol*, 20(6), 1899-1910.
- Volkert, F. C., & Broach, J. R. (1986). Site-specific recombination promotes plasmid amplification in yeast. *Cell*, 46(4), 541-550.
- Wang, Q., Song, C., Irizarry, L., Dai, R., Zhang, X., & Li, C. C. (2005). Multifunctional roles of the conserved Arg residues in the second region of homology of p97/valosin-containing protein. *J Biol Chem*, 280(49), 40515-40523. doi:10.1074/jbc.M509636200

- Wang, X., & Terpstra, E. J. (2013). Ubiquitin receptors and protein quality control. *J Mol Cell Cardiol*, *55*, 73-84. doi:10.1016/j.yjmcc.2012.09.012
- Ward, T. A., Dudasova, Z., Sarkar, S., Bhide, M. R., Vlasakova, D., Chovanec, M., & McHugh, P. J. (2012). Components of a Fanconi-like pathway control Pso2-independent DNA interstrand crosslink repair in yeast. *PLoS Genet*, *8*(8), e1002884. doi:10.1371/journal.pgen.1002884
- Waters, L. S., Minesinger, B. K., Wilttrout, M. E., D'Souza, S., Woodruff, R. V., & Walker, G. C. (2009). Eukaryotic translesion polymerases and their roles and regulation in DNA damage tolerance. *Microbiol Mol Biol Rev*, *73*(1), 134-154. doi:10.1128/mnbr.00034-08
- Watkins, J. F., Sung, P., Prakash, L., & Prakash, S. (1993). The *Saccharomyces cerevisiae* DNA repair gene RAD23 encodes a nuclear protein containing a ubiquitin-like domain required for biological function. *Mol Cell Biol*, *13*(12), 7757-7765.
- Weasner, B. M., Zhu, J., & Kumar, J. P. (2017). FLPing Genes On and Off in *Drosophila*. *Methods Mol Biol*, *1642*, 195-209. doi:10.1007/978-1-4939-7169-5_13
- Weinert, T. A., & Hartwell, L. H. (1988). The RAD9 gene controls the cell cycle response to DNA damage in *Saccharomyces cerevisiae*. *Science*, *241*(4863), 317-322.
- Wellinger, R. J., & Zakian, V. A. (2012). Everything you ever wanted to know about *Saccharomyces cerevisiae* telomeres: beginning to end. *Genetics*, *191*(4), 1073-1105. doi:10.1534/genetics.111.137851
- Wilson, C. J., Chao, D. M., Imbalzano, A. N., Schnitzler, G. R., Kingston, R. E., & Young, R. A. (1996). RNA polymerase II holoenzyme contains SWI/SNF regulators involved in chromatin remodeling. *Cell*, *84*(2), 235-244.
- Wilson, T. E., Grawunder, U., & Lieber, M. R. (1997). Yeast DNA ligase IV mediates non-homologous DNA end joining. *Nature*, *388*(6641), 495-498. doi:10.1038/41365
- Wong, M. C., Scott-Drew, S. R., Hayes, M. J., Howard, P. J., & Murray, J. A. (2002). RSC2, encoding a component of the RSC nucleosome remodeling complex, is essential for 2 microm plasmid maintenance in *Saccharomyces cerevisiae*. *Mol Cell Biol*, *22*(12), 4218-4229.

- Xiao, W., Chow, B. L., Broomfield, S., & Hanna, M. (2000). The *Saccharomyces cerevisiae* RAD6 group is composed of an error-prone and two error-free postreplication repair pathways. *Genetics*, *155*(4), 1633-1641.
- Xiao, W., Chow, B. L., Fontanie, T., Ma, L., Bacchetti, S., Hryciw, T., & Broomfield, S. (1999). Genetic interactions between error-prone and error-free postreplication repair pathways in *Saccharomyces cerevisiae*. *Mutat Res*, *435*(1), 1-11.
- Xie, Y., Kerscher, O., Kroetz, M. B., McConchie, H. F., Sung, P., & Hochstrasser, M. (2007). The yeast Hex3.Slx8 heterodimer is a ubiquitin ligase stimulated by substrate sumoylation. *J Biol Chem*, *282*(47), 34176-34184. doi:10.1074/jbc.M706025200
- Xiong, L., Chen, X. L., Silver, H. R., Ahmed, N. T., & Johnson, E. S. (2009). Deficient SUMO attachment to Flp recombinase leads to homologous recombination-dependent hyperamplification of the yeast 2 microm circle plasmid. *Mol Biol Cell*, *20*(4), 1241-1251. doi:10.1091/mbc.E08-06-0659
- Xu, P., Duong, D. M., Seyfried, N. T., Cheng, D., Xie, Y., Robert, J., . . . Peng, J. (2009). Quantitative proteomics reveals the function of unconventional ubiquitin chains in proteasomal degradation. *Cell*, *137*(1), 133-145. doi:10.1016/j.cell.2009.01.041
- Yang, J. G., Madrid, T. S., Sevastopoulos, E., & Narlikar, G. J. (2006). The chromatin-remodeling enzyme ACF is an ATP-dependent DNA length sensor that regulates nucleosome spacing. *Nat Struct Mol Biol*, *13*(12), 1078-1083. doi:10.1038/nsmb1170
- Ye, Y. (2006). Diverse functions with a common regulator: ubiquitin takes command of an AAA ATPase. *J Struct Biol*, *156*(1), 29-40. doi:10.1016/j.jsb.2006.01.005
- Yen Ting, L., Sau, S., Ma, C. H., Kachroo, A. H., Rowley, P. A., Chang, K. M., . . . Jayaram, M. (2014). The partitioning and copy number control systems of the selfish yeast plasmid: an optimized molecular design for stable persistence in host cells. *Microbiol Spectr*, *2*(5). doi:10.1128/microbiolspec.PLAS-0003-2013
- You, H. J., Swanson, R. L., Harrington, C., Corbett, A. H., Jinks-Robertson, S., Senturker, S., . . . Doetsch, P. W. (1999). *Saccharomyces cerevisiae* Ntg1p and Ntg2p: broad specificity N-glycosylases for the repair of oxidative DNA

damage in the nucleus and mitochondria. *Biochemistry*, 38(35), 11298-11306. doi:10.1021/bi991121i

- You, J., Croyle, J. L., Nishimura, A., Ozato, K., & Howley, P. M. (2004). Interaction of the bovine papillomavirus E2 protein with Brd4 tethers the viral DNA to host mitotic chromosomes. *Cell*, 117(3), 349-360.
- Young, C. L., Britton, Z. T., & Robinson, A. S. (2012). Recombinant protein expression and purification: a comprehensive review of affinity tags and microbial applications. *Biotechnol J*, 7(5), 620-634. doi:10.1002/biot.201100155
- Zeman, M. K., Lin, J. R., Freire, R., & Cimprich, K. A. (2014). DNA damage-specific deubiquitination regulates Rad18 functions to suppress mutagenesis. *J Cell Biol*, 206(2), 183-197. doi:10.1083/jcb.201311063
- Zhang, C., Roberts, T. M., Yang, J., Desai, R., & Brown, G. W. (2006). Suppression of genomic instability by SLX5 and SLX8 in *Saccharomyces cerevisiae*. *DNA Repair (Amst)*, 5(3), 336-346. doi:10.1016/j.dnarep.2005.10.010
- Zhao, X., Wu, C. Y., & Blobel, G. (2004). Mlp-dependent anchorage and stabilization of a desumoylating enzyme is required to prevent clonal lethality. *J Cell Biol*, 167(4), 605-611. doi:10.1083/jcb.200405168
- Zhou, W., Ryan, J. J., & Zhou, H. (2004). Global analyses of sumoylated proteins in *Saccharomyces cerevisiae*. Induction of protein sumoylation by cellular stresses. *J Biol Chem*, 279(31), 32262-32268. doi:10.1074/jbc.M404173200
- Zimmerman, E. S., Schulman, B. A., & Zheng, N. (2010). Structural assembly of cullin-RING ubiquitin ligase complexes. *Curr Opin Struct Biol*, 20(6), 714-721. doi:10.1016/j.sbi.2010.08.010

Appendix

Table 3: Top hits for mass spectrometry results for TAP-Irc20

*dNSAF is Distributed Normalized Spectral Abundance Factor, and refers to the relative amount of interested protein compared to total amount of proteins existed in the prep (total =1). **The list excludes ribosomal proteins, heat shock proteins, proteins of unknown function and mitochondrial proteins.

dNSAF * Rank	Gene**	dNSAF value for fractions:		Description
		21-23	24-26	
2	CDC10	0.0197	0.0536	Component of the septin ring , required for cytokinesis
3	CDC3	0.0147	0.0091	Component of the septin ring
4	CDC12	0.0130	0.0328	Component of the septin ring
5	SHS1	0.0127	0.0130	Component of the septin ring
7	EIS1	0.0084	0.0010	Component of the eisosome
10	FAS1	0.0075	0.0009	Beta subunit of fatty acid synthetase
11	FAS2	0.0071	0.0007	Alpha subunit of fatty acid synthetase
12	YGP1	0.0067	0.0006	Cell wall-related secretory glycoprotein
15	TDH1	0.0059	0.0011	Glyceraldehyde-3-phosphate dehydrogenase (GAPDH)
16	SSE1	0.0057	0.0024	ATPase component of heat shock protein Hsp90 chaperone complex
17	IMH1	0.0055	0.0001	Protein involved in vesicular transport
20	KGD2	0.0038	0.0009	Dihydrolipoyl transsuccinylase
22	CDC11	0.0030	0.0042	Component of the septin ring
23	CHC1	0.0023	0.0005	Clathrin heavy chain; involved in intracellular protein transport and endocytosis
25	CLC1	0.0020	0.0004	Clathrin light chain
28	NAP1	0.0017	0.0005	Histone chaperone
29	EDE1	0.0016	0.0001	Scaffold protein involved in the formation of early endocytic sites
30	MYO2	0.0015	0.0007	Type V myosin motor involved in actin-based transport of cargos
31	TEF4	0.0015	0.0007	Gamma subunit of translational elongation factor eEF1B
32	PSA1	0.0012	0.0009	GDP-mannose pyrophosphorylase
33	BMH2	0.0012	0.0054	14-3-3 protein, controls proteome at post-transcriptional level

Table 3: Top hits for mass spectrometry results for TAP-Irc20 (continued)

dNSAF * Rank	Gene**	dNSAF value for fractions:		Description
		21-23	24-26	
35	TAF6	0.0010	0.0005	Subunit of TFIID and SAGA complexes; involved in transcription initiation of RNA polymerase II and in chromatin modification
36	GYP1	0.0010	0.0004	Cis-golgi GTPase-activating protein (GAP) for yeast Rabs
37	LAT1	0.0009	0.0002	Dihydrolipoamide acetyltransferase component of the pyruvate dehydrogenase complex (PDC)
38	PDA1	0.0009	0.0002	E1 alpha subunit of the pyruvate dehydrogenase (PDH) complex
41	SSA3	0.0008	0.0003	ATPase involved in protein folding and the response to stress
43	CDC27	0.0008	0.0004	Subunit of the Anaphase-Promoting Complex/Cyclosome (APC/C)
44	KEL1	0.0008	0.0001	Protein required for proper cell fusion and cell morphology
45	AHA1	0.0008	0.0006	Co-chaperone that binds Hsp82p and activates its ATPase activity
47	CKA2	0.0008	0.0076	Alpha' catalytic subunit of casein kinase 2 (CK2)
50	VAC14	0.0007	0.0001	Enzyme regulator, in control of trafficking of some proteins to the vacuole lumen via the MVB, and in maintenance of vacuole size and acidity
51	TAF11	0.0007	0.0023	TFIID subunit; involved in RNA polymerase II transcription initiation
52	SEC31	0.0007	0.0011	Component of the Sec13p-Sec31p complex of the COPII vesicle coat
53	TUP1	0.0007	0.0002	General repressor of transcription; forms complex with Cyc8p, involved in the establishment of repressive chromatin structure
55	URA2	0.0006	0.0003	Bifunctional carbamoylphosphate synthetase/aspartate transcarbamylase
56	RVS161	0.0006	0.0006	Regulates polarization of the actin cytoskeleton, endocytosis, cell polarity, cell fusion and viability following starvation or osmotic stress

Table 3: Top hits for mass spectrometry results for TAP-Irc20 (continued)

dNSAF * Rank	Gene**	dNSAF value for fractions:		Description
		21-23	24-26	
57	SRP1	0.0006	0.0022	Karyopherin alpha homolog mediates import of nuclear proteins
58	RPT1	0.0006	0.0003	ATPase of the 19S regulatory particle of the 26S proteasome
59	CYR1	0.0006	0.0003	Adenylate cyclase; required for cAMP production and cAMP-dependent protein kinase signaling
60	SNF1	0.0006	0.0005	Forms a complex with Snf4p and members of the Sip1p/Sip2p/Gal83p family; required for transcription of glucose-repressed genes
62	SWC4	0.0005	0.0010	Component of the Swr1p complex that incorporates Htz1p into chromatin
64	YAF9	0.0005	0.0015	Subunit of NuA4 histone H4 acetyltransferase and SWR1 complexes
65	CKB1	0.0005	0.0003	Beta regulatory subunit of casein kinase 2 (CK2)
66	HCM1	0.0005	0.0004	Forkhead transcription factor
67	TIF34	0.0005	0.0014	eIF3i subunit of the eukaryotic translation initiation factor 3 (eIF3)
68	NOG1	0.0005	0.0001	Associates with free 60S ribosomal subunits in the nucleolus and is required for 60S ribosomal subunit biogenesis
69	IES3	0.0005	0.0002	Subunit of the INO80 chromatin remodeling complex
70	PRE6	0.0005	0.0007	Alpha 4 subunit of the 20S proteasome
71	TRX1	0.0005	0.0016	Cytoplasmic thioredoxin isoenzyme
72	CDC23	0.0004	0.0001	Subunit of the (APC/C)
75	RXT2	0.0004	0.0002	Component of the histone deacetylase Rpd3L complex
76	ACS2	0.0004	0.0005	Acetyl-coA synthetase isoform
77	CLA4	0.0004	0.0000	Cdc42p-activated signal transducing kinase
79	MRC1	0.0004	0.0004	S-phase checkpoint protein required for DNA replication
80	PDB1	0.0004	0.0005	E1 beta subunit of the pyruvate dehydrogenase (PDH) complex

Table 3: Top hits for mass spectrometry results for TAP-Irc20 (continued)

dNSAF * Rank	Gene**	dNSAF value for fractions:		Description
		21-23	24-26	
81	CKA1	0.0004	0.0019	Alpha catalytic subunit of casein kinase 2
82	ARO8	0.0004	0.0002	Aromatic aminotransferase I
83	TAF1	0.0004	0.0002	TFIID subunit, involved in RNA pol II transcription initiation
85	APC9	0.0004	0.0006	Subunit of the (APC/C)
86	COP1	0.0004	0.0009	Alpha subunit of COPI vesicle coatomer complex
87	CDC48	0.0003	0.0006	AAA ATPase; subunit of polyUb-selective segregase complex
88	EAP1	0.0003	0.0006	eIF4E-associated protein, competes with eIF4G for binding to eIF4E
90	SPT7	0.0003	0.0001	Subunit of the SAGA transcriptional regulatory complex
91	ADH2	0.0003	0.0002	Glucose-repressible alcohol dehydrogenase II
92	MKT1	0.0003	0.0001	Protein similar to nucleases that forms a complex with Pbp1p; complex may mediate posttranscriptional regulation of HO
93	PMA1	0.0003	0.0002	Plasma membrane P2-type H ⁺ -ATPase
94	YPI1	0.0003	0.0003	Regulatory subunit of the type I protein phosphatase (PP1) Glc7p
97	CCT8	0.0003	0.0012	Subunit of the cytosolic chaperonin Cct ring complex
98	NIP1	0.0003	0.0003	eIF3c subunit of the eukaryotic translation initiation factor 3 (eIF3)
99	NOG2	0.0003	0.0003	Associates with pre-60S ribosomal subunits in the nucleolus and is required for their nuclear export and maturation
100	CCT4	0.0003	0.0014	Subunit of the Cct ring complex
102	GCN1	0.0003	0.0003	Positive regulator of the Gcn2p kinase activity; forms a complex with Gcn20p; proposed to stimulate Gcn2p activation by an uncharged tRNA
103	CDC16	0.0003	0.0003	Subunit of the (APC/C)
105	PRE2	0.0002	0.0006	Beta 5 subunit of the 20S proteasome

Table 3: Top hits for mass spectrometry results for TAP-Irc20 (continued)

dNSAF * Rank	Gene**	dNSAF value for fractions:		Description
		21-23	24-26	
106	APC1	0.0002	0.0001	Largest subunit of the (APC/C)
108	PFK1	0.0002	0.0022	Alpha subunit of heterooctameric phosphofructokinase
109	SEC13	0.0002	0.0013	Structural component of 3 complexes; subunit of the Nup84p nuclear pore subcomplex that contributes to nucleocytoplasmic transport and NPC biogenesis
110	LPD1	0.0002	0.0002	Dihydrolipoamide dehydrogenase
111	FAA1	0.0002	0.0001	Long chain fatty acyl-CoA synthetase
112	SAP30	0.0002	0.0004	Component of Rpd3L histone deacetylase complex; involved in silencing at telomeres, rDNA, and silent mating-type loci
113	RPO21	0.0002	0.0001	RNA polymerase II largest subunit B220
114	LIP5	0.0002	0.0005	Protein involved in biosynthesis of the coenzyme lipoic acid
115	FAB1	0.0002	0.0000	1-phosphatidylinositol-3-phosphate 5-kinase
116	IRC20	0.0002	0.0001	
117	GCD11	0.0002	0.0004	Gamma subunit of the translation initiation factor eIF2; involved in the identification of the start codon
118	INO80	0.0002	0.0001	ATPase and nucleosome spacing factor; subunit of complex containing actin and actin-related proteins that has chromatin remodeling activity and 3' to 5' DNA helicase activity in vitro; has a role in modulating stress gene transcription
119	MEU1	0.0002	0.0002	Methylthioadenosine phosphorylase (MTAP)
120	BUG1	0.0002	0.0017	Cis-golgi localized protein involved in ER to Golgi transport
121	MDN1	0.0002	0.0000	Huge dynein-related AAA-type ATPase (midasin)
122	STE5	0.0002	0.0001	Pheromone-responsive MAPK scaffold protein
123	SES1	0.0002	0.0002	Cytosolic seryl-tRNA synthetase

Table 3: Top hits for mass spectrometry results for TAP-Irc20 (continued)

dNSAF * Rank	Gene**	dNSAF value for fractions:		Description
		21-23	24-26	
124	TRP5	0.0002	0.0001	Tryptophan synthase
125	SPT20	0.0002	0.0001	Subunit of the SAGA transcriptional regulatory complex; involved in maintaining the integrity of the complex
129	UGP1	0.0002	0.0002	UDP-glucose pyrophosphorylase (UGPase)
130	FAR8	0.0002	0.0038	Protein involved in recovery from arrest in response to pheromone
133	SEC26	0.0002	0.0006	Essential beta-coat protein of the COPI coatomer
134	STE11	0.0002	0.0001	Signal transducing MEK kinase
135	DBF2	0.0002	0.0001	Ser/Thr kinase involved in transcription and stress response
136	RPT2	0.0002	0.0006	ATPase of the 19S regulatory particle of the 26S proteasome
137	SUP45	0.0002	0.0001	Polypeptide release factor (eRF1) in translation termination
138	RGT1	0.0002	0.0001	Glucose-responsive transcription factor
139	SAN1	0.0002	0.0001	Ubiquitin-protein ligase
143	TCO89	0.0001	0.0003	Subunit of TORC1 (Tor1p or Tor2p-Kog1p-Lst8p-Tco89p)
144	SNF4	0.0001	0.0026	Activating gamma subunit of the AMP-activated Snf1p kinase complex; additional subunits of the complex are Snf1p and a Sip1p/Sip2p/Gal83p family member; activates glucose-repressed genes, represses glucose-induced genes; role in sporulation, and peroxisome biogenesis
145	CYC8	0.0001	0.0001	General transcriptional co-repressor; acts together with Tup1p; also acts as part of a transcriptional co-activator complex that recruits the SWI/SNF and SAGA complexes to promoters
147	TFB4	0.0001	0.0002	Subunit of TFIIH complex; involved in transcription initiation
148	LSP1	0.0001	0.0001	Eisosome core component

Table 3: Top hits for mass spectrometry results for TAP-Irc20 (continued)

dNSAF * Rank	Gene**	dNSAF value for fractions:		Description
		21-23	24-26	
152	GDE1	0.0001	0.0003	Glycerophosphocholine (GroPCho) phosphodiesterase
153	FBA1	0.0001	0.0002	Fructose 1,6-bisphosphate aldolase
155	BCK1	0.0001	0.0001	MAPKKK acting in the protein kinase C signaling pathway
157	TSA1	0.0001	0.0013	Thioredoxin peroxidase
158	YHB1	0.0001	0.0001	Nitric oxide oxidoreductase
159	ACC1	0.0001	0.0001	Acetyl-CoA carboxylase
160	PUP3	0.0001	0.0018	Beta 3 subunit of the 20S proteasome
162	MIL1	0.0001	0.0000	Predicted lipase
163	CRN1	0.0001	0.0007	Coronin
164	TSL1	0.0001	0.0002	Large subunit of trehalose 6-phosphate synthase/phosphatase complex
165	CMK1	0.0001	0.0005	Calmodulin-dependent protein kinase
166	PAF1	0.0001	0.0001	Component of the Paf1p complex involved in transcription elongation
169	SLA2	0.0001	0.0000	Adaptor protein that links actin to clathrin and endocytosis
170	RPB2	0.0001	0.0001	RNA polymerase II second largest subunit B150
171	MES1	0.0001	0.0001	Methionyl-tRNA synthetase
172	PRT1	0.0001	0.0002	eIF3b subunit of the eukaryotic translation initiation factor 3 (eIF3)
173	OSH2	0.0001	0.0004	Member of an oxysterol-binding protein family with seven members
176	KAR2	0.0001	0.0002	ATPase involved in protein import into the ER
177	APL6	0.0001	0.0001	Beta3-like subunit of the yeast AP-3 complex
178	CCT7	0.0001	0.0006	Subunit of the Cct ring complex
179	PHB1	0.0001	0.0004	Subunit of the prohibitin complex (Phb1p-Phb2p)
181	COG4	0.0001	0.0000	Essential component of the conserved oligomeric Golgi complex
182	CMS1	0.0001	0.0001	Putative subunit of the 90S preribosome processome complex
183	GPH1	0.0001	0.0000	Glycogen phosphorylase required for the mobilization of glycogen

Table 3: Top hits for mass spectrometry results for TAP-Irc20 (continued)

dNSAF * Rank	Gene**	dNSAF value for fractions:		Description
		21-23	24-26	
184	KAP104	0.0001	0.0000	Transportin or cytosolic karyopherin beta 2
185	PHB2	0.0001	0.0001	Subunit of the prohibitin complex (Phb1p-Phb2p)
186	SEC21	0.0001	0.0000	Gamma subunit of coatomer; coatomer is a heptameric protein complex that together with Arf1p forms the COPI coat; involved in ER to Golgi transport of selective cargo
187	TPD3	0.0001	0.0003	Regulatory subunit A of the heterotrimeric PP2A complex
188	APC4	0.0001	0.0001	Subunit of the (APC/C)
189	FIP1	0.0001	0.0001	Subunit of cleavage polyadenylation factor (CPF)
190	NUP145	0.0001	0.0000	Essential protein in two nuclear pore subcomplexes
191	SPT16	0.0001	0.0000	Subunit of the heterodimeric FACT complex (Spt16p-Pob3p); FACT associates with chromatin and reorganizes nucleosomes to facilitate access to DNA by RNA and DNA polymerases
192	MND2	0.0001	0.0002	Subunit of the (APC/C)
193	GCD7	0.0001	0.0010	Beta subunit of the translation initiation factor eIF2B
194	VMA5	0.0001	0.0001	Subunit C of the V1 peripheral membrane domain of V-ATPase
196	RPA49	0.0001	0.0002	RNA polymerase I subunit A49
197	RPT3	0.0001	0.0010	ATPase of the 19S regulatory particle of the 26S proteasome
199	CCT5	0.0000	0.0003	Subunit of the Cct ring complex
200	SMC3	0.00001	0.00001	Subunit of the multiprotein cohesin complex

Table 4: Top hits for mass spectrometry for TAP-Irc20 *C1239A*

*Signal Intensity refers to the sum of intensity measurements for total peptides detected for the protein. **The list excludes ribosomal proteins, heat shock proteins, proteins of unknown function and mitochondrial proteins. Highlighted in grey are proteins pulled down with both wild type and mutant Irc20.

Gene Symbol	Signal Intensity*		Description
	<i>Irc20 C1239A</i>	Control	
KOG1	220000000	0	Subunit of TORC1
SWI1	130000000	0	SWI/SNF chromatin-remodeling complex subunit
FAB1	110000000	0	1-phosphatidylinositol-3-phosphate 5-kinase
COP1	99000000	0	Alpha subunit of COPI vesicle coatomer complex
FAA3	98000000	0	Long chain fatty acyl-CoA synthetase
PMA1	92000000	0	Plasma membrane P2-type H ⁺ -ATPase
SEC26	83000000	0	Essential beta-coat protein of the COPI coatomer
FAA1	75000000	0	Long chain fatty acyl-CoA synthetase
TY1B	66000000	0	Transposon TyH3 Gag-Pol polyprotein
TRA1	60000000	0	Subunit of SAGA and NuA4 histone acetyltransferase complexes
VMA2	59000000	0	Subunit B of V1 peripheral membrane domain of vacuolar H ⁺ -ATPase
CKA2	53000000	0	Alpha' catalytic subunit of casein kinase 2 (CK2)
URA2	50000000	0	Bifunctional carbamoylphosphate synthetase/aspartate transcarbamylase
APC1	47000000	0	Largest subunit of the (APC/C)
RPO21	46000000	0	RNA polymerase II largest subunit B220
FAS1	45000000	0	Beta subunit of fatty acid synthetase
BNI1	35000000	0	Formin; polarisome component; nucleates the formation of linear actin filaments
ADH1	31000000	0	Alcohol dehydrogenase
RGA2	30000000	0	GTPase-activating protein for polarity-establishment protein Cdc42p
PFK2	29000000	0	Beta subunit of heterooctameric phosphofructokinase
RNQ1	29000000	0	Prion; an infectious protein conformation that is generally an ordered protein aggregate

Table 4: Top hits for mass spectrometry for TAP-*Irc20 C1239A* (continued)

Gene Symbol	Signal Intensity*		Description
	<i>Irc20 C1239A</i>	Control	
BIM1	24000000	0	Microtubule plus end-tracking protein
EBS1	24000000	0	Protein involved in translation inhibition and nonsense-mediated decay
PDR1	23000000	0	Transcription factor that regulates the pleiotropic drug response
TUB2	23000000	0	Tubulin beta chain
AVL9	22000000	0	Conserved protein involved in exocytic transport from the Golgi
RLP7	21000000	0	Nucleolar protein similar to large ribosomal subunit L7 proteins
APC2	21000000	0	Subunit of the (APC/C)
BNI4	21000000	0	Targeting subunit for Glc7p protein phosphatase
SNT1	20000000	0	Subunit of the Set3C deacetylase complex
KAP123	19000000	0	Karyopherin beta; mediates nuclear import of ribosomal proteins prior to assembly into ribosomes
TPD3	19000000	0	Regulatory subunit A of the heterotrimeric PP2A complex
FAS2	19000000	0	Alpha subunit of fatty acid synthetase
ELG1	19000000	0	Subunit of an alternative replication factor C complex
YMR1	19000000	0	Phosphatidylinositol 3-phosphate (PI3P) phosphatase
TFB1	19000000	0	Subunit of TFIIH and NEF3 complexes
GLT1	18000000	0	NAD(+)-dependent glutamate synthase
RPA190	18000000	0	RNA polymerase I largest subunit A190
NOP1	18000000	0	Histone glutamine methyltransferase
IQG1	18000000	0	Essential protein required for determination of budding pattern
YJL049W	17000000	0	Localizes to the ER presumably as part of an ESCRT-III like complex
CDC23	17000000	0	Subunit of the (APC/C)
SWP82	17000000	0	Member of the SWI/SNF chromatin remodeling complex
NUT1	16000000	0	Component of the RNA polymerase II mediator complex

Table 4: Top hits for mass spectrometry for TAP-*Irc20 C1239A* (continued)

Gene Symbol	Signal Intensity*		Description
	<i>Irc20 C1239A</i>	Control	
CDC39	16000000	0	Subunit of the CCR4-NOT1 core complex has multiple roles in regulation of mRNA levels
SST2	16000000	0	GTPase-activating protein for Gpa1p; regulates desensitization to alpha factor pheromone
APL3	16000000	0	Alpha-adaptin; large subunit of the clathrin associated protein complex(AP-2)
RTS1	16000000	0	B-type regulatory subunit of protein phosphatase 2A (PP2A)
CDC27	16000000	0	Subunit of the (APC/C)
NUP145	16000000	0	Essential protein in two nuclear pore subcomplexes
NAB6	16000000	0	Putative RNA-binding protein
SSD1	16000000	0	Translational repressor with a role in polar growth and wall integrity
ATG26	16000000	0	UDP-glucose:sterol glucosyltransferase
UBP13	16000000	0	Ubiquitin-specific protease that cleaves Ub-protein fusions
APC5	15000000	0	Subunit of the (APC/C)
MYO4	15000000	0	Type V myosin motor
SEC7	15000000	0	Guanine nucleotide exchange factor (GEF) for ADP ribosylation factors
BOI1	15000000	0	Protein implicated in polar growth
NEW1	15000000	0	ATP binding cassette protein; required for biogenesis of the small ribosomal subunit
ACS2	15000000	0	Acetyl-coA synthetase isoform
MTC5	14000000	0	Subunit of SEACAT, a subcomplex of the SEA complex, a coatomer-related complex
XRN1	13000000	0	Evolutionarily-conserved 5'-3' exonuclease
ACE2	13000000	0	Transcription factor required for septum destruction after cytokinesis
SPT7	13000000	0	Subunit of the SAGA transcriptional regulatory complex
DHH1	13000000	0	Cytoplasmic DEAD-box helicase
KAR2	13000000	0	ATPase involved in protein import into the ER
GFA1	13000000	0	Glutamine-fructose-6-phosphate amidotransferase
ACC1	12000000	0	Acetyl-CoA carboxylase
TFB2	12000000	0	Subunit of TFIIF and NEF3 complexes

Table 4: Top hits for mass spectrometry for TAP-*Irc20 C1239A* (continued)

Gene Symbol	Signal Intensity*		Description
	<i>Irc20 C1239A</i>	Control	
GLC7	12000000	0	Type 1 S/T protein phosphatase (PP1) catalytic subunit
TAF6	12000000	0	Subunit of TFIID and SAGA complexes; involved in transcription initiation of RNA polymerase II and in chromatin modification
DAL81	11000000	0	Positive regulator of genes in multiple nitrogen degradation pathways
TAF4	11000000	0	TFIID subunit; involved in RNA polymerase II transcription initiation
MDN1	10000000	0	Huge dynein-related AAA-type ATPase (midasin)
SIN4	10000000	0	Subunit of the RNA polymerase II mediator complex
SEA4	10000000	0	Subunit of SEACAT, a subcomplex of the SEA complex
URA7	10000000	0	Major CTP synthase isozyme
TBF1	9900000	0	Telobox-containing general regulatory factor
STE11	9800000	0	Signal transducing MEK kinase
ECM21	9700000	0	Protein involved in regulating endocytosis of plasma membrane proteins
TY1B-BR	9600000	0	Transposon Ty1-BR Gag-Pol polyprotein
BNA3	9200000	0	Kynurenine aminotransferase
CHC1	8900000	0	Clathrin heavy chain; involved in intracellular protein transport and endocytosis
RPA135	8900000	0	RNA polymerase I second largest subunit A135
PFK1	8900000	0	Alpha subunit of heterooctameric phosphofructokinase
PGK1	8800000	0	3-phosphoglycerate kinase
ARP7	8700000	0	Component of both the SWI/SNF and RSC chromatin remodeling complexes
RFC4	8600000	0	Subunit of heteropentameric Replication factor C (RF-C)
GCN1	8500000	0	Positive regulator of the Gcn2p kinase activity
CDC55	8400000	0	Regulatory subunit B of protein phosphatase 2A (PP2A)
MMS1	8300000	0	Subunit of E3 ubiquitin ligase complex involved in replication repair

Table 4: Top hits for mass spectrometry for TAP-*Irc20 C1239A* (continued)

Gene Symbol	Signal Intensity*		Description
	<i>Irc20 C1239A</i>	Control	
INO80	8300000	0	ATPase and nucleosome spacing factor; subunit of complex containing actin and actin-related proteins that has chromatin remodeling activity and 3' to 5' DNA helicase activity in vitro; has a role in modulating stress gene transcription
MPE1	8100000	0	Essential conserved subunit of CPF cleavage and polyadenylation factor
SNF1	8100000	0	Forms a complex with Snf4p and members of the Sip1p/Sip2p/Gal83p family; required for transcription of glucose-repressed genes
EDC3	8000000	0	Non-essential conserved protein with a role in mRNA decapping
MES1	8000000	0	Methionine--tRNA ligase
UFD4	7700000	0	Ubiquitin-protein ligase (E3); interacts with Rpt4p and Rpt6p, two subunits of the 19S particle of the 26S proteasome
YEF3	7700000	0	Translation elongation factor 3
RFC2	7700000	0	Subunit of heteropentameric Replication factor C (RF-C)
DOT6	7300000	0	Protein involved in rRNA and ribosome biogenesis
NIP1	7300000	0	eIF3c subunit of the eukaryotic translation initiation factor 3 (eIF3)
SWH1	7200000	0	Contains ankyrin repeats and FFAT motif; interacts with ER anchor Scs2p at the nucleus-vacuole junction
GDE1	7200000	0	Glycerophosphocholine (GroPCho) phosphodiesterase
KAP95	7100000	0	Karyopherin beta; interacts with nucleoporins to mediate nuclear import of NLS-containing cargo proteins via the nuclear pore complex
RTC1	7100000	0	Subunit of SEACAT, a subcomplex of the SEA complex
SET3	7100000	0	Defining member of the SET3 histone deacetylase complex
MEU1	7100000	0	Methylthioadenosine phosphorylase (MTAP)
VAC14	7000000	0	Enzyme regulator; involved in synthesis of phosphatidylinositol 3,5-bisphosphate
CDC53	7000000	0	Cullin; structural protein of SCF complexes

Table 4: Top hits for mass spectrometry for TAP-*Irc20 C1239A* (continued)

Gene Symbol	Signal Intensity*		Description
	<i>Irc20 C1239A</i>	Control	
NUP133	6800000	0	Subunit of Nup84p subcomplex of nuclear pore complex (NPC)
RFC5	6800000	0	Subunit of heteropentameric Replication factor C (RF-C)
ARO1	6700000	0	Pentafunctional arom protein
NSR1	6700000	0	Nucleolar protein that binds nuclear localization sequences
IRC20	6500000	0	
EDE1	6400000	0	Scaffold protein involved in the formation of early endocytic sites
PUF3	6300000	0	Protein of the mitochondrial outer surface
APC4	6300000	0	Subunit of the (APC/C)
TAF1	6300000	0	TFIID subunit
GSY1	6200000	0	Glycogen synthase
MSB3	6200000	0	Rab GTPase-activating protein
PSA1	6200000	0	GDP-mannose pyrophosphorylase (mannose-1-phosphate guanyltransferase)
TUB3	6200000	0	Alpha-tubulin
SIN3	6200000	0	Component of both the Rpd3S and Rpd3L histone deacetylase complexes
SRV2	6000000	0	CAP (cyclase-associated protein)
TDH1	5900000	0	Glyceraldehyde-3-phosphate dehydrogenase (GAPDH), isozyme 1
SAF1	5900000	0	F-Box protein involved in proteasome-dependent degradation of Aah1p
URB1	5700000	0	Protein required for the normal accumulation of 25S and 5.8S rRNAs
GCD11	5700000	0	Gamma subunit of the translation initiation factor eIF2
ULS1	5600000	0	Swi2/Snf2-related translocase and STUbL
MSL5	5600000	0	Component of commitment complex; which defines first step in splicing pathway
YPR097W	5500000	0	Protein that contains a PX domain and binds phosphoinositides
PTR3	5500000	0	Component of the SPS plasma membrane amino acid sensor system
RAM1	5500000	0	Beta subunit of the CAAX farnesyltransferase (FTase)

Table 4: Top hits for mass spectrometry for TAP-*Irc20 C1239A* (continued)

Gene Symbol	Signal Intensity*		Description
	<i>Irc20 C1239A</i>	Control	
NUP82	5400000	0	Linker nucleoporin component of the nuclear pore complex (NPC)
SEN1	5400000	0	ATP-dependent 5' to 3' RNA/DNA and DNA helicase
PDR16	5400000	0	Phosphatidylinositol transfer protein (PITP)
PRT1	5400000	0	eIF3b subunit of the eukaryotic translation initiation factor 3 (eIF3)
HSL1	5300000	0	Nim1p-related protein kinase; septin-binding kinase
PIK1	5300000	0	Phosphatidylinositol 4-kinase
RGR1	5200000	0	Subunit of the RNA polymerase II mediator complex
CCT8	5200000	0	Subunit of the cytosolic chaperonin Cct ring complex
TOR2	5100000	0	PIK-related protein kinase and rapamycin target
TAO3	5100000	0	Component of the RAM signaling network
GPH1	5100000	0	Glycogen phosphorylase required for the mobilization of glycogen
PDR17	5100000	0	Phosphatidylinositol transfer protein (PITP)
ARP9	5100000	0	Component of both the SWI/SNF and RSC chromatin remodeling complexes
RPT1	5100000	0	ATPase of the 19S regulatory particle of the 26S proteasome
BUD2	5000000	0	GTPase activating factor for Rsr1p/Bud1p
MKT1	5000000	0	Protein similar to nucleases that forms a complex with Pbp1p
SYF1	4900000	0	Member of the NineTeen Complex (NTC), stabilizes U6 snRNA in catalytic forms of the spliceosome
IMD3	4700000	0	Inosine monophosphate dehydrogenase
COG6	4700000	0	Component of the conserved oligomeric Golgi complex
PDC2	4700000	0	Transcription factor for thiamine-regulated genes
PRP19	4600000	0	Splicing factor associated with the spliceosome
CKB1	4600000	0	Beta regulatory subunit of casein kinase 2 (CK2)
DBP5	4500000	0	Cytoplasmic ATP-dependent RNA helicase of the DEAD-box family

Table 4: Top hits for mass spectrometry for TAP-*Irc20 C1239A* (continued)

Gene Symbol	Signal Intensity*		Description
	<i>Irc20 C1239A</i>	Control	
FKH2	4500000	0	Forkhead family transcription factor
APL2	4400000	0	Beta-adaptin subunit of the clathrin-associated protein (AP-1) complex
NUP60	4400000	0	FG-nucleoporin component of central core of the nuclear pore complex
FKS1	4300000	0	Catalytic subunit of 1,3-beta-D-glucan synthase
CKA1	4300000	0	Alpha catalytic subunit of casein kinase 2 (CK2)
ZDS2	4300000	0	Protein with a role in regulating Swe1p-dependent polarized growth
RVB1	4200000	0	ATP-dependent DNA helicase, also known as pontin; member of the AAA+ and RuvB-like protein families
OSH2	4200000	0	Member of an oxysterol-binding protein family with seven members
NUG1	4200000	0	GTPase that associates with nuclear 60S pre-ribosomes
RFC3	4200000	0	Subunit of heteropentameric Replication factor C (RF-C)
TIF4631	4100000	0	Translation initiation factor eIF4G
BMS1	4100000	0	GTPase required for ribosomal subunit synthesis and rRNA processing
RDH54	4100000	0	DNA-dependent ATPase; DNA recombination/repair translocase
SEC28	4000000	0	Epsilon-COP subunit of the coatomer
NUP159	4000000	0	FG-nucleoporin component of central core of the nuclear pore complex
SIF2	3900000	0	WD40 repeat-containing subunit of Set3C histone deacetylase complex
APL1	3900000	0	Beta-adaptin; large subunit of the clathrin associated protein complex (AP-2)
EAF3	3900000	0	Component of the Rpd3S histone deacetylase complex
SPT6	3900000	0	Nucleosome remodeling protein
NOG1	3900000	0	Associates with free 60S ribosomal subunits in the nucleolus and is required for 60S ribosomal subunit biogenesis